

Gamma-ray burst prompt correlations

Dainotti M. G.^{1,2,3}, Del Vecchio R.³, Tarnopolski M.³

ABSTRACT

The mechanism responsible for the prompt emission of gamma-ray bursts (GRBs) is still a debated issue. The prompt phase-related GRB correlations can allow to discriminate among the most plausible theoretical models explaining this emission. We present an overview of the observational two-parameter correlations, their physical interpretations, their use as redshift estimators and possibly as cosmological tools. The nowadays challenge is to make GRBs, the farthest stellar-scaled objects observed (up to redshift $z = 9.4$), standard candles through well established and robust correlations. However, GRBs spanning several orders of magnitude in their energetics are far from being standard candles. We describe the advances in the prompt correlation research in the past decades, with particular focus paid to the discoveries in the last 20 years.

Subject headings: gamma-ray bursts, prompt emission, correlations

¹Physics Department, Stanford University, Via Pueblo Mall 382, Stanford, CA, USA, E-mail: mdainott@stanford.edu

²INAF-Istituto di Astrofisica Spaziale e Fisica cosmica, Via Gobetti 101, 40129, Bologna, Italy

³Astronomical Observatory, Jagiellonian University, Orla 171, 30-244 Kraków, Poland, E-mails: delvecchioroberta@hotmail.it, mariagiovannadainotti@yahoo.it, mariusz.tarnopolski@uj.edu.pl

Contents

1	Introduction	4
2	Notations and nomenclature	7
3	The Prompt Correlations	10
3.1	The $L_{\text{peak}} - \tau_{\text{lag}}$ correlation	10
3.1.1	Literature overview	10
3.1.2	Physical interpretation of the $L_{\text{peak}} - \tau_{\text{lag}}$ relation	14
3.2	The $L_{\text{peak}} - V$ correlation	16
3.2.1	Literature overview	16
3.2.2	Physical interpretation of the $L_{\text{peak}} - V$ relation	19
3.3	The $L_{\text{iso}} - \tau_{\text{RT}}$ correlation and its physical interpretation	19
3.4	The $\Gamma_0 - E_{\text{prompt}}$ and $\Gamma_0 - L_{\text{iso}}$ correlations and their physical interpretation	21
3.5	Correlations between the energetics and the peak energy	24
3.5.1	The $\langle E_{\text{peak}} \rangle - F_{\text{peak}}$ and the $E_{\text{peak}} - S_{\text{tot}}$ correlations	24
3.5.2	The $E_{\text{peak}} - E_{\text{iso}}$ correlation	27
3.5.3	The $E_{\text{peak}} - E_{\gamma}$ correlation	32
3.5.4	Physical interpretation of the energetics vs. peak energy relations . .	33
3.6	Correlations between the luminosity and the peak energy	38
3.6.1	The $L_{\text{iso}} - E_{\text{peak}}$ correlation	38
3.6.2	The $L_{\text{peak}} - E_{\text{peak}}$ correlation	40
3.6.3	Physical interpretation of the luminosity vs. peak energy relations . .	43
3.7	Comparisons between $E_{\text{peak}} - E_{\text{iso}}$ and $E_{\text{peak}} - L_{\text{peak}}$ correlation	45
3.8	The $L_{X,p} - T_p^*$ correlation and its physical interpretation	46
3.9	The $L_f - T_f$ correlation and its physical interpretation	49

4 Summary	52
References	52

1. Introduction

Gamma-ray bursts (GRBs) are highly energetic events with the total isotropic energy released of the order of $10^{48} - 10^{55}$ erg (for recent reviews, see Nakar 2007; Zhang 2011; Gehrels and Razzaque 2013; Berger 2014; Kumar and Zhang 2015; Mészáros and Rees 2015). GRBs were discovered by military satellites *Vela* in late 1960’s and were recognized early to be of extrasolar origin (Klebesadel et al. 1973). A bimodal structure (reported first by Mazets et al. 1981) in the duration distribution of GRBs detected by the Burst and Transient Source Experiment (BATSE) onboard the *Compton Gamma-Ray Observatory* (*CGRO*) (Meegan et al. 1992), based on which GRBs are nowadays commonly classified into short (with durations $T_{90} < 2$ s, SGRBs) and long (with $T_{90} > 2$ s, LGRBs), was found (Kouveliotou et al. 1993). BATSE observations allowed also to confirm the hypothesis of Klebesadel et al. (1973) that GRBs are of extragalactic origin due to isotropic angular distribution in the sky combined with the fact that they exhibited an intensity distribution that deviated strongly from the $-3/2$ power law (Paczynski 1991a,b; Meegan et al. 1992; Fishman and Meegan 1995; Briggs et al. 1996). This was later corroborated by establishing the first redshift measurement, taken for GRB970508, which with $0.835 < z \lesssim 2.3$ was placed at a cosmological distance of at least 2.9 Gpc (Metzger et al. 1997). Despite initial isotropy, SGRBs were shown to be distributed anisotropically on the sky, while LGRBs are distributed isotropically (Balazs et al. 1998; Mészáros et al. 2000a,b; Mészáros and Štoček 2003; Magliocchetti et al. 2003; Bernui et al. 2008; Vavrek et al. 2008; Tarnopolski 2015a). Cosmological consequences of the anisotropic celestial distribution of SGRBs were discussed lately by Mészáros et al. (2009) and Mészáros and Rees (2015). Finally, the progenitors of LGRBs are associated with supernovae (SNe) (Hjorth et al. 2003; Malesani et al. 2004; Woosley and Bloom 2006; Sparre et al. 2011; Schulze et al. 2014) related with collapse of massive stars. Progenitors of SGRBs are thought to be neutron star–black hole (NS–BH) or NS–NS mergers (Eichler et al. 1989; Paczynski 1991b; Narayan et al. 1992; Nakar and Piran 2005), and no connection between SGRBs and SNe has been proven (Zhang et al. 2009).

While the recent first direct detection of gravitational waves (GW), termed GW150914, by the Laser Interferometer Gravitational Wave Observatory (LIGO) (Abbott et al. 2016), interpreted as a merger of two stellar-mass BHs with masses $36_{-4}^{+5}M_{\odot}$ and $29_{-4}^{+4}M_{\odot}$, is by itself a discovery of prime importance, it becomes especially interesting in light of the finding of Connaughton et al. (2016) who reported a weak transient source lasting 1 s and detected by *Fermi*/GBM (Narayana Bhat et al. 2016) only 0.4 s after the GW150914, termed GW150914-GBM. Its false alarm probability is estimated to be 0.0022. The fluence in the energy band 1 keV – 10 MeV is computed to be $1.8_{-1.0}^{+1.5} \times 10^{49}$ erg s $^{-1}$. While these GW and GRB events are consistent in direction, its connection is tentative due to relatively large uncertainties in their localization. This association is unexpected as SGRBs have been thought to originate

from NS–NS or NS–BH mergers. Moreover, neither *INTEGRAL* (Savchenko et al. 2016), nor *Swift* (Evans et al. 2016) detected any signals that could be ascribed to a GRB. Even if it turns out that it is only a chance coincidence (Lyutikov 2016), it has already triggered scenarios explaining how a BH–BH merger can become a GRB, e.g. the nascent BH could generate a GRB via accretion of a mass $\simeq 10^{-5}M_{\odot}$ (Li et al. 2016), indicating its location in a dense medium (see also Loeb 2016), or two high-mass, low-metallicity stars could undergo an SN explosion, and the matter ejected from the last exploding star can form—after some time—an accretion disk producing an SGRB (Perna et al. 2016). Also the possible detection of an afterglow that can be visible many months after the event (Morsony et al. 2016) could shed light on the nature of the GW and SGRB association.

From a phenomenological point of view, a GRB is composed of the prompt emission, which consists of high-energy photons such as γ -rays and hard X-rays, and the afterglow emission, i.e. a long lasting multi-wavelength emission (X-ray, optical, and sometimes also radio), which follows the prompt phase. The first afterglow observation (for GRB970228) was due to the *BeppoSAX* satellite (Costa et al. 1997; van Paradijs et al. 1997). Another class, besides SGRBs and LGRBs, i.e. intermediate in duration, was proposed to be present in univariate duration distributions (Horváth 1998, 2002; Horváth et al. 2008; Horváth 2009; Huja et al. 2009; Řípa et al. 2009), as well as in higher dimensional parameter spaces (Mukherjee et al. 1998; Horváth et al. 2006; Řípa et al. 2009; Horváth et al. 2010; Veres et al. 2010; Koen and Bere 2012). On the other hand, this elusive intermediate class might be a statistical feature that can be explained by modelling the duration distribution with skewed distributions, instead of the commonly applied standard Gaussians (Zitouni et al. 2015; Tarnopolski 2015b, 2016a,b,c). Additionally, GRB classification was shown to be detector dependent (Nakar 2007; Bromberg et al. 2013; Tarnopolski 2015c). Moreover, a subclass classification of LGRBs was proposed (Gao et al. 2010), and Norris and Bonnell (2006) discovered the existence of an intermediate class or SGRBs with extended emission, that show mixed properties between SGRBs and LGRBs. GRBs with very long durations (ultra-long GRBs, with $T_{90} > 1000$ s) are statistically different than regular (i.e., with $T_{90} < 500$ s) LGRBs (Boër et al. 2015), and hence might form a different class (see also Virgili et al. 2013; Zhang et al. 2014; Levan et al. 2014; Levan 2015). Another relevant classification appears related to the spectral features distinguishing normal GRBs from X-ray flashes (XRFs). The XRFs (Heise et al. 2001; Kippen et al. 2001) are extragalactic transient X-ray sources with spatial distribution, spectral and temporal characteristics similar to LGRBs. The remarkable property that distinguishes XRFs from GRBs is that their νF_{ν} prompt emission spectrum peaks at energies which are observed to be typically an order of magnitude lower than the observed peak energies of GRBs. XRFs are empirically defined by a greater fluence (time integrated flux) in the X-ray band (2–30 keV) than in the

γ -ray band (30 – 400 keV). This classification is also relevant for the investigation of GRB correlations since some of them become stronger or weaker by introducing different GRB categories. Grupe et al. (2013), using 754 *Swift* GRBs, performed an exhaustive analysis of several correlations as well as the GRB redshift distribution, discovering that the bright bursts are more common in the high- z (i.e., $z \gtrsim 3$) than in the local universe.

This classification has further enhanced the knowledge of the progenitor system from which GRBs originate. It was soon after their discovery that LGRBs were thought to originate from distant star-forming galaxies. Since then, LGRBs have been firmly associated with powerful core-collapse SNe and the association seems solid. Nevertheless, there have been puzzling cases of LGRBs that were not associated with bright SNe (Fynbo et al. 2006; Della Valle et al. 2006). This implies that it is possible to observe GRBs without an associated bright SNe or there are other progenitors for LGRBs than core-collapse of massive stars. Another relevant uncertainty concerning the progenitor systems for LGRBs is the role of metallicity Z . In the collapsar model (Woosley and Bloom 2006), LGRBs are only formed by massive stars with Z/Z_{\odot} below $\simeq 0.1 - 0.3$. However, several GRBs have been located in very metal-rich systems (Perley et al. 2015) and it is an important goal to understand whether there are other ways to form LGRBs than through the collapsar scenario (Greiner et al. 2015). One of the models used to explain the GRB phenomenon is the “fireball” model (Wijers et al. 1997; Mészáros 1998, 2006b) in which a compact central engine (either the collapsed core of a massive star or the merger product of an NS–NS binary) launches a highly relativistic, jetted electron-positron-baryon plasma. Interactions of blobs within the jet are believed to produce the prompt emission. Instead, the interaction of the jet with the ambient material causes the afterglow phase. However, problems in explaining the light curves within this model have been shown by Willingale et al. (2007). Specifically, for $\simeq 50\%$ of GRBs the observed afterglows are in agreement with the model, but for the rest the temporal and spectral indices do not conform and suggest a continued late energy injection. Melandri et al. (2008) performed a multiwavelength analysis and found that the forward shock (FS) model does not explain almost 50% of the examined GRBs, even after taking into account energy injection. Rykoff et al. (2009) showed that the fireball model does not model correctly early afterglows. (Oates et al. 2011) analyzed the prompt and afterglow light curves, and pointed out that some GRBs required energy injection to explain the outflows. The crisis of the standard fireball models appeared when *Swift* (Gehrels et al. 2004) observations revealed a more complex behaviour of the light curves than observed in the past (O’Brien et al. 2006; Sakamoto et al. 2007; Zhang et al. 2007) and pointed out that GRBs often follow “canonical” light curves (Nousek et al. 2006). Therefore, the discovery of correlations among relevant physical parameters in the prompt phase is very important in this context in order to use them as possible model discriminators. In fact, many the-

oretical models have been presented in the literature in order to explain the wide variety of observations, but each model has some advantages as well as drawbacks, and the use of the phenomenological correlations can boost the understanding of the mechanism responsible for the prompt emission. Moreover, given the much larger (compared to SNe) redshift range over which GRBs can be observed, it is tempting to include them as cosmological probes, extending the redshift range by almost an order of magnitude further than the available SNe Ia. GRBs are observed up to redshift $z = 9.4$ (Cucchiara et al. 2011), much more distant than SNe Ia, observed up to $z = 2.26$ (Rodney et al. 2015), and therefore they can help to understand the nature of dark energy and determine the evolution of its equation of state at very high z . However, contrary to SNe Ia, which originate from white dwarves reaching the Chandrasekhar limit and always releasing the same amount of energy, GRBs cannot yet be considered standard candles with their (isotropic-equivalent) energies spanning 8 orders of magnitude (see also Lin et al. 2015 and references therein). Therefore, finding universal relations among observable properties can help to standardize their energetics and/or luminosities. They can serve as a tracer of the history of the cosmic star formation rate (Totani 1997; Porciani and Madau 2001; Bromm and Loeb 2006; Kistler et al. 2009; de Souza et al. 2011) and provide invaluable information on the physics in the intergalactic medium (Barkana and Loeb 2004; Ioka and Mészáros 2005; Inoue et al. 2007). This is the reason why the study of GRB correlations is so relevant for understanding the GRB emission mechanism, for finding a good distance indicator, and for exploring the high-redshift universe (Salvaterra 2015).

This paper is organized in the following manner. In Sect. 2 we explain the nomenclature and definitions adopted in this work, and in Sect. 3 we analyze the correlations between various prompt parameters. We summarize in Sect. 4.

2. Notations and nomenclature

For clarity we report a summary of the nomenclature adopted in the review. L , F , E , S and T indicate the luminosity, the energy flux, the energy, the fluence and the timescale, respectively, which can be measured in several wavelengths. More specifically:

- T_{90} is the time interval in which 90% of the GRB’s fluence is accumulated, starting from the time at which 5% of the total fluence was detected (Kouveliotou et al. 1993).
- T_{50} is defined, similarly to T_{90} , as the time interval from 25% to 75% of the total detected fluence.

- T_{45} is the time spanned by the brightest 45% of the total counts detected above background (Reichart et al. 2001).
- T_{peak} is the time at which the pulse (i.e., a sharp rise and a slower, smooth decay (Fishman et al. 1994; Norris et al. 1996; Stern and Svensson 1996; Ryde and Svensson 2002)) in the prompt light curve peaks (see Fig. 1).

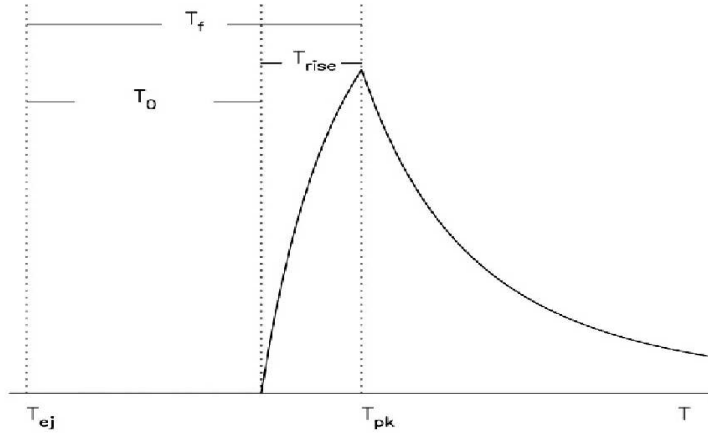


Fig. 1.— A sketch of the pulse displaying T_{ej} and T_{peak} (denoted by T_{pk} here) and the quantities T_f and $T_0 = T_f - T_{\text{rise}}$. (Figure after Willingale et al. (2010); see Fig. 1 therein.)

- T_{break} is the time of a power law break in the afterglow light curve (Sari et al. 1999; Willingale et al. 2010), i.e. the time when the afterglow brightness has a power law decline that suddenly steepens due to the slowing down of the jet until the relativistic beaming angle roughly equals the jet opening angle θ_{jet} (Rhoads 1997)
- τ_{lag} and τ_{RT} are the difference of arrival times to the observer of the high energy photons and low energy photons defined between 25 – 50 keV and 100 – 300 keV energy band, and the shortest time over which the light curve increases by 50% of the peak flux of the pulse.
- T_p is the end time prompt phase at which the exponential decay switches to a power law, which is usually followed by a shallow decay called the plateau phase, and T_a is the time at the end of this plateau phase (Willingale et al. 2007).
- T_f is the pulse width since the burst trigger at the time T_{ej} of the ejecta.

- E_{peak} , E_{iso} , E_{γ} and E_{prompt} are the peak energy, i.e. the energy at the peak of the νF_{ν} spectrum (Mallozzi et al. 1995), the total isotropic energy emitted during the whole burst (e.g., Amati et al. 2002), the total energy corrected for the beaming factor [the latter two are connected via $E_{\gamma} = (1 - \cos \theta_{\text{jet}})E_{\text{iso}}$], and the isotropic energy emitted in the prompt phase, respectively.
- F_{peak} , F_{tot} are the peak and the total fluxes respectively (Lee and Petrosian 1996).
- L_a , $L_{X,p}$ and L_f are the luminosities respective to T_a , T_p (specified in the X-ray band) and T_f .
- L is the observed luminosity, and specifically L_{peak} and L_{iso} are the peak luminosity (i.e., the luminosity at the pulse peak, Norris et al. 2000) and the total isotropic luminosity, both in a given energy band. More precisely, L_{peak} is defined as follows:

$$L_{\text{peak}} = 4\pi D_L(z, \Omega_M, \Omega_{\Lambda})^2 F_{\text{peak}}, \quad (1)$$

with $D_L(z, \Omega_M, \Omega_{\Lambda})$ the luminosity distance given by

$$D_L(z, \Omega_M, \Omega_{\Lambda}) = \frac{c(1+z)}{H_0} \int_0^z \frac{dz'}{\sqrt{\Omega_M(1+z')^3 + \Omega_{\Lambda}}}, \quad (2)$$

where Ω_M and Ω_{Λ} are the matter and dark energy density parameters, H_0 is the present-day Hubble constant, and z is the redshift. Similarly, L_{iso} is given by

$$L_{\text{iso}} = 4\pi D_L(z, \Omega_M, \Omega_{\Lambda})^2 F_{\text{tot}}. \quad (3)$$

- S_{γ} , S_{obs} , S_{tot} indicate the prompt fluence in the whole gamma band (i.e., from a few hundred keV to a few MeV), the observed fluence in the range 50 – 300 keV and the total fluence in the 20 keV – 1.5 MeV energy band.
- V is the variability of the GRB’s light curve. It is computed by taking the difference between the observed light curve and its smoothed version, squaring this difference, summing these squared differences over time intervals, and appropriately normalizing the resulting sum (Reichart et al. 2001). Different smoothing filters may be applied (see also Li and Paczyński 2006 for a different approach). V_f denotes the variability for a certain fraction of the smoothing timescale in the light curve.

Most of the quantities described above are given in the observer frame, except for E_{iso} , E_{prompt} , L_{peak} and L_{iso} , which are already defined in the rest frame. With the upper index “*” we explicitly denote the observables in the GRB rest frame. The rest frame times are the

observed times divided by the cosmic time expansion, for example the rest frame time in the prompt phase is denoted with $T_p^* = T_p / (1 + z)$. The energetics are transformed differently, e.g. $E_{\text{peak}}^* = E_{\text{peak}}(1 + z)$.

The Band function (Band et al. 1993) is a commonly applied phenomenological spectral profile, such that

$$N_E(E) = A_{\text{norm}} \times \begin{cases} \left(\frac{E}{100 \text{ keV}}\right)^\alpha \exp\left(-\frac{E}{E_0}\right), & E \leq (\alpha - \beta)E_0 \\ \left[\frac{(\alpha - \beta)E_0}{100 \text{ keV}}\right]^{\alpha - \beta} \left(\frac{E}{100 \text{ keV}}\right)^\beta \exp(\alpha - \beta), & E \geq (\alpha - \beta)E_0 \end{cases} \quad (4)$$

where A_{norm} is the normalization. Here, α and β are the low- and high-energy indices of the Band function, respectively. $N_E(E)$ is in units of photons $\text{cm}^{-2} \text{s}^{-1} \text{keV}^{-1}$. For the cases $\beta < -2$ and $\alpha > -2$, the E_{peak} can be derived as $E_{\text{peak}} = (2 + \alpha)E_0$, which corresponds to the energy at the maximum flux in the νF_ν spectra (Band et al. 1993; Yonetoku et al. 2004).

The Pearson correlation coefficient (Kendall and Stuart 1973; Bevington and Robinson 2003) is denoted with r , the Spearman correlation coefficient (Spearman 1904) with ρ , and the p -value (a probability that a correlation is drawn by chance) is denoted with P .

Finally, we mostly deal with correlations of the form $y = ax + b$. However, when the intercept b is neglected in the text, but its value is non-negligible (or not known due to lacking in the original paper), we use the notation $y \sim ax$ to emphasize the slope.

3. The Prompt Correlations

Several physical relations between relevant quantities in GRBs were found since the 1990's. In each paragraph below we follow the discovery of the correlation with the definition of the quantities, the discussions presented in literature and their physical interpretation.

3.1. The $L_{\text{peak}} - \tau_{\text{lag}}$ correlation

3.1.1. Literature overview

Liang and Kargatis (1996), using 34 bright GRBs detected by BATSE, found that E_{peak} depends linearly on the previous flux emitted by the pulse, i.e. that the rate of change of E_{peak} is proportional to the instantaneous luminosity. Quantitatively,

$$\frac{L_{\text{peak}}}{N} = -\frac{dE_{\text{peak}}}{dt}, \quad (5)$$

where N is a normalization constant expressing the luminosity for each pulse within a burst, and L_{peak} was calculated from the observed flux via Eq. (1).

The $L_{\text{peak}} - \tau_{\text{lag}}$ correlation was introduced for the first time by Norris et al. (2000) who examined a sample of 174 GRBs detected by BATSE, among which 6 GRBs had an established redshift and those were used to find an anticorrelation between L_{peak} and τ_{lag} in the form of (see the left panel of Fig. 2)

$$\log L_{\text{peak}} = 55.11 - 1.14 \log \tau_{\text{lag}}^*, \quad (6)$$

with L_{peak} , in units of $10^{53} \text{ erg s}^{-1}$, computed in the 50 – 300 keV range, and τ_{lag}^* is measured in seconds. A remarkably consistent relation was found by Schaefer et al. (2001), who used a sample of 112 BATSE GRBs and reported that

$$\log L_{\text{peak}} = 52.46 - (1.14 \pm 0.20) \log \tau_{\text{lag}}, \quad (7)$$

being in perfect agreement with the result of Norris et al. (2000). Here, L_{peak} is in units of $10^{51} \text{ erg s}^{-1}$, and τ_{lag} in seconds. This relation has been confirmed by several studies (e.g. Salmonson 2000; Daigne and Mochkovitch 2003; Zhang et al. 2006).

Schaefer (2004) showed that the $L_{\text{peak}} - \tau_{\text{lag}}$ relation is a consequence of the Liang and Kargatis (1996) empirical relation from Eq. (5), and he derived this dependence to be of the form $\log L_{\text{peak}} \sim -\log \tau_{\text{lag}}$. This correlation was useful in the investigation of Kocevski and Liang (2003), who used a sample of 19 BATSE GRBs and the $L_{\text{peak}} - \tau_{\text{lag}}$ relation from (Schaefer et al. 2001) to infer their pseudo-redshifts. Their approach was to vary the guessed z until it allowed to match the luminosity distance D_L measured with the GRB’s energy flux and the D_L that can be calculated from the guessed redshift within a flat Λ CDM model, until the agreement among the two converged to within 10^{-3} . Next, the rate of E_{peak} decay, as in (Liang and Kargatis 1996), was measured. Finally, Kocevski and Liang (2003) showed that the L_{peak} is directly related to the GRB’s spectral evolution. However, Hakkila et al. (2008) found a different slope, -0.62 ± 0.04 , and argued that the $L_{\text{peak}} - \tau_{\text{lag}}$ relation is a pulse rather than a burst property, i.e. each pulse is characterized by its own τ_{lag} , distinct for various pulses within a GRB.

Tsutsui et al. (2008), using pseudo-redshifts estimated via the Yonetoku relation (see Sect. 3.6.2) for 565 BATSE GRBs, found that the $L_{\text{peak}} - \tau_{\text{lag}}$ relation has a ρ of only 0.38 (see the right panel of Fig. 2). However, assuming that the luminosity is a function of both the redshift and the lag, a new redshift-dependent $L_{\text{peak}} - \tau_{\text{lag}}$ relation was found as

$$\log L_{\text{peak}} = 50.88 + 2.53 \log(1 + z) - 0.282 \log \tau_{\text{lag}}, \quad (8)$$

with L_{peak} in units of $10^{50} \text{ erg s}^{-1}$, τ_{lag} in seconds, $\rho = 0.77$ and $P = 7.9 \times 10^{-75}$. Although the spectral lag is computed from two channels of BATSE, this new $L_{\text{peak}} - \tau_{\text{lag}}$ relation suggests

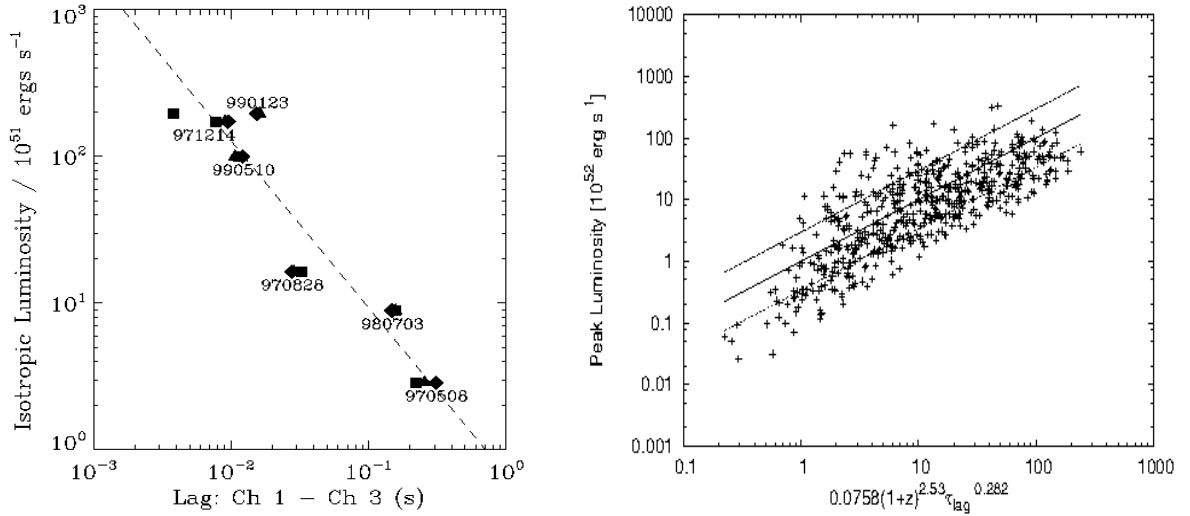


Fig. 2.— **Left panel:** L_{peak} vs. τ_{lag}^* distribution for six GRBs with measured redshifts. The dashed line represents the power law fit to the lag times for ranges consisting of count rates larger than $0.1 \times$ peak intensity (squares), yielding $\log L_{\text{peak}} \sim -1.14 \log(\tau_{\text{lag}}^*/0.01 \text{ s})$. The lag time is computed using channel 1 (25 – 50 keV) and channel 3 (100 – 300 keV) of the BATSE instrument. (Figure after Norris et al. (2000); see Fig. 6 therein. © AAS. Reproduced with permission.) **Right panel:** The $L_{\text{peak}} - \tau_{\text{lag}}$ distribution in the $\log L_{\text{peak}}$ vs. $\sim 2.53 \log(1+z) - 0.282 \log \tau_{\text{lag}}$ plane. The correlation coefficient is $\rho = 0.77$, $P = 7.9 \times 10^{-75}$. The solid line represents the best fit line and two dashed lines delineate 1σ deviation. (Figure after Tsutsui et al. (2008); see Fig. 4 therein. Copyright © 2008 AIP Publishing.)

that a future lag-luminosity relation defined within the *Swift* data should also depend on the redshift.

Afterwards, Sultana et al. (2012) presented a relation between the z - and k -corrected τ_{lag} for the *Swift* energy bands 50–100 keV and 100–200 keV, and L_{peak} , for a subset of 12 *Swift* long GRBs. The z -correction takes into account the time dilatation effect by multiplying the observed lag by $(1+z)^{-1}$ to translate it into the rest frame. The k -correction takes into account a similar effect caused by energy bands being different in the observer and rest frames via multiplication by $(1+z)^{0.33}$ (Gehrels et al. 2006). The net corrected τ_{lag}^* is thence $(1+z)^{-0.67}\tau_{\text{lag}}$. In addition, Sultana et al. (2012) demonstrated that this correlation in the prompt phase can be extrapolated into the $L_a - T_a^*$ relation (Dainotti et al. 2008, 2010, 2011a, 2013). Sultana et al. (2012) found¹:

$$\log L_{\text{peak}} = (54.87 \pm 0.29) - (1.19 \pm 0.17) \log [(1+z)^{-0.67} \tau_{\text{lag}}], \quad (9)$$

and

$$\log L_a = (51.57 \pm 0.10) - (1.10 \pm 0.03) \log T_a^*, \quad (10)$$

with τ_{lag} in ms, T_a^* in seconds, and L in erg s^{-1} . The correlation coefficient is significant for these two relations ($\rho = -0.65$ for the $L_{\text{peak}} - \tau_{\text{lag}}$ and $\rho = -0.88$ for the $L_a - T_a^*$ relations) and have surprisingly similar best-fit power law indices (-1.19 ± 0.17 and -1.10 ± 0.03 , respectively). Although τ_{lag} and T_a^* represent different GRB time variables, it appears distinctly that the $L_{\text{peak}} - \tau_{\text{lag}}$ relation extrapolates into $L_a - T_a^*$ for timescales $\tau_{\text{lag}} \simeq T_a^*$. A discussion and comparison of this extrapolation with the $L_f - T_f$ relation is extensively presented in (Dainotti et al. 2015).

Ukwatta et al. (2010) confirmed that there is a correlation between L_{peak}^* and the z - and k -corrected τ_{lag} among 31 GRBs observed by *Swift*, with $r = -0.68$, $P = 7 \times 10^{-2}$ and the slope equal to -1.4 ± 0.3 , hence confirming the $L_{\text{peak}} - \tau_{\text{lag}}$ relation, although with a large scatter. This was followed by another confirmation of this correlation (Ukwatta et al. 2012) with the use of 43 *Swift* GRBs with known redshift, which yielded $r = -0.82$, $P = 5.5 \times 10^{-5}$, and a slope of -1.2 ± 0.2 , being consistent with the previous results.

Finally, Margutti et al. (2010) established that the X-ray flares obey the same $L_{\text{peak}} - \tau_{\text{lag}}^*$ relation (in the rest-frame energy band 0.3–10 keV) as GRBs, and proposed that their underlying mechanism is similar.

¹Note that Sultana et al. (2012) used L_{iso} to denote the peak isotropic luminosity.

3.1.2. Physical interpretation of the $L_{\text{peak}} - \tau_{\text{lag}}$ relation

The physical assumption on which the work by Norris et al. (2000) was based is that the initial mechanism for the energy formation affects the development of the pulse much more than dissipation. From the study of several pulses in bright, long BATSE GRBs, it was claimed that for pulses with precisely defined shape, the rise-to-decay ratio is ≤ 1 . In addition, when the ratio diminishes, pulses show a tendency to be broader and weaker.

Salmonson (2000) proposed that the $L_{\text{peak}} - \tau_{\text{lag}}$ relation arises from an entirely kinematic effect. In this scenario, an emitting region with constant (among the bursts) luminosity is the source of the GRB's radiation. He also claimed that variations in the line-of-sight velocity should affect the observed luminosity proportionally to the Lorentz factor of the jet's expansion, $\Gamma = [1 - (v/c)^2]^{-1/2}$ (where v is the relative velocity between the inertial reference frames and c is the speed of light), while the apparent τ_{lag} is proportional to $1/\Gamma$. The variations in the velocity among the line-of-sight is a result of the jet's expansion velocity combined with the cosmological expansion. The differences of luminosity and lag between different bursts are due to the different velocities of the individual emitting regions. In this case, the luminosity is expected to be proportional to $1/\tau_{\text{lag}}$, which is consistent with the observed relation. This explanation, however, requires the comoving luminosity to be nearly constant among the bursts, which is a very strong condition to be fulfilled. Moreover, this scenario has several other problems (as pointed out by Schaefer 2004):

1. it requires the Lorentz factor and luminosity to have the same range of variation. However, the observed L_{peak} span more than three orders of magnitude (e.g., Schaefer et al. 2001), while the Lorentz factors span less than one order of magnitude (i.e., a factor of 5) (Panaitescu and Kumar 2002);
2. it follows that the observed luminosity should be linearly dependent on the jet's Lorentz factor, yet this claim is not justified. In fact, a number of corrections is to be taken into account, leading to a significantly nonlinear dependence. The forward motion of the jet introduces by itself an additional quadratic dependence (Fenimore et al. 1996).

Ioka and Nakamura (2001) proposed another interpretation for the $L_{\text{peak}} - \tau_{\text{lag}}$ correlation. From their analysis, a model in which the peak luminosity depends on the viewing angle is elaborated: the viewing angle is the off-axis angular position from which the observer examines the emission. Indeed, it is found that a high-luminosity peak in GRBs with brief spectral lag is due to an emitted jet with a smaller viewing angle than a fainter peak with extended lag. It is also claimed that the viewing angle can have implications on other correlations, such as the luminosity-variability relation presented in Sect. 3.2. As an additional

result from this study, it was pointed out that XRFs can be seen as GRBs detected from large angles with high spectral lag and small variability.

On the other hand, regarding the jet angle distributions, Liang et al. (2008) found an anticorrelation between the jet opening angle and the isotropic kinetic energy among 179 X-ray GRB light curves and the afterglow data of 57 GRBs. Assuming that the GRB rate follows the star formation rate, and after a careful consideration of selection effects, Lü et al. (2012b) found in a sample of 77 GRBs an anticorrelation between the jet opening angle θ_{jet} and the redshift in the form

$$\log \theta_{\text{jet}} = (-0.90 \pm 0.09) - (0.94 \pm 0.19) \log(1 + z), \quad (11)$$

with $\rho = 0.55$ and $P < 10^{-4}$. Using a mock sample and bootstrap technique, they showed that the observed $\theta_{\text{jet}} - z$ relation is most likely due to instrumental selection effects. Moreover, they argued that other types of relation, e.g. $\tau_{\text{lag}} - z$ (Yi et al. 2008) or the redshift dependence of the shallow decays in X-ray afterglows Stratta et al. (2009), while might have connections with the jet geometry, are also likely to stem from observational biases or sample selection effects. Also, Ryan et al. (2015) investigated the jet opening angle properties using a sample of 226 *Swift*/XRT GRBs with known redshift. They found that most of the observed afterglows were observed off-axis, hence the expected behaviour of the afterglow light curves can be significantly affected by the viewing angle.

Zhang et al. (2009) argued, on the basis of the kinematic model, that the origin of the $L_{\text{peak}} - \tau_{\text{lag}}$ relation is due to a more intrinsic $L_{\text{peak}} - V$ relation (see Sect. 3.2). They also gave an interpretation of the latter relation within the internal shock model (see Sect. 3.2.2). Recently, Uhm and Zhang (2016) constructed a model based on the synchrotron radiation mechanism that explains the physical origin of the spectral lags and is consistent with observations.

Another explanation for the origin of the $L_{\text{peak}} - \tau_{\text{lag}}$ relation, given by Sultana et al. (2012), involves only kinematic effects. In this case, L_{peak} and τ_{lag} depend on the quantity:

$$D = \frac{1}{\Gamma(1 - \beta_0 \cos \theta)(1 + z)}, \quad (12)$$

depicting the Doppler factor of a jet at a viewing angle θ and with velocity $\beta_0 \equiv v/c$ at redshift z . In this study there is no reference to the masses and forces involved and, as a consequence of the Doppler effect, the factor D associates the GRB rest frame timescale τ with the observed time t in the following way:

$$t = \frac{\tau}{D}. \quad (13)$$

Therefore, considering a decay timescale $\Delta\tau$ in the GRB rest frame, Eq. (13) in the observer frame will give $\Delta t = \Delta\tau/D$. Furthermore, taking into account a spectrum given by $\Phi(E) \propto E^{-\alpha}$, the peak luminosity (as already pointed out by Salmonson 2000) can be computed as

$$L_{\text{peak}} \propto D^\alpha, \quad (14)$$

with $\alpha \approx 1$. In such a way, Eqs. (13) and (14) allow to retrieve the observed $L_{\text{peak}} - \tau_{\text{lag}}$ relation. Finally, the analogous correlation coefficients and best-fit slopes of the $L_{\text{peak}} - \tau_{\text{lag}}$ and $L_a - T_a^*$ correlations obtained by Sultana et al. (2012) seem to hint toward a similar origin for these two relations.

3.2. The $L_{\text{peak}} - V$ correlation

The first correlation between L_{peak} and V was discovered by Fenimore and Ramirez-Ruiz (2000), and was given as

$$\log L_{\text{peak}} = 56.49 + 3.35 \log V, \quad (15)$$

with L_{peak} measured in ergs^{-1} . Here, the luminosity is per steradian in a specified (rest frame) energy bandpass (50 – 300 keV), averaged over 256 ms. First, seven BATSE GRBs with a measured redshift were used to calibrate the $L_{\text{peak}} - V$ relation. Next, the obtained relationship was applied to 220 bright BATSE GRBs in order to obtain the luminosities and distances, and to infer that the GRB formation rate scales as $(1+z)^{3.3 \pm 0.3}$. Finally, the authors emphasized the need of confirmation of the proposed $L_{\text{peak}} - V$ relation.

3.2.1. Literature overview

Reichart et al. (2001) used a total of 20 GRBs observed by *CGRO*/BATSE (13 bursts), the *KONUS*/Wind (5 bursts), the *Ulysses*/GRB (1 burst), and the *NEAR*/XGRS (1 burst), finding:

$$\log L_{\text{peak}} \sim (3.3_{-0.9}^{+1.1}) \log V. \quad (16)$$

with $\rho = 0.8$ and $P = 1.4 \times 10^{-4}$ (see the left panel of Fig. 3); L_{peak} was computed in the 50 – 300 keV observer-frame energy band, which corresponds roughly to the range 100 – 1000 keV in the rest frame for $z \simeq 1 - 2$, typical for GRBs in the sample examined. The distribution of the sample’s bursts in the $\log L_{\text{peak}} - \log V_f$ plane appears to be well modeled by the following parameterization:

$$\log V_f(L) = \log \bar{V}_f + b + m(\log L_{\text{peak}} - \log \bar{L}_{\text{peak}}), \quad (17)$$

where $b = 0.013_{-0.092}^{+0.075}$ is the intercept of the line, $m = 0.302_{-0.075}^{+0.112}$ is its slope, and \bar{V}_f and \bar{L}_{peak} are the median values of V_f and L_{peak} for the bursts in the sample for which spectroscopic redshifts, peak fluxes, and 64-ms or better resolution light curves are available.

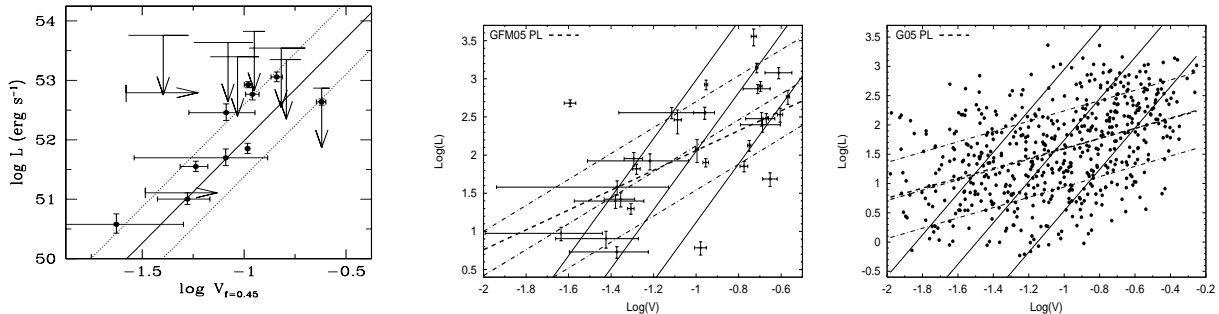


Fig. 3.— **Left panel:** the variabilities $V_{f=0.45}$ and peak luminosities L_{peak} of the data set, excluding GRB980425. In this case, $V_{f=0.45}$ indicates the variabilities for the 45% smoothing timescale of the light curve. The solid and dotted lines are the best fit line and 1σ deviation respectively in the $\log L_{\text{peak}} - \log V_{f=0.45}$ plane. (Figure after Reichart et al. (2001); see Fig. 9 therein. @ AAS. Reproduced with permission.) **Middle panel:** The $\log L_{\text{peak}} - \log V$ plane for the sample of 32 GRBs with measured redshift. The best fit lines and 1σ deviations are also displayed: solid lines are computed with the Reichart et al. (2001) method, dashed-dotted lines with the D’Agostini (2005) method and the dashed lines are recovered by Guidorzi et al. (2005). (Figure after Guidorzi et al. (2006); see Fig. 1 therein.) **Right panel:** $\log L_{\text{peak}} - \log V$ relation for the set of 551 BATSE GRBs. The best-fit lines and 1σ regions are also shown, the solid lines are fitted with the Reichart et al. (2001) method, the dashed-dotted lines with the D’Agostini (2005) method and the dashed lines are recovered by Guidorzi et al. (2005). (Figure after Guidorzi et al. (2006); see Fig. 2 therein.)

Later, Guidorzi et al. (2005) updated the sample to 32 GRBs detected by different satellites, i.e. *BeppoSAX*, *CGRO/BATSE*, *HETE-2* and *KONUS* (see the middle panel of Fig. 3). The existence of a correlation was confirmed, but they found a dramatically different relationship with respect to the original one:

$$\log L_{\text{peak}} = 3.36_{-0.43}^{+0.89} + 1.30_{-0.44}^{+0.84} \log V, \quad (18)$$

with $\rho = 0.625$ and $P = 10^{-4}$, and L_{peak} in units of $10^{50} \text{ erg s}^{-1}$.

However, Reichart and Nysewander (2005) using the same sample claimed that this result was the outcome of an improper statistical methodology, and confirmed the previous work of Reichart et al. (2001). Indeed, they showed that the difference among their results and the ones from Guidorzi et al. (2005) was due to the fact that the variance of the sample in the fit in (Guidorzi et al. 2005) was not taken into account. They used an updated data

set, finding that the fit was well described by the slope $m = 3.4_{-0.6}^{+0.9}$, with a sample variance $\sigma_V = 0.2 \pm 0.04$.

Subsequently, Guidorzi et al. (2006) using a sample of 551 BATSE GRBs with pseudo-redshifts derived using the $L_{\text{peak}} - \tau_{\text{lag}}$ relation (Guidorzi 2005), tested the $L_{\text{peak}} - V$ correlation (see right panel of Fig. 3). They also calculated the slope of the correlation of the samples using the methods implemented by Reichart et al. (2001) and D’Agostini (2005). The former method provided a value of the slope in the $L_{\text{peak}} - V$ correlation consistent with respect to the previous works:

$$\log L_{\text{peak}} \sim 3.5_{-0.4}^{+0.6} \log V. \quad (19)$$

Instead, the slope for this sample using the latter method is much lower than the value in (Reichart et al. 2001):

$$\log L_{\text{peak}} \sim 0.88_{-0.13}^{+0.12} \log V. \quad (20)$$

The latter slope m is consistent with the results obtained by Guidorzi et al. (2005), but inconsistent with the results derived by Reichart and Nysewander (2005).

Afterwards, Rizzuto et al. (2007) tested this correlation with a sample of 36 LGRBs detected by *Swift* in the 15–350 keV energy range and known redshifts. The sample consisted of bright GRBs with $L_{\text{peak}} > 5 \times 10^{50} \text{ erg s}^{-1}$ within a 100 – 1000 keV energy range. In their study, they adopted two definitions of variability, presented by Reichart et al. (2001), called V_R , and by Li and Paczyński (2006), hereafter V_{LP} . V_R and V_{LP} differ from each other with a different smoothing filter which, in the second case, selects only high-frequency variability. Finally, Rizzuto et al. (2007) confirmed the correlation and its intrinsic dispersion around the best-fitting power law given by

$$\log L_{\text{peak}} \sim (2.3 \pm 0.17) \log V_{LP}, \quad (21)$$

with $\rho = 0.758$ and $P = 0.011$, and

$$\log L_{\text{peak}} \sim (1.7 \pm 0.4) \log V_R, \quad (22)$$

with $\sigma_{\log L} = 0.58_{-0.12}^{+0.15}$, $\rho = 0.115$, and $P = 0.506$. Six low-luminosity GRBs (i.e., GRB050223, GRB050416A, GRB050803, GRB051016B, GRB060614 and GRB060729), out of a total of 36 in the sample, are outliers of the correlation, showing values of V_R higher than expected. Thus, the correlation is not valid for low-luminosity GRBs.

As is visible from this discussion, the scatter in this relation is not negligible, thus making it less reliable than the previously discussed ones. However, investigating the physical explanation of this correlation is worth to be depicted for further developments.

3.2.2. Physical interpretation of the $L_{\text{peak}} - V$ relation

We here briefly describe the internal and external shock model (Piran 2004; Mészáros 2006a), in which the GRB is caused by emission from a relativistic, expanding baryonic shell with a Lorentz bulk factor Γ . Let there be a spherical section with an opening angle θ_{jet} . In general, θ_{jet} can be greater than Γ^{-1} , but the observer can detect radiation coming only from the angular region with size $\simeq \Gamma^{-1}$. An external shock is formed when the expanding shell collides with the external medium. In general, there might be more than one shell, and the internal shock takes place when a faster shell reaches a slower one. In both cases one distinguishes an FS, when the shock propagates into the external shell or the external medium, and a reverse shock (RS), when it propagates into the inner shell.

Fenimore and Ramirez-Ruiz (2000) pointed out that the underlying cause of the $L_{\text{peak}} - V$ relation is unclear. In the context of the internal shock model, larger initial Γ factors tend to produce more efficient collisions. After changing some quantities such as the Γ factors, the ambient density, and/or the initial mass of the shells, the observed variability values are not recovered. Therefore, the central engine seems to play a relevant role in the explanation for the observed $L_{\text{peak}} - V$ correlation. In fact, this correlation was also explored within the context of a model in which the GRB variability is due to a change in the jet-opening angles and narrower jets have faster outflows (Salmonson and Galama 2002). As a result, this model predicts bright luminosities, small pulse lags and large variability as well as an early jet break time for on-axis observed bursts. On the other hand, dimmer luminosities, longer pulse lags, flatter bursts and later jet break times will cause larger viewing angles.

Guidorzi et al. (2006) gave an interpretation for the smaller value of the correlation in the context of the jet-emission scenario where a stronger dependence of the Γ of the expanding shells on the jet-opening angle is expected. However, Schaefer (2007) attributed the origin of the $L_{\text{peak}} - V$ relation to be based on relativistically shocked jets. Indeed, V and L_{peak} are both functions of Γ , where L_{peak} is proportional to a high power of Γ , as was already demonstrated in the context of the $L_{\text{peak}} - \tau_{\text{lag}}$ relation (see Sect. 3.1.2), and hence fast rise times and short pulse durations imply high variability.

3.3. The $L_{\text{iso}} - \tau_{\text{RT}}$ correlation and its physical interpretation

Schaefer (2002) predicted that τ_{RT} should be connected with L_{iso} in a following manner:

$$L_{\text{iso}} \propto \tau_{\text{RT}}^{-N/2}, \quad (23)$$

with the exponent $N \simeq 3$ (see also Schaefer 2002, 2007). Therefore, fast rises indicate high luminosities and slow rises low luminosities. The τ_{RT} can be directly connected to the physics of the shocked jet. Indeed, for a sudden collision of a material within a jet (with the shock creating an individual pulse in the GRB light curve), τ_{RT} will be determined as the maximum delay between the arrival time of photons from the center of the visible region versus their arrival time from its edge.

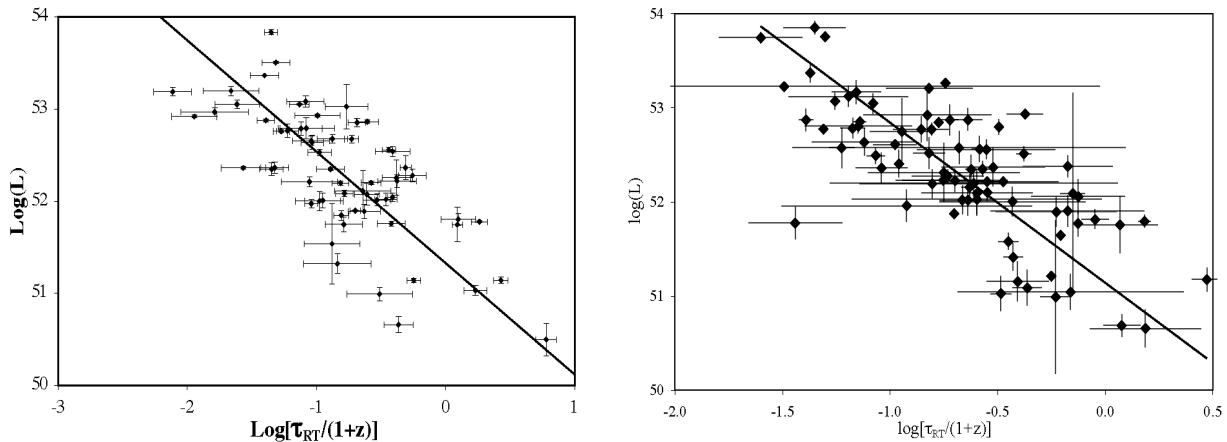


Fig. 4.— **Left panel:** the $\log L_{\text{iso}} - \log \tau_{\text{RT}}^*$ relation with the best fit line displayed. The errors are given by the 1σ confidence interval. (Figure after Schaefer (2007); see Fig. 5 therein. © AAS. Reproduced with permission.) **Right panel:** the $\log L_{\text{iso}} - \log \tau_{\text{RT}}^*$ correlation with the best fit line. (Figure after Xiao and Schaefer (2009); see Fig. 3 therein. © AAS. Reproduced with permission.)

The angular opening of the emitted jet, usually associated with Γ , could cause this delay leading to a relation $\tau_{\text{RT}} \propto \Gamma^{-2}$. The radius at which the material is shocked affects the proportionality constant, and the minimum radius under which the material cannot radiate efficiently anymore should be the same for each GRB (Panaitescu and Kumar 2002). In addition, a large scatter is expected because it will depend on how near this minimum radius the collisions are observed.

With both τ_{RT} and L_{iso} being functions of Γ , Schaefer (2007) confirmed that $\log L_{\text{iso}}$ should be $\sim -N/2 \log \tau_{\text{RT}}$. From 69 GRBs detected by BATSE and *Swift*, the following relation was obtained:

$$\log L_{\text{iso}} = 53.54 - 1.21 \log \tau_{\text{RT}}^*, \quad (24)$$

with L_{iso} in erg s^{-1} and τ_{RT}^* measured in seconds. The 1σ uncertainties in the intercept and slope are $\sigma_a = 0.06$ and $\sigma_b = 0.06$ (see the left panel of Fig. 4). The uncertainty in the log

of the burst luminosity is

$$\sigma_{\log L_{\text{iso}}}^2 = \sigma_a^2 + \left[\sigma_b \log \frac{\tau_{\text{RT}}^*}{0.1 \text{ s}} \right]^2 + \left(\frac{0.43b\sigma_{\text{RT}}}{\tau_{\text{RT}}} \right)^2 + \sigma_{\text{RT,sys}}^2, \quad (25)$$

where Schaefer (2007) takes into account the extra scatter, σ_{sys} . When $\sigma_{\text{RT,sys}} = 0.47$, the χ^2 of the best fit line is unity.

Xiao and Schaefer (2009) explained in details the procedure of how they calculated the τ_{RT} using 107 GRBs with known spectroscopic redshift observed by BATSE, *HETE*, *KONUS* and *Swift* (see the right panel of Fig. 4), taking into account also the Poissonian noise. Their analysis yielded

$$\log L_{\text{iso}} = 53.84 - 1.70 \log \tau_{\text{RT}}^*, \quad (26)$$

with the same units as in Eq. (24). As a consequence, the flattening of the light curve before computing the rise time is an important step. The problem is that the flattening should be done carefully, in fact if the light curve is flattened too much, a rise time comparable with the smoothing-time bin is obtained, while if it is flattened not enough, the Poissonian noise dominates the apparent fastest rise time, giving a too small rise time. Therefore, for some of the dimmest bursts, the Poissonian-noise dominant region and the smoothing-effect dominant region can coincide, thus not yielding τ_{RT} values for the weakest bursts. Finally, the physical interpretation of this correlation is given by Schaefer (2007). It is shown that the fastest rise in a light curve is related to the Lorentz factor Γ simply due to the geometrical rise time for a region subtending an angle of $1/\Gamma$, assuming that the minimum radius for which the optical depth of the jet material is of order of unity remains constant. The luminosity of the burst is also a power law of Γ , which scales as Γ^N for $3 < N < 5$. Therefore, the $\tau_{\text{RT}} - \Gamma$ and the $L_{\text{iso}} - \Gamma$ relations together yield the observed $L_{\text{iso}} - \tau_{\text{RT}}$ relation.

3.4. The $\Gamma_0 - E_{\text{prompt}}$ and $\Gamma_0 - L_{\text{iso}}$ correlations and their physical interpretation

Freedman and Waxman (2001) in their analysis of the GRB emission, considering a relativistic velocity for the fireball, showed that the radiation detected by an observer is within an opening angle $\simeq 1/\Gamma(t)$. Hence, the total fireball energy E should be interpreted as the energy that the fireball would have carried if this is assumed spherically symmetric. In particular, it was claimed that the afterglow flux measurements in X-rays gave a strong evaluation for the fireball energy per unit solid angle represented by $\epsilon_e = \xi_e E/4\pi$, within the observable opening angle $1/\Gamma(t)$, where ξ_e is the electron energy fraction. It was found that

$$\Gamma(t) = 10.6 \left(\frac{1+z}{2} \right)^{3/8} \left(\frac{E_{\text{prompt}}}{n_0} \right)^{1/8} t^{-3/8}, \quad (27)$$

where E_{prompt} is in units of 10^{53} erg, n_0 is the uniform ambient density of the expanding fireball in units of cm^{-3} , and t is the time of the fireball expansion in days. Finally, it was pointed out that ξ_e from the afterglow observations should be close to equipartition, namely $\xi_e \simeq \frac{1}{3}$. For example, for GRB970508 it was found that $\xi_e \simeq 0.2$ (Waxman 1997; Wijers and Galama 1999; Granot et al. 1999). A similar conclusion, i.e. that it is also close to equipartition, could be drawn for GRB971214, however Wijers and Galama (1999) proposed another interpretation for this GRB’s data, demanding $\xi_e \simeq 1$.

Liang et al. (2010) selected from the *Swift* catalogue 20 optical and 12 X-ray GRBs showing the onset of the afterglow shaped by the deceleration of the fireball due to the circumburst medium. The optically selected GRBs were used to fit a linear relation in the $\log \Gamma_0 - \log E_{\text{prompt}}$ plane, where Γ_0 is the initial Lorentz factor of the fireball and E_{prompt} is in units of 10^{52} erg (see left panel of Fig. 5). The best fit line of the $\Gamma_0 - E_{\text{prompt}}$ relation is given by

$$\log \Gamma_0 = (2.26 \pm 0.03) + (0.25 \pm 0.03) \log E_{\text{prompt}}, \quad (28)$$

with $\rho = 0.89$, $P < 10^{-4}$, and $\sigma = 0.11$ which can be measured with the deviation of the ratio $\Gamma_0/E_{\text{prompt}}^{0.25}$. It was found that most of the GRBs with a lower limit of Γ_0 are enclosed within the 2σ region represented by the dashed lines in the left panel of Fig. 5, and it was pointed out that GRBs with a tentative Γ_0 derived from RS peaks or the afterglow peaks, as well as those which lower limits of Γ_0 were derived from light curves with a single power law, are systematically above the best fit line. The lower values of Γ_0 , obtained from a set of optical afterglow light curves with a decaying trend since the start of the detection, were compatible with this correlation.

Later, this correlation was verified by Ghirlanda et al. (2011) and Lü et al. (2012a). Ghirlanda et al. (2011), studying the spectral evolution of 13 SGRBs detected by *Fermi*/GBM, investigated spectra resolved in the 8 keV – 35 MeV energy range and confirmed the results of Liang et al. (2010).

Lü et al. (2012a) enlarged this sample reaching a total of 51 GRBs with spectroscopically confirmed redshifts, and engaged three methods to constrain Γ_0 : (1) the afterglow onset method (Sari and Piran 1999) which considers T_{peak} of the early afterglow light curve as the deceleration time of the external FS; (2) the pair opacity constraint method (Lithwick and Sari 2001) which requires that the observed high energy γ -rays (i.e., those in the GeV range) are optically thin to electron-positron pair production, thus leading to a lower limit on Γ_0 of the emitting region; (3) the early external forward emission method (Zou and Piran 2010) where an upper limit of Γ_0 can be derived from the quiescent periods between the prompt emission pulses, in which the signal of external shock has to go down the instrument thresholds. Considering some aspects of the external shock emission, the $\Gamma_0 - E_{\text{prompt}}$ correlation was

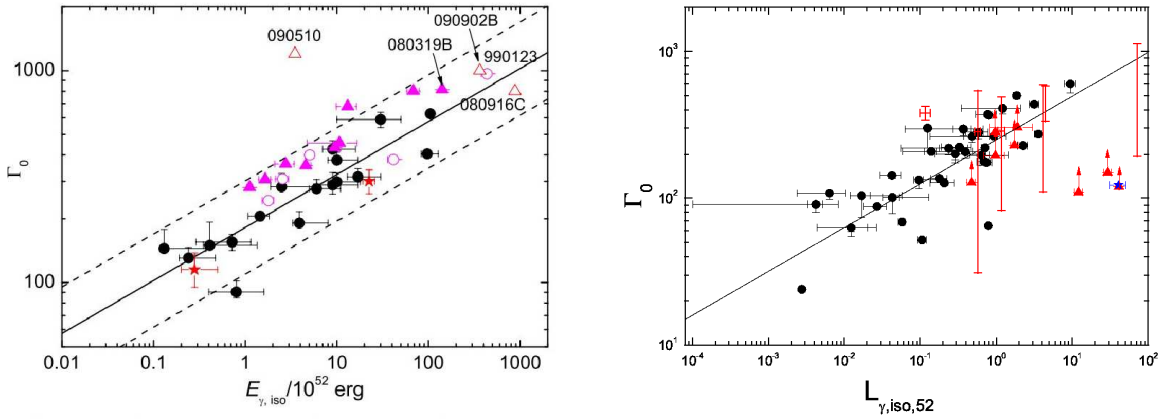


Fig. 5.— **Left panel:** $\log \Gamma_0 - \log E_{\text{prompt}}$ relation with the addition of GRBs with an onset trend in the X-ray band (GRBs 070208 and 080319C; red stars), Γ_0 computed by RS peaks or probable afterglow peaks (pink open circles), lower values of Γ_0 obtained from single power law decay light curves (pink solid triangles), and strong lower values of Γ_0 for *Fermi*/LAT GRBs 080916C, 090902B, and 090510 (red open triangles) calculated from opacity limits with *Fermi*/LAT observations. The solid line indicates the best fit of the $\Gamma_0 - E_{\text{prompt}}$ relation, $\log \Gamma_0 = 2.26 + 0.25 \log E_{\text{prompt}}$. The two dashed lines represent the 2σ deviation, where the standard deviation of the ratio $\Gamma_0/E_{\text{prompt}}^{0.25}$ for the data sample is $\sigma = 0.11$. (Figure after Liang et al. (2010); see Fig. 8 therein. © AAS. Reproduced with permission.) **Right panel:** $\log \Gamma_0$ vs. $\log L_{\text{iso}}$ distribution. The best fit line is given by $\log \Gamma_0 \simeq 2.40 + 0.30 \log L_{\text{iso}}$ with $r = 0.79$. The triangles represent the bursts with only lower values and the star indicates the only short burst in the sample, GRB090510. (Figure after Lü et al. (2012a); see Fig. 2 therein. © AAS. Reproduced with permission.)

statistically re-analysed using 38 GRBs with Γ_0 calculated using method (1) (as the other two provide only a range of the Lorentz factors, not a definite value), finding

$$\log \Gamma_0 = (1.96 \pm 0.002) + (0.29 \pm 0.002) \log E_{\text{prompt}}, \quad (29)$$

with $r = 0.67$, and E_{prompt} in units of 10^{52} erg. In addition, applying the beaming correction, a relation between Γ_0 and L_{iso} , using the same sample (see right panel of Fig. 5), was found to be

$$\log \Gamma_0 = (2.40 \pm 0.002) + (0.30 \pm 0.002) \log L_{\text{iso}}, \quad (30)$$

with $r = 0.79$, and L_{iso} in units of $10^{52} \text{ erg s}^{-1}$.

Regarding the physical interpretation, Liang et al. (2010) claimed that this correlation clearly shows the association of E_{prompt} with Γ_0 angular structure, and this result yielded another evidence for the fireball deceleration model. Instead, Lü et al. (2012a) found that this relation is well explained by a neutrino-annihilation-powered jet during the emission, indicating a high accretion rate and not very fast BH spin. Besides, evidence for a jet dominated by a magnetic field have already been presented (Zhang and Pe'er 2009; Fan 2010; Zhang and Yan 2011). From the studies of the BH central engine models it was also indicated that magnetic fields are a fundamental feature (Lei et al. 2009). Nevertheless, the baryon loading mechanism in a strongly magnetized jet is more complex, and it has still to be fully investigated.

3.5. Correlations between the energetics and the peak energy

3.5.1. The $\langle E_{\text{peak}} \rangle - F_{\text{peak}}$ and the $E_{\text{peak}} - S_{\text{tot}}$ correlations

Mallozzi et al. (1995) analysed 399 GRBs observed by BATSE and discovered a correlation between the logarithmic average peak energies $\langle E_{\text{peak}} \rangle$ and F_{peak} . Choosing as a selection criterion for the bursts $F_{\text{peak}} \geq 1 \text{ ph cm}^{-2} \text{ s}^{-1}$, they derived F_{peak} from the count rate data in 256 ms time bins in the energy band 50–300 keV and used the E_{peak} distribution derived from the Comptonized photon model (the differential photon number flux per unit energy):

$$\frac{dN}{dE} = A e^{-E(2+\beta_S)/E_{\text{peak}}} \left(\frac{E}{E_{\text{piv}}} \right)^{\beta_S}, \quad (31)$$

with A the normalization, β_S the spectral index, and $E_{\text{piv}} = 100 \text{ keV}$. Then, they grouped the sample into 5 different width F_{peak} bins of about 80 events each (see Fig. 6). The bursts were ranked such that group 1 had the lowest peak flux values and group 5 had the highest

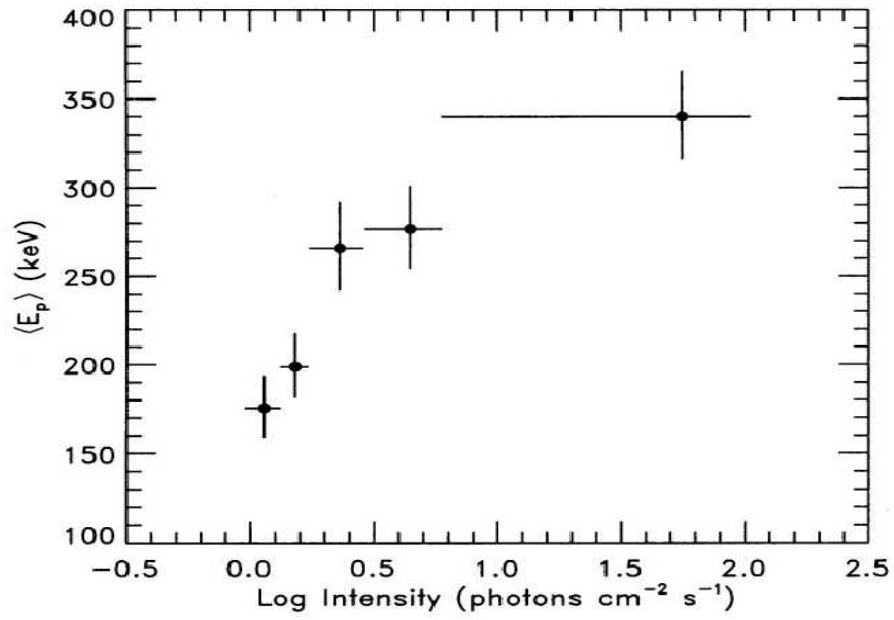


Fig. 6.— The average νF_ν peak energies as a function of intensity for five groups of GRB spectra. The vertical bars represent a 1σ estimated error in the mean, where the peak energy distributions were assumed to be approximately Gaussian in logarithm of energy. The horizontal bars mark the bin widths. (Figure after Mallozzi et al. (1995); see Fig. 2 therein. © AAS. Reproduced with permission.)

values. They found a correlation with $\rho = 0.90$ and $P = 0.04$. Lower intensity GRBs exhibited a lower $\langle E_{\text{peak}} \rangle$.

Later, Lloyd et al. (2000a) examined the $E_{\text{peak}} - S_{\text{tot}}$ correlation with 1000 simulated bursts in the same energy range as Mallozzi et al. (1995), and found a strong correlation between E_{peak} and S_{tot} (see the left panel of Fig. 7). The relation between the two variables was as follows:

$$\log E_{\text{peak}} \sim 0.29 \log S_{\text{tot}}, \quad (32)$$

with the Kendall correlation coefficient (Kendall 1938) $\tau = 0.80$ and $P = 10^{-13}$. In addition, they compared it to the $E_{\text{peak}} - F_{\text{peak}}$ relation (see right panel of Fig. 7). This relation was for the whole spectral sample, and consistent with earlier results (Mallozzi et al. 1995, 1998). However, they selected a subsample composed of only the most luminous GRBs, because spectral parameters obtained from bursts near the detector threshold are not robust. Therefore, to better understand the selection effects relevant to E_{peak} and burst strength, they considered the following selection criteria: $F_{\text{peak}} \geq 3 \text{ ph cm}^{-2} \text{ s}^{-1}$, $S_{\text{obs}} \geq 10^{-6} \text{ erg cm}^{-2}$, and $S_{\text{tot}} \geq 5 \times 10^{-6} \text{ erg cm}^{-2}$. Due to the sensitivity over a certain energy band of all the detectors, especially BATSE, and to some restrictions to the trigger, the selection effects are inevitable. However, the subsample of the most luminous GRBs presents a weak $E_{\text{peak}} - F_{\text{peak}}$ correlation. Instead, a tight $E_{\text{peak}} - S_{\text{tot}}$ correlation was found for the whole sample as well as the subsample of the brightest GRBs. Lloyd et al. (2000a) paid more attention to the $E_{\text{peak}} - S_{\text{tot}}$ correlation for the brightest GRBs because it is easier to deal with the truncation effects in this case, and the cosmological interpretation is simpler.

This correlation has been the basis for the investigation of the Amati relation (see Sect. 3.5.2), and the Ghirlanda relation (see Sect. 3.5.3). Lloyd et al. (2000a) concluded that “the observed correlation can be explained by cosmological expansion alone if the total radiated energy (in the γ -ray range) is constant”. In fact, their finding does not depend on the GRB rate density or on the distribution of other parameters. However, the data from GRBs with known redshift are incompatible with a narrow distribution of radiated energy or luminosity.

Following a different approach, Goldstein et al. (2010) pointed out that the ratio $E_{\text{peak}}/S_{\text{tot}}$ can serve as an indicator of the ratio of the energy at which most of the γ -rays are radiated to the total energy, and claimed that the $E_{\text{peak}} - S_{\text{tot}}$ relation is a significant tool for classifying LGRBs and SGRBs. The fluence indicates the duration of the burst without providing a biased value of T_{90} , and $E_{\text{peak}}/S_{\text{tot}}$ displays, as a spectral hardness ratio, an increased hardness for SGRBs in respect to LGRBs, in agreement with (Kouveliotou et al. 1993). This correlation is quite interesting, since the energy ratio, being dependent only on the square of the luminosity distance, gets rid of the cosmological dependence for the

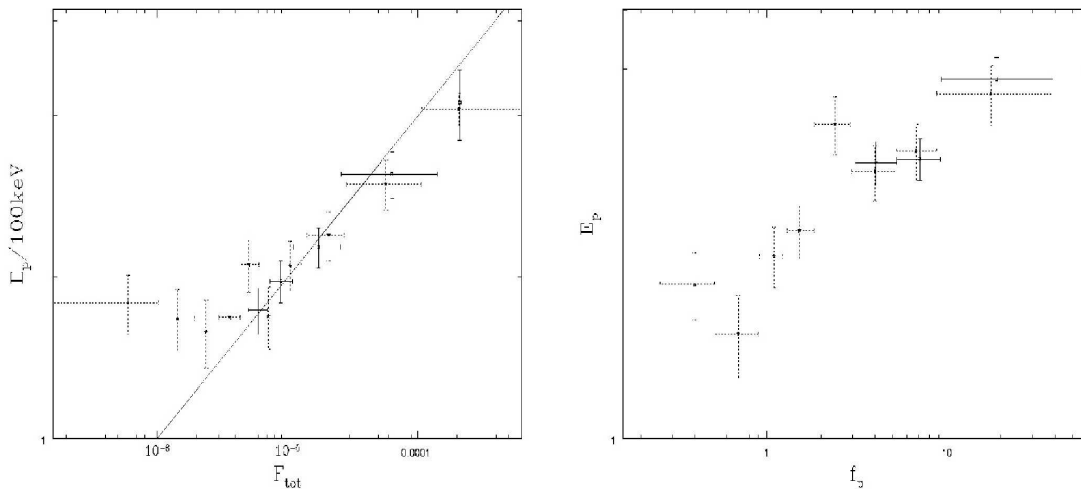


Fig. 7.— E_{peak} vs. (**left panel**) S_{tot} and (**right panel**) F_{peak} distributions for the complete (dashed elements) and sub (solid elements) spectral sample. The flux suggests a tight correlation at low values, but not for the most luminous GRBs. The solid line represents a least squares fit compatible with the correlation computed by statistical methods. (Figures after Lloyd et al. (2000a); see Fig. 3 therein. © AAS. Reproduced with permission.)

considered quantities. Therefore, it was evaluated that the energy ratio could be used as a GRB classifier.

Later, Lu et al. (2012) with the results of time-resolved spectral analysis, computed the $E_{\text{peak}} - S_{\text{tot}}$ relation for 51 LGRBs and 11 bright SGRBs observed with *Fermi*/GBM. For each GRB, they fitted a simple power law function. They measured its scatter with the distance of the data points from the best fit line. The measured scatter of the $E_{\text{peak}} - S_{\text{tot}}$ relation is 0.17 ± 0.08 . This result was reported for the first time by Golenetskii et al. (1983), and later confirmed by Borgonovo and Ryde (2001); Ghirlanda et al. (2010); Guiriec et al. (2010); Ghirlanda et al. (2011).

3.5.2. The $E_{\text{peak}} - E_{\text{iso}}$ correlation

Evidence for a correlation between E_{peak} and S_{tot} was first found by Lloyd and Petrosian (1999) and Lloyd et al. (2000b) based on 46 BATSE events, but this relation was in the observer frame due to the paucity of the data with precise redshift measurement, as was shown in previous paragraphs. Evidence for a stronger correlation between E_{peak} and E_{iso} , also called the Amati relation, was reported by Amati et al. (2002) based on a limited sample of 12 GRBs with known redshifts (9 with firm redshift and 3 with plausible values) detected

by *BeppoSAX*. They found that

$$\log E_{\text{peak}} \sim (0.52 \pm 0.06) \log E_{\text{iso}}, \quad (33)$$

with $r = 0.949$, $P = 0.005$, and E_{iso} calculated as

$$E_{\text{iso}} = 4\pi D_L(z, \Omega_M, \Omega_\Lambda)^2 S_{\text{tot}}(1+z)^{-2}. \quad (34)$$

Regarding the methodology considered, instead of fitting the observed spectra, as done for example by Bloom et al. (2001), the GRB spectra were blue-shifted to the rest frames to obtain their intrinsic form. Then, the total emitted energy is calculated by integrating the Band et al. (1993) spectral model in $1 - 10^4$ keV energy band and scaling for the luminosity distance. This was computed employing a flat Friedman-Lemaître-Robertson-Walker cosmological model with $H_0 = 65 \text{ km s}^{-1} \text{ Mpc}^{-1}$, $\Omega_M = 0.3$, $\Omega_\Lambda = 0.7$, and taking into account both the cosmological time dilation and spectral redshift.

Amati et al. (2003) enlarged the set of Amati et al. (2002) by including 20 GRBs from *BeppoSAX* with known redshift for which new spectral data (*BeppoSAX* events) or published best-fitting spectral parameters (BATSE and *HETE-2* events) were accessible. The relation was found to be

$$\log E_{\text{peak}} = (2.07 \pm 0.03) + (0.35 \pm 0.06) \log E_{\text{iso}}, \quad (35)$$

with $r = 0.92$, $P = 1.1 \times 10^{-8}$, E_{peak} in keV and E_{iso} in units of 10^{52} erg. Therefore, its statistical significance increased, providing a correlation coefficient comparable to that obtained by Amati et al. (2002), but based on a larger set.

Based on *HETE-2* measurements, Lamb et al. (2004) and Sakamoto et al. (2004) verified the previous results and considered also XRFs, finding out that the Amati relation remains valid over three orders of magnitude in E_{peak} and five orders of magnitude in E_{iso} . The increasing amount of GRBs with measured redshift allowed to verify this relation and strengthen its validity, as found by Ghirlanda et al. (2004b) with 29 events ($r = 0.803$ and $P = 7.6 \times 10^{-7}$; see left panel in Fig. 9).

Ghirlanda et al. (2005a) verified the $E_{\text{peak}} - E_{\text{iso}}$ correlation among LGRBs considering a set of 442 BATSE GRBs with measured E_{peak} and with pseudo-redshifts computed via the $L_{\text{peak}} - \tau_{\text{lag}}$ correlation. It was shown that the scatter of the sample around the best fitting line is comparable with that of another set composed of 27 GRBs with measured spectroscopic redshifts. This is because the weights of the outliers were marginal. It was noted that the relation for the 442 BATSE GRBs has a slope slightly smaller (0.47) than the one obtained for the 27 GRBs with measured spectroscopic redshifts (0.56).

Afterwards, Amati (2006) (see the upper left and bottom left panels in Fig. 8) updated the study of the $E_{\text{peak}} - E_{\text{iso}}$ correlation considering a sample of 41 LGRBs/XRFs

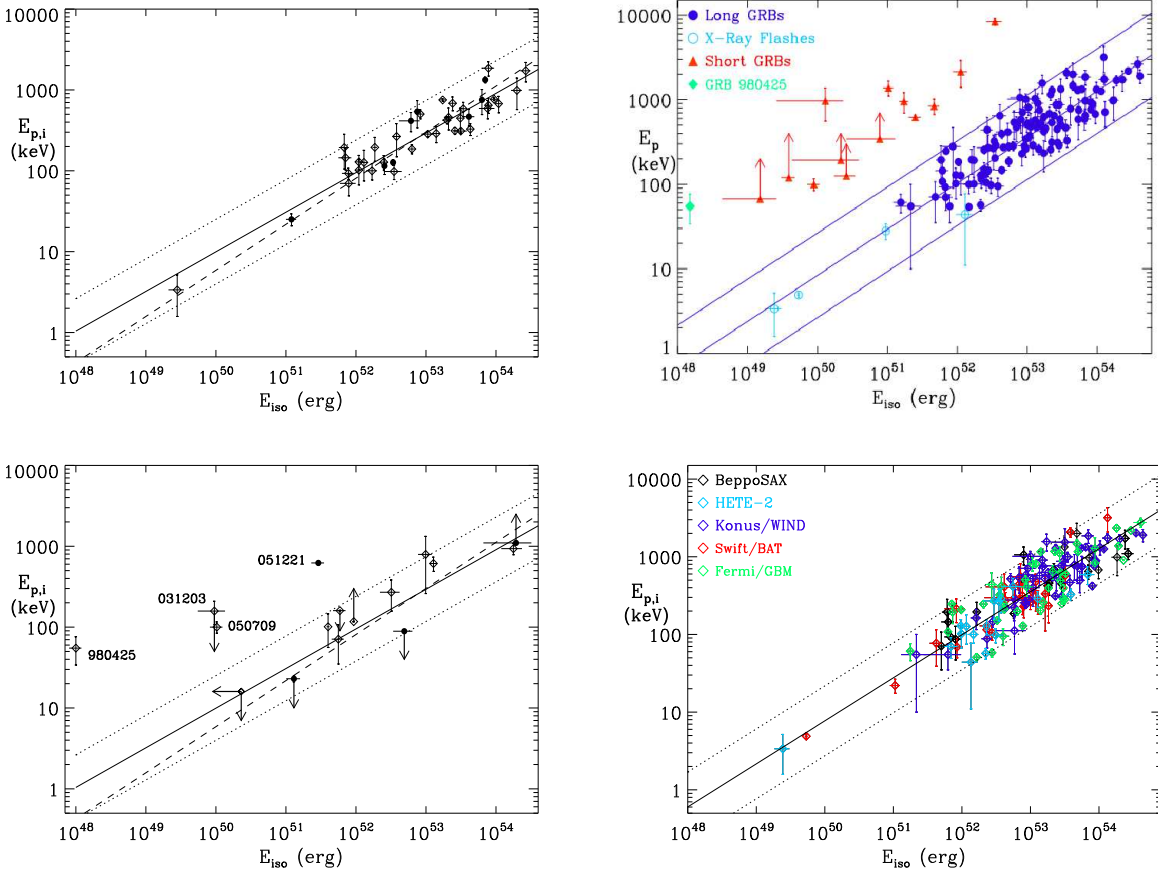


Fig. 8.— **Upper left panel:** $E_{\text{peak}} - E_{\text{iso}}$ distribution for 41 GRBs/XRFs with measured redshifts and E_{peak} values. Filled circles indicate Swift GRBs. The solid line represents the best fit line $\log E_{\text{peak}} = 1.98 + 0.49 \log E_{\text{iso}}$; the dotted lines show the region within a vertical logarithmic deviation of 0.4. The dashed line represents the best fit line $\log E_{\text{peak}} = 1.89 + 0.57 \log E_{\text{iso}}$ computed without taking into account the sample variance. (Figure after Amati (2006); see Fig. 2 therein.) **Upper right panel:** the distribution of the sample in the $E_{\text{peak}} - E_{\text{iso}}$ plane. The lines indicate the best fit line and the $\pm 2\sigma$ confidence region for LGRBs and XRFs. (Figure after Amati (2012); see Fig. 4 therein. Copyright © 2012 World Scientific Publishing Company.) **Bottom left panel:** $E_{\text{peak}} - E_{\text{iso}}$ distribution of 12 GRBs with uncertain values of z and/or E_{peak} , for the sub-energetic event GRB980425 and for the two SGRBs 050709 and 051221. Filled circles represent *Swift* GRBs. The solid line is the best fit line $\log E_{\text{peak}} = 1.98 + 0.49 \log E_{\text{iso}}$; the dotted lines mark the region within a vertical deviation in logarithmic scale of 0.4. The dashed line is the best fit line $\log E_{\text{peak}} = 1.89 + 0.57 \log E_{\text{iso}}$ computed without taking into account the sample variance. (Figure after Amati (2006); see Fig. 3 therein.) **Bottom right panel:** the $E_{\text{peak}} - E_{\text{iso}}$ distribution for the LGRBs. The black line represents the best fit line and, for each point, the color indicates the instrument which performed the spectral measurement. (Figure after Amati and Della Valle (2013); see Fig. 4 therein. Copyright © 2013 World Scientific Publishing Company.)

with firm values of z and E_{peak} , 12 GRBs with uncertain z and/or E_{peak} , 2 SGRBs with certain values of z and E_{peak} , and the sub-energetic events GRB980425/SN1998bw and GRB031203/SN2003lw. The different sets are displayed in the upper right panel in Fig. 8. Taking into account also the sample variance it was found:

$$\log E_{\text{peak}} = 1.98_{-0.04}^{+0.05} + (0.49_{-0.05}^{+0.06}) \log E_{\text{iso}}, \quad (36)$$

with $\rho = 0.89$, $P = 7 \times 10^{-15}$, and units the same as in Eq. (35). Moreover, sub-energetic GRBs (980425 and possibly 031203) and SGRBs were incompatible with the $E_{\text{peak}} - E_{\text{iso}}$ relation, suggesting that it can be an important tool for distinguishing different classes of GRBs. Indeed, the increasing number of GRBs with measured z and E_{peak} can provide the most reliable evidence for the existence of two or more subclasses of outliers for the $E_{\text{peak}} - E_{\text{iso}}$ relation. Moreover, the relation is valid also for the particular sub-energetic event GRB060218. Finally, the normalization considered by Amati (2006) is consistent with those obtained by other instruments.

Ghirlanda et al. (2008) confirmed the $E_{\text{peak}} - E_{\text{iso}}$ correlation for softer events (XRFs). The sample consisted of 76 GRBs observed by several satellites, mainly *HETE-2*, *KONUS/Wind*, *Swift* and *Fermi/GBM*. The most important outcome is a tight correlation with no new outliers (with respect to the classical GRB980425 and GRB031203) in the $E_{\text{peak}} - E_{\text{iso}}$ plane. The obtained relation was

$$\log E_{\text{peak}} \sim (0.54 \pm 0.01) \log E_{\text{iso}}. \quad (37)$$

Amati et al. (2009) studied 95 *Fermi* GRBs with measured z and obtained an updated $E_{\text{peak}} - E_{\text{iso}}$ relation, which read

$$\log E_{\text{peak}} \sim 0.57 \log E_{\text{iso}}, \quad (38)$$

with $\rho = 0.88$ and $P < 10^{-3}$. In particular, they investigated two GRBs (080916C and 090323) with very energetic prompt emission, and found that they follow the $E_{\text{peak}} - E_{\text{iso}}$ relation well. On the other hand, an SGRB, 090510, also a very luminous and energetic event, was found not to obey the relation. Hence, Amati et al. (2009) proposed that the correlation might serve as a discriminating factor among high-energetic GRBs. In addition, they claimed that the physics of the radiation process for really luminous and energetic GRBs is identical to that for average-luminous and soft-dim long events (XRFs), because all these groups follow the Amati relation.

Later, Amati (2012) provided an update of the analysis by Amati et al. (2008) with a larger sample of 120 GRBs (see the upper right panel of Fig. 8) finding it to be consistent with the following relation:

$$\log E_{\text{peak}} = 2 + 0.5 \log E_{\text{iso}}. \quad (39)$$

with units the same as in Eqs. (35) and (36). Afterwards, Qin and Chen (2013) analysed a sample of 153 GRBs with measured z , E_{peak} , E_{iso} and T_{90} , observed by various instruments up to 2012 May. The distribution of the logarithmic deviation of E_{peak} from the Amati relation displayed a clear bimodality which was well represented by a mixture of two Gaussian distributions. Moreover, it was suggested to use the logarithmic deviation of the E_{peak} value for distinguishing GRBs in the E_{peak} versus E_{iso} plane. This procedure separated GRBs into two classes: the Amati type bursts, which follow the Amati relation, and the non-Amati type bursts, which do not follow it. For the Amati type bursts it was found that

$$\log E_{\text{peak}} = (2.06 \pm 0.16) + (0.51 \pm 0.12) \log E_{\text{iso}} \quad (40)$$

with $r = 0.83$ and $P < 10^{-36}$, while for non-Amati bursts:

$$\log E_{\text{peak}} = (3.16 \pm 0.65) + (0.39 \pm 0.33) \log E_{\text{iso}} \quad (41)$$

with $r = 0.91$ and $P < 10^{-7}$. In both relations E_{peak} is in keV, and E_{iso} is in units of 10^{52} erg.

In addition, it was pointed out that almost all Amati type bursts are LGRBs at higher energies, as opposed to non-Amati type bursts which are mostly SGRBs. An improvement to this classification procedure is that the two types of GRBs are clearly separated, hence different GRBs can be easily classified.

Heussaff et al. (2013), applying particular selection criteria for the duration and the spectral indices, obtained a set of *Fermi* GRBs and analysed their locations in the $E_{\text{peak}} - E_{\text{iso}}$ plane. The sample, composed of 43 GRBs with known redshifts, yielded the following relation:

$$\log E_{\text{peak}} = 2.07 + 0.49 \log E_{\text{iso}}, \quad (42)$$

with $\rho = 0.70$, $P = 1.7 \times 10^{-7}$, and the same units as in previous relations of this type.

Amati and Della Valle (2013) pointed out that an enlarged sample of 156 LGRBs with known z and E_{peak} also follows the Amati relation with a slope $\simeq 0.5$ (see the bottom right panel of Fig. 8). Additionally, Basak and Rao (2012) showed that a time-resolved Amati relation also holds within each single GRB with normalization and slope consistent with those obtained with time-averaged spectra and energetics/luminosity, and is even better than the time-integrated relation (Basak and Rao 2013). Time-resolved E_{peak} and E_{iso} are obtained at different times during the prompt phase (see also Ghirlanda et al. 2010; Lu et al. 2012; Frontera et al. 2012 and Sect. 3.6).

3.5.3. The $E_{\text{peak}} - E_{\gamma}$ correlation

The $E_{\text{peak}} - E_{\gamma}$ relation (also called the Ghirlanda relation) was first discovered by Ghirlanda et al. (2004b), who used 40 GRBs with z and E_{peak} known at their time of writing. Considering the time T_{break} , its value can be used to deduce E_{γ} from E_{iso} . Indeed, even if only a little less than half of the bursts have observed jet breaks (47%), from (Sari et al. 1999) we know that

$$\theta_{\text{jet}} = 0.161 \left(\frac{T_{\text{break}}}{1+z} \right)^{3/8} (n\eta_{\gamma}E_{\text{iso}})^{1/8}, \quad (43)$$

where T_{break} is measured in days, n is the density of the circumburst medium in particles per cm^3 , η_{γ} is the radiative efficiency, and E_{iso} is in units of 10^{52} erg. Here, θ_{jet} is in degrees and it is the angular radius (the half opening angle) subtended by the jet. For GRBs with no measured n , the median value $n = 3 \text{ cm}^{-3}$ of the distribution of the computed densities, extending between 1 and 10 cm^{-3} , was considered (Frail et al. 2000; Yost et al. 2002; Panaitescu and Kumar 2002; Schaefer 2003a).

Later, Liang and Zhang (2005) using a sample of 15 GRBs with measured z , E_{peak} and T_{break} , considered a purely phenomenological T_{break}^* of the optical afterglow light curves, thus avoiding the assumption of any theoretical model, contrary to what was done by Ghirlanda et al. (2004b). The functional form of this correlation is given by:

$$\log E_{\gamma} = (0.85 \pm 0.21) + (1.94 \pm 0.17) \log E_{\text{peak}}^* - (1.24 \pm 0.23) \log T_{\text{break}}^*, \quad (44)$$

where E_{γ} is in units of 10^{52} erg, E_{peak}^* in units of 100 keV, T_{break}^* is measured in days, and $\rho = 0.96$ and $P < 10^{-4}$.

Nava et al. (2006) found that the Ghirlanda relation, assuming a wind-like circumburst medium, is as strong as the one considering a homogeneous medium. They analysed the discrepancy between the correlations in the observed and in the comoving frame (with Lorentz factor identical to the fireball's one). Since both E_{peak} and E_{γ} transform in the same way, the wind-like Ghirlanda relation remains linear also in the comoving frame, no matter what the Lorentz factor's distribution is. The wind-like relation corresponds to bursts with the same number of photons emitted. Instead, for the homogeneous density medium scenario, it is common to consider a tight relation between the Lorentz factor and the total energy, thus limiting the emission models of the prompt radiation. Using 18 GRBs with firm z , E_{peak} and T_{break} , Nava et al. (2006) found for the homogeneous density case

$$\log \frac{E_{\text{peak}}^*}{100 \text{ keV}} = 0.45_{-0.03}^{+0.02} + (0.69 \pm 0.04) \log \frac{E_{\gamma}}{2.72 \times 10^{52} \text{ erg}}, \quad (45)$$

with $\rho = 0.93$ and $P = 2.3 \times 10^{-8}$. Instead, for the wind case

$$\log \frac{E_{\text{peak}}^*}{100 \text{ keV}} = 0.48_{-0.03}^{+0.02} + (1.03 \pm 0.06) \log \frac{E_\gamma}{2.2 \times 10^{50} \text{ erg}}, \quad (46)$$

with $\rho = 0.92$ and $P = 6.9 \times 10^{-8}$.

Ghirlanda et al. (2007) tested the $E_{\text{peak}} - E_\gamma$ correlation using 33 GRBs (16 new bursts detected by *Swift* with firm z and E_{peak} up to December 2006, and 17 pre-*Swift* GRBs). They claimed that for computing the T_{break} it is required that:

1. the detection of the jet break should be in the optical,
2. the optical light curve should continue up to a time longer than the T_{break} ,
3. the host galaxy flux and the flux from a probable SN should be removed,
4. the break should not depend on the frequency in the optical, and a coincident break in the X-ray light curve is not necessary, because the flux in X-rays could be controlled by another feature,
5. the considered T_{break} should be different from the one at the end of the plateau emission (the time T_a in Willingale et al. 2007), otherwise the feature affecting the X-ray flux is also influencing the optical one.

Therefore, considering all these restrictions, the sample was reduced to 16 GRBs, all compatible with the following $E_{\text{peak}} - E_\gamma$ relation:

$$\log \frac{E_{\text{peak}}}{100 \text{ keV}} = (0.48 \pm 0.02) + (0.70 \pm 0.04) \log \frac{E_\gamma}{4.4 \times 10^{50} \text{ erg}}. \quad (47)$$

No outliers were detected. Therefore, the reduced scatter of the $E_{\text{peak}} - E_\gamma$ relation corroborates the use of GRBs as standardizable candles.

3.5.4. *Physical interpretation of the energetics vs. peak energy relations*

Lloyd et al. (2000a) investigated the physical explanation of the $E_{\text{peak}} - S_{\text{tot}}$ correlation assuming the emission process to be a synchrotron radiation from internal and external shocks. Indeed, they claimed that this correlation is easily obtained considering a thin synchrotron radiation by a power law distribution of electrons with Γ larger than some minimum threshold value, Γ_m . Moreover, the internal shock model illustrates the tight $E_{\text{peak}} - S_{\text{tot}}$ relation and the emitted energy better than the external shock model.

Lloyd-Ronning and Petrosian (2002) pointed out that the GRB particle acceleration is not a well analysed issue. Generally, the main hypothesis is that the emitted particles are accelerated via recurrent scatterings through the (internal) shocks. They found that the recurrent crossings of the shock come from a power law distribution of the particles with a precise index, providing a large energy synchrotron photon index. Moreover, the connection between E_{peak} and the photon flux can be justified by the variation of the magnetic field or electron energy in the emission events. Finally, they claimed that in the majority of GRBs, the acceleration of particles is not an isotropic mechanism, but occurs along the magnetic field lines.

Amati et al. (2002) confirmed the findings of Lloyd et al. (2000b) that the $\log E_{\text{peak}} \sim 0.5 \log E_{\text{iso}}$ relation is obtained assuming an optically thin synchrotron shock model. This model considers electrons following the $N(\Gamma) = N_0 \Gamma^{-p}$ distribution for $\Gamma > \Gamma_m$ with Γ_m , GRB duration, and N_0 constant in each GRB. However, the above assumptions are not fully justifiable. In fact the duration is different in each GRB and E_{iso} might be smaller in the case of beamed emission.

Amati (2006) pointed out the impact that the correlation has on the modeling of the prompt emission and on the possible unification of the two classes of GRBs and XRFs. In addition, this correlation is often applied for checking GRB synthesis models (e.g. Zhang and Mészáros 2002; Ghirlanda et al. 2013).

In every model, E_{peak} and E_{iso} depend on Γ , and the $E_{\text{peak}} - E_{\text{iso}}$ relation can help to relate the parameters of the synchrotron shock model and inverse Compton model (Zhang and Mészáros 2002; Schaefer 2003a). Specifically, Zhang and Mészáros (2002) and Rees and Mészáros (2005) found that, for an electron distribution given by a power law and produced by an internal shock in a fireball with velocity Γ , the peak energy is given as

$$\log E_{\text{peak}}^* \sim -2 \log \Gamma + 0.5 \log L - \log t_\nu, \quad (48)$$

where L is the total fireball luminosity and t_ν the variability timescale. However, to recover the $E_{\text{peak}} - E_{\text{iso}}$ relation from this relation, Γ and t_ν should be similar for each GRB, a condition that cannot be easily supported. A further issue arises when one considers that $L \propto \Gamma^N$, with N between 2 and 3 in different models (Zhang and Mészáros 2002; Schaefer 2003a; Ramirez-Ruiz 2005). An explanation could be that direct or Comptonized thermal radiation from the fireball photosphere (Zhang and Mészáros 2002; Ramirez-Ruiz 2005; Ryde 2005; Rees and Mészáros 2005; Beloborodov 2010; Guiriec et al. 2011; Hascoët et al. 2013; Guiriec et al. 2013; Vurm and Beloborodov 2015; Guiriec et al. 2015a,b) can affect significantly the GRB prompt emission. This can be a good interpretation of the really energetic spectra presented for many events (Frontera et al. 2000; Preece et al. 2000; Ghirlanda et al. 2003) and the flat shape in GRB average spectra. In such cases, E_{peak} depends on the peak

temperature $T_{bb,peak}$ of photons distributed as by a blackbody, and therefore it is associated to the luminosity or emitted energy. For Comptonized radiation from the photosphere the relations are

$$\log E_{peak} \sim \log \Gamma + \log T_{bb,peak} \sim 2 \log \Gamma - 0.25 \log L \quad (49)$$

or

$$\log E_{peak} \sim \log \Gamma + \log T_{bb,peak} \sim -0.5 \log r_0 + 0.25 \log L, \quad (50)$$

where r_0 is a particular distance between the central engine and the energy radiating area, such that the Lorentz factor evolves as $\Gamma \simeq r/r_0$ up to some saturation radius r_s (Rees and Mészáros 2005). As suggested by Rees and Mészáros (2005), in this scenario the $E_{peak} - E_{iso}$ relation could be recovered for particular physical cases just underneath the photosphere, though it would rely on an undefined number of unknown parameters.

Also for high-energetic GRBs (i.e., $E_{iso} \approx 10^{55}$ erg) the nonthermal synchrotron emission model can explain the $E_{peak} - E_{iso}$ correlation. This can be possible either considering the minimum Lorentz factor and the normalization of the power law distribution of the emitting electrons constant in each GRB, or by constraints on the slope of the relation between Γ and the luminosity (Lloyd et al. 2000b; Zhang and Mészáros 2002).

Panaitescu (2009) used 76 GRBs with measured redshifts to analyse the case in which the $E_{peak} - E_{iso}$ relation for LGRBs is due to the external shock generated by a relativistic outflow interacting with the ambient medium. He considered the effect of each parameter defining the $E_{peak} - E_{iso}$ relation on the radial distribution of the external medium density and pointed out that the $\log E_{peak} \sim 0.5 \log E_{iso}$ relation is recovered if the external medium is radially stratified. For some combinations of radiative (synchrotron or inverse-Compton) and dissipation (such as RS or FS) mechanisms, it is concluded that the external medium requires a particle density distributed distinctly from R^{-2} , with R the distance at which the GRB radiation is generated. This tendency should be commonly associated to uniform mass-loss rate and final velocity.

Mochkovitch and Nava (2015) checked whether the $E_{peak} - E_{iso}$ relation can be recovered in a case when the prompt emission is due to internal shocks, or alternatively if the correlation can give some limits for the internal shock scenario defined through the impact of only two shells. Simulated GRB samples were obtained considering different model parameter distributions, such as the emitted power in the relativistic emission and Γ . Simulated $E_{peak} - E_{iso}$ distributions were plotted for each case and analysed together with the observed relation (based on 58 GRBs). The sample contained only luminous *Swift* GRBs with $F_{peak} > 2.6 \text{ ph cm}^{-2} \text{ s}^{-1}$ in the 15 – 150 keV energy band. In conclusion, a correspondence between the model and data was found, but exclusively if the following restrictions for the dynamics of the emission and for the dispersion of the energy are assumed:

1. the majority of the dispersed energy should be radiated in few electrons;
2. the spread between the highest and the lowest Lorentz factor should be small;
3. if the mean Lorentz factor grows as $\bar{\Gamma} \propto \dot{E}^{1/2}$ (where \dot{E} is the rate of injected energy, or mean emitted power, in the relativistic outflow), the $E_{\text{peak}} - E_{\text{iso}}$ relation is not retrieved and E_{peak} is diminishing with larger E_{iso} . However, the $E_{\text{peak}} - E_{\text{iso}}$ relation can be regained if $\bar{\Gamma} \propto \dot{E}^{1/2}$ is a lower constraint for a particular \dot{E} ;
4. when the timescale or the width of the variability of the Lorentz factor is associated with $\bar{\Gamma}$, $E_{\text{peak}} - E_{\text{iso}}$ relation is recovered.

For the Ghirlanda relation (Ghirlanda et al. 2004b), with the assumption that the line of sight is within the jet angle, the $E_{\text{peak}} - E_{\gamma}$ relation indicates its invariance when moving from the rest frame to the comoving frame. As a result, the number of radiated photons in each GRBs is comparable and should be about 10^{57} . The last characteristic could be important for understanding the dynamics of GRBs and the radiative mechanisms (see also right panel of Fig. 9).

Collazzi et al. (2011) found that the mean E_{peak}^* is near to 511 keV, the electron rest-mass energy $m_e c^2$. Therefore, it is claimed that the tight shape of the E_{peak} distribution does not stem only from selection effects. No studied mechanism can drive this effect, however with the E_{peak}^* compatible with the effective temperature of the γ -ray radiating area, the almost constant temperature needs some mechanism similar to a thermostat, keeping the temperature at a steady value. It was suggested that such a mechanism could be an electron-positron annihilation.

Ghirlanda et al. (2013), using a simulated sample, analysed if different intrinsic distributions of Γ and θ_{jet} can replicate a grid of observational constraints. With the assumption that in the comoving frame each GRB has similar E_{peak} and E_{γ} , it was found that the distributions of Γ and θ_{jet} cannot be power laws. Instead, the highest concordance between simulation and data is given by log-normal distributions, and a connection between their maxima, like $\theta_{\text{jet,max}}^{2.5} \Gamma_{\text{max}} = \text{const}$. In this work θ_{jet} and Γ are important quantities for the calculation of the GRB energetics. Indeed, from a sample of ≈ 30 GRBs with known θ_{jet} or Γ it was found that the E_{γ} distribution is centered at $10^{50} - 10^{51}$ erg and it is tightly related to E_{peak} . It was obtained that

$$\log E_{\text{peak}} \sim \log \frac{E_{\gamma}}{5 - 2\beta_0}. \quad (51)$$

Present values of Γ and θ_{jet} rely on incomplete data sets and their distributions could be

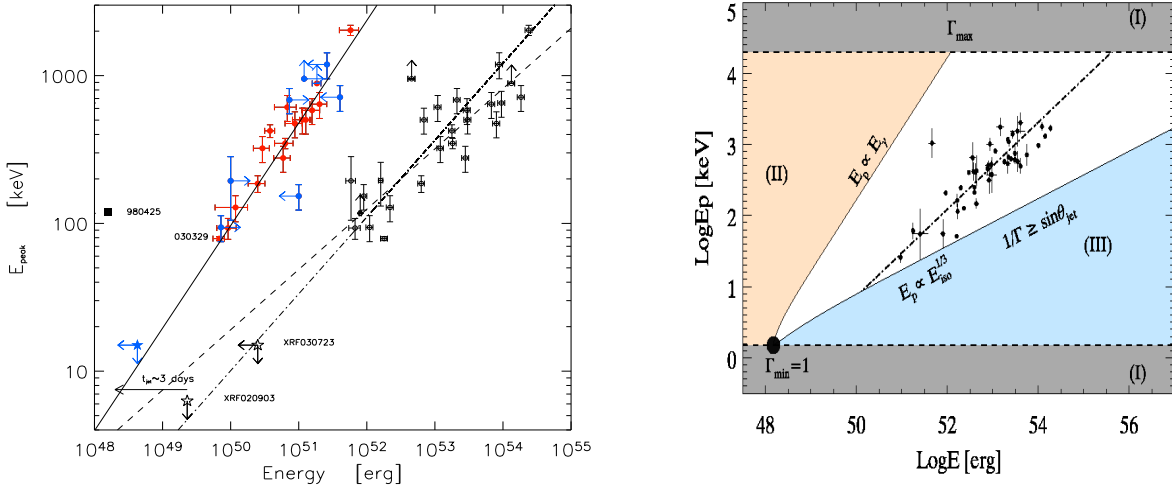


Fig. 9.— **Left panel:** $E_{\text{peak}}^* - E_{\gamma}$ relation for GRBs with known redshift. The filled circles represent E_{γ} for the events where a jet break was detected. Grey symbols indicate lower/upper limits. The solid line represents the best fit, i.e. $\log E_{\text{peak}} \sim 53.68 + 0.7 \log E_{\gamma}$. Open circles denote E_{iso} for the GRBs. The dashed line represents the best fit to these points and the dash-dotted line is the relation shown by Amati et al. (2002). (Figure after Ghirlanda et al. (2004b); see Fig. 1 therein. © AAS. Reproduced with permission.) **Right panel:** rest frame plane of GRB energy. The large black dot indicates that all simulated GRBs were assigned $E_{\text{peak}}^* = 1.5$ keV and $E_{\gamma}^* = 1.5 \times 10^{48}$ erg. Since $\Gamma > 1$ but less than 8000, regions (I) are forbidden. Since for all the simulated GRBs $\theta_{\text{jet}} \leq 90^\circ$, they cannot stay in region (II). When Γ is small, the beaming cone turns out to be larger than the jet. Therefore, the isotropic equivalent energy is given by $\log E_{\text{iso}} = \log E_{\gamma} + \log(1 + \beta_0) + 2 \log \Gamma$, lower than the energy computed by $\log E_{\text{iso}} = \log E_{\gamma} - \log(1 - \cos \theta_{\text{jet}})$. This brings in a constraint, $\log E_{\text{peak}} \sim 1/3 \times \log E_{\text{iso}}$, and GRBs cannot lie to the right of this constraint. Hence, region (III) is not allowed. The black dots indicate the actual GRBs of the *Swift* sample. The fit to the Swift sample is displayed as the dot-dashed line. (Figure after Ghirlanda et al. (2013); see Fig. 1 therein.)

affected by biases. Nevertheless, Ghirlanda et al. (2013) claimed that greater values of Γ are related to smaller θ_{jet} values, i.e. the faster a GRB, the narrower its jet.

Furthermore, GRBs fulfilling the condition $\sin \theta_{\text{jet}} < 1/\Gamma$ might not display any jet break in the afterglow light curve, and Ghirlanda et al. (2013) predicted that this group should comprise $\approx 6\%$ of the on-axis GRBs. Finally, their work is crucial as it allowed to find that the local rate of GRBs is $\approx 0.3\%$ of the local SNe Ib/c rate, and $\approx 4.3\%$ of the local hypernovae (i.e., SNe Ib/c with wide-lines) rate.

3.6. Correlations between the luminosity and the peak energy

3.6.1. The $L_{\text{iso}} - E_{\text{peak}}$ correlation

The $L_{\text{iso}} - E_{\text{peak}}$ relation was discovered by Schaefer (2003a) who used 84 GRBs with known E_{peak} from the BATSE catalogue (Schaefer et al. 2001), and 20 GRBs with luminosities based on optically measured redshift (Amati et al. 2002; Schaefer 2003b). It was found that (see Fig. 10) for the 20 GRBs

$$\log E_{\text{peak}} \sim (0.38 \pm 0.11) \log L_{\text{iso}}, \quad (52)$$

with $r = 0.90$ and $P = 3 \times 10^{-8}$, and among the 84 GRBs the relation was

$$\log E_{\text{peak}} \sim (0.36 \pm 0.03) \log L_{\text{iso}}. \quad (53)$$

The underlying idea is that the L_{iso} varies as a power of Γ , as we have already discussed in Sect. 3.1.2, and the E_{peak} also varies as some other power of Γ , so that E_{peak} and L_{iso} will be correlated to each other through their dependence on Γ . For the general case where the luminosity varies as Γ^N and E_{peak} varies as Γ^M , and therefore $\log E_{\text{peak}}$ will vary as $(M + 1)/N \times \log L_{\text{iso}}$.

Frontera et al. (2012), using a sample of 9 GRBs detected simultaneously with the Wide Field Camera (WFC) on board the *BeppoSAX* satellite, and by the BATSE instrument, reported the results of a systematic study of the broadband (2 – 2000 keV) time-resolved prompt emission spectra. However, only 4 of those GRBs (970111, 980329, 990123, 990510) were bright enough to allow a fine time-resolved spectral analysis, resulting in a total of 40 spectra. Finally, the study of the time-resolved dependence (see also the end of Sect. 3.5.2) of E_{peak} on the corresponding L_{iso} was possible for two bursts with known redshift (i.e., 990123 and 990510), and found using the least squares method (see Fig. 11):

$$\log E_{\text{peak}}^* \sim (0.66 \pm 0.03) \log L_{\text{iso}}, \quad (54)$$

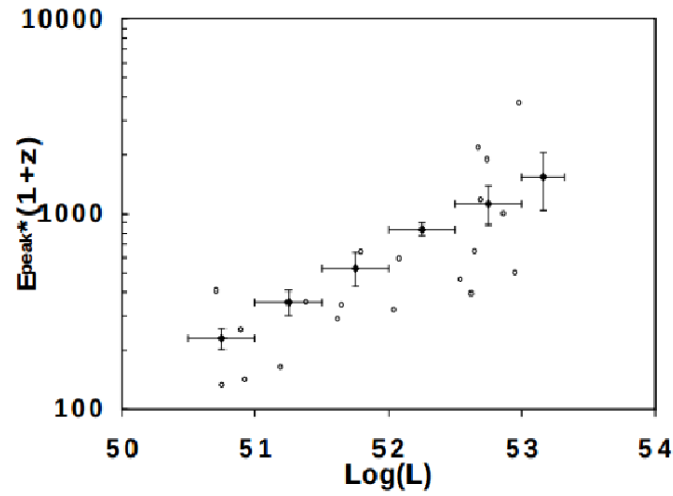


Fig. 10.— Direct fit of $\log L_{\text{iso}} - \log E_{\text{peak}}$ data. This is shown here for two independent data sets for which the luminosities are derived by two independent methods. The first data set consists of 20 bursts with spectroscopically measured redshifts (the open circles). The second one is for 84 bursts (whose binned values are shown as filled diamonds, and the horizontal bars are the bin widths) whose luminosity (and then redshift) were determined with the spectral lag and variability light curve parameters. Both data sets show a highly significant and similar power law relations. (Figure after Schaefer (2003a); see Fig. 3 therein. © AAS. Reproduced with permission.)

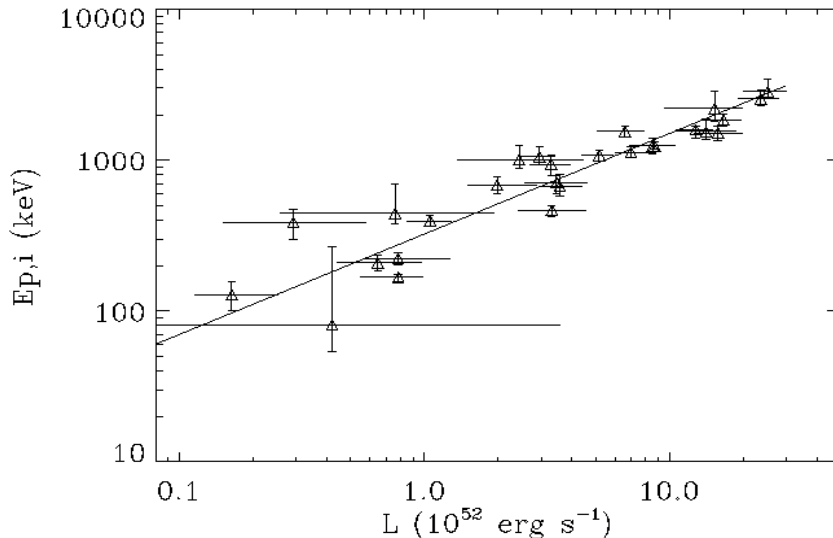


Fig. 11.— E_{peak}^* vs. L_{iso} , obtained from data for GRBs 990123 and 990510. The solid line is the best-fit power law. (Figure after Frontera et al. (2012); see Fig. 6 therein. © AAS. Reproduced with permission.)

with $\rho = 0.94$ and $P = 1.57 \times 10^{-13}$.

Afterwards, Nava et al. (2012), using a sample of 46 *Swift* GRBs with measured z and E_{peak} , found a strong $L_{\text{iso}} - E_{\text{peak}}$ correlation, with a functional form of

$$\log E_{\text{peak}}^* = -(25.33 \pm 3.26) + (0.53 \pm 0.06) \log L_{\text{iso}}, \quad (55)$$

with $\rho = 0.65$ and $P = 10^{-6}$; E_{peak} is in keV, and L_{iso} is in units of $10^{51} \text{ erg s}^{-1}$. Furthermore, using 12 GRBs with only an upper limit on z (3 events) or no redshift at all (3 events), or with a lower limit on E_{peak} (3 events) or no estimate at all (3 events), they found that these bursts also obey the obtained $L_{\text{iso}} - E_{\text{peak}}$ relation.

3.6.2. The $L_{\text{peak}} - E_{\text{peak}}$ correlation

It was also found that the Amati relation holds even if E_{iso} is substituted with L_{iso} and L_{peak} , which is not surprising given that these “energy indicators” are strongly correlated. To this end, the Yonetoku correlation (Yonetoku et al. 2004, see the left panel of Fig. 12), relates E_{peak} with L_{peak} . The relation was obtained employing 11 GRBs with known redshifts detected by BATSE, together with *BeppoSAX* GRBs from (Amati et al. 2002). This relation uses the L_{peak} of the burst instead of L_{iso} , and it is tighter than previous prompt correlations.

The best-fit line is given by

$$\log L_{\text{peak}} \sim (2.0 \pm 0.2) \log E_{\text{peak}}^*, \quad (56)$$

with $r = 0.958$, $P = 5.31 \times 10^{-9}$, and the uncertainties are 1σ error. This relation agrees well with the standard synchrotron model (Zhang and Mészáros 2002; Lloyd et al. 2000b). Finally, it has been used to estimate pseudo-redshifts of 689 BATSE LGRBs with unknown distances and to derive their formation rate as a function of z .

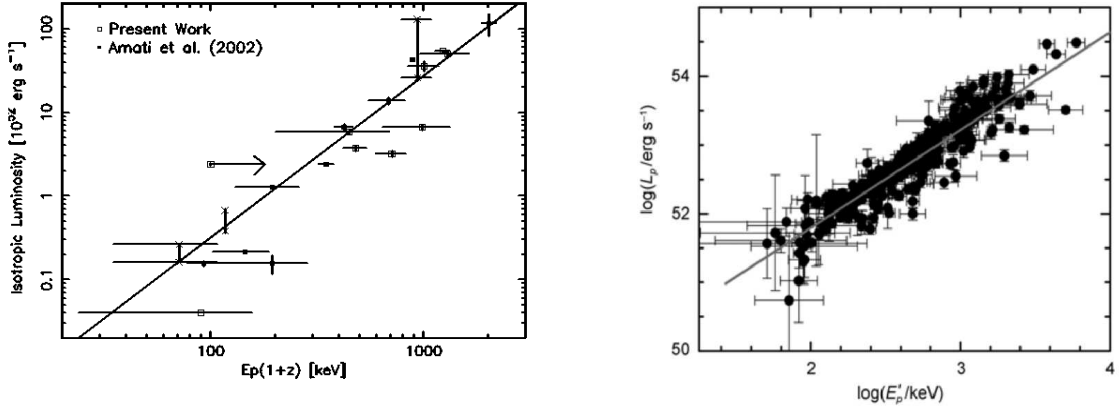


Fig. 12.— **Left panel:** the $\log L_{\text{peak}} - \log E_{\text{peak}}$ relation. The open squares mark the BATSE data. *BeppoSAX* events, which are converted into the energy range of 30 – 10000 keV, are shown as filled squares and the cross points. The solid line indicates the best-fit line. (Figure after Yonetoku et al. (2004); see Fig. 1 therein. © AAS. Reproduced with permission.) **Right panel:** $\log L_{\text{peak}}$ vs. $\log E_{\text{peak}}$ for 276 time-resolved spectra within the decay pulses for the sample. The solid line stands for the best fit to the data. (Figure after Lu and Liang (2010); see Fig. 4 therein. Copyright © 2010 Springer.)

Ghirlanda et al. (2004a) selected 36 bright SGRBs detected by BATSE, with an F_{peak} on the 64 ms timescale in the 50 – 300 keV energy range exceeding $10 \text{ ph cm}^{-2} \text{ s}^{-1}$. In 7 cases, the signal-to-noise-ratio was too low to reliably constrain the spectral best-fit parameters. One case yielded missing data. Hence, the sample consisted of 28 events. Due to unknown redshifts, E_{peak}^* , E_{iso} and L_{peak} were expressed as functions of the redshift in the range $z \in [0.001, 10]$. It was found that SGRBs are unlikely to obey the Amati relation, $E_{\text{iso}} - E_{\text{peak}}^*$, but the results were consistent with the $L_{\text{peak}} - E_{\text{peak}}^*$ relation of Yonetoku et al. (2004). Hence, assuming that this relation indeed holds for SGRBs, their pseudo-redshifts were estimated and found to have a similar distribution as LGRBs, with a slightly smaller average redshift.

Afterwards, Yonetoku et al. (2010) investigated the prompt emission of 101 GRBs with measured redshifts and a reported F_{peak} detected until the end of 2009. The sample comes

from events detected in a number of independent missions: the satellites used for this purpose are *KONUS*, *Swift*, *HXD-WAM* and *RHESSI*. Using this data set, the $E_{\text{peak}} - L_{\text{peak}}$ correlation was revised, and its functional form could be written as

$$\log L_{\text{peak}} = (52.43 \pm 0.037) + (1.60 \pm 0.082) \log E_{\text{peak}}^*, \quad (57)$$

with $r = 0.889$ for 99 degrees of freedom and an associated $P = 2.18 \times 10^{-35}$; L_{peak} is expressed in ergs^{-1} , and E_{peak}^* in units of 355 keV. To provide reference to previous works, the $1 - 10^4$ keV energy band in the GRB rest frame was used to calculate the bolometric energy and L_{peak} . Finally, it was demonstrated that this relation is intrinsic to GRBs and affected by the truncation effects imposed by the detector threshold.

Lu and Liang (2010), using time-resolved spectral data for a sample of 30 pulses in 27 bright GRBs detected by BATSE, investigated the $L_{\text{peak}} - E_{\text{peak}}$ relation in the decay phases of these pulses (see right panel of Fig. 12). Quite all of the pulses followed a narrow $L_{\text{peak}} - E_{\text{peak}}$ relation given by

$$\log L_{\text{peak}} \sim (1.42 \pm 0.03) \log E_{\text{peak}}^*, \quad (58)$$

with $r = 0.91$ and $P < 10^{-4}$, but the power law index varied. The statistical or observational effects could not account for the large scatter of the power law index, and it was suggested to be an intrinsic feature, indicating that no relation common for all GRB pulses $L_{\text{peak}} - E_{\text{peak}}$ would be expected. However, in the light of *Fermi* observations that revealed deviations from the Band function (Abdo et al. 2009; Guiriec et al. 2010; Ackermann et al. 2010, 2011, 2013; see also Lin et al. 2016), it was proposed recently that the GRB spectra should be modelled not with the Band function itself (constituting a non-thermal component), but with additional black-body (BB, thermal) and power law (PL, non-thermal) components (Guiriec et al. 2013, 2015a,b, 2016). The non-thermal component was well described within the context of synchrotron radiation from particles in the jet, while the thermal component was interpreted by the emission from the jet photosphere. The PL component was claimed to originate most likely from the inverse Compton process. The results point toward a universal relation between L_{peak} and E_{peak}^* related to the non-thermal components.

Tsutsui et al. (2013) analysed 13 SGRB candidates (i.e., an SGRB with $T_{90}^* < 2$ s), from among which they selected 8 events considering them as secure ones. An SGRB candidate is regarded as a misguided SGRB if it is located within the $3\sigma_{\text{int}}$ dispersion region from the best-fit $E_{\text{peak}}^* - E_{\text{iso}}$ function of the correlation for LGRBs, while the others are regarded as secure SGRBs. The relation obtained with secure GRBs is the following:

$$\log L_{\text{peak}} = (52.29 \pm 0.066) + (1.59 \pm 0.11) \log E_{\text{peak}}^*, \quad (59)$$

with $r = 0.98$ and $P = 1.5 \times 10^{-5}$, where E_{peak}^* (in units of 774.5 keV) is from the time-integrated spectrum, while L_{peak} (in erg s^{-1}) was taken as the luminosity integrated for 64 ms at the peak considering the shorter duration of SGRBs. Application of this relation to 71 bright BATSE SGRBs resulted in pseudo-redshifts distributed in the range $z \in [0.097, 2.258]$, with $\langle z \rangle = 1.05$, which is apparently lower than $\langle z \rangle = 2.2$ for LGRBs. Finally, Yonetoku et al. (2014), using 72 SGRBs with well determined spectral features as observed by BATSE, determined their pseudo-redshifts and luminosities by employing the $L_{\text{peak}} - E_{\text{peak}}$ correlation for SGRBs found by Tsutsui et al. (2013). It was found that the obtained redshift distribution for $z \leq 1$ was in agreement with that of 22 *Swift* SGRBs, indicating the reliability of the redshift determination via the $E_{\text{peak}}^* - L_{\text{peak}}$ relation.

3.6.3. Physical interpretation of the luminosity vs. peak energy relations

As pointed out by Schaefer et al. (2001) and Schaefer (2003a), E_{peak} and L_{iso} are correlated because of their dependence on Γ . The $L_{\text{iso}} - E_{\text{peak}}$ relation could shed light on the structure of the ultra relativistic outflow, the shock acceleration and the magnetic field generation (Lloyd-Ronning and Ramirez-Ruiz 2002). However, since only few SGRBs are included in the samples used, the correlations and interpretations are currently only applicable to LGRBs.

Schaefer et al. (2001) and Schaefer (2003a) claimed that the values of E_{peak} are approximately constant for all the bursts with $z \geq 5$. However, with the launch of the *Swift* satellite in the end of 2004 the hunt for “standard candles” via a number of GRB correlations is still ongoing. Thus, the great challenge is to find universal constancy in some GRB parameters, despite the substantial diversity exhibited by their light curves. If this goal is achieved, GRBs might prove to be a useful cosmological tool (Wang et al. 2015).

Liang et al. (2004) defined a parameter $\omega = (L_{\text{iso}}/10^{52} \text{ erg s}^{-1})^{0.5}/(E_{\text{peak}}/200 \text{ keV})$ and discussed possible implications of the $E_{\text{peak}} - L_{\text{iso}}$ relation for the fireball models. They found that ω is limited to the range $\simeq 0.1 - 1$. They constrained some parameters, such as the combined internal shock parameter, ζ_i , for the internal as well as external shock models, with an assumption of uncorrelated model parameters. Their distributions suggest that the production of prompt γ -rays within internal shocks dominated by kinetic energy is in agreement with the standard internal shock model. Similarly in case when the γ -rays come from external shocks dominated by magnetic dissipation. These results imply that both models can provide a physical interpretation of the $L_{\text{iso}} \propto E_{\text{peak}}^2$ relation as well as the parameter ω .

To explain the origin of this correlation, Mendoza et al. (2009) considered simple laws of mass and linear momentum conservation on the emission surface to give a full description of the working surface flow parameterized by the initial velocity and mass injection rate. They assumed a source-ejecting matter in a preferred direction x with a velocity $v(t)$ and a mass ejection rate $\dot{m}(t)$, both dependent on time t as measured from the jet's source; i.e., they studied the case of a uniform release of mass and the luminosity was measured considering simple periodic oscillations of the particle velocity, a common assumption in the internal shock model scenario.

Due to the presence of a velocity shear with a considerable variation in Γ at the boundary of the spine and sheath region, a fraction of the injected photons are accelerated via a Fermi-like acceleration mechanism such that a high energy power law tail is formed in the resultant spectrum. Ito et al. (2013) showed in particular that if a velocity shear with a considerable variance in Γ is present, the high energy part of the observed GRB photon spectrum can be explained by this photon acceleration mechanism. The accelerated photons may also account for the origin of the extra hard power law component above the bump of the thermal-like peak seen in some peculiar GRBs (090510, 090902B, 090926A). It was demonstrated that time-integrated spectra can also reproduce the low energy spectra of GRBs consistently due to a multi-temperature effect when time evolution of the outflow is considered.

Regarding the Yonetoku relation, its implications are related to the GRB formation rate and the luminosity function of GRBs. In fact, the analysis of Yonetoku et al. (2004) showed that the existence of the luminosity evolution of GRBs, assuming as a function a simple power law dependence on the redshift, such as $g(z) = (1+z)^{1.85}$, may indicate the evolution of GRB progenitor itself (mass) or the jet evolution. To study the evolution of jet opening angle they considered two assumptions: either the maximum jet opening angle decreases or the total jet energy increases. In the former case, the GRB formation rate obtained may be an underestimation since the chance probability to observe the high redshift GRBs will decrease. If so, the evolution of the ratio of the GRB formation rate to the star formation rate becomes more rapid. On the other hand, in the latter case, GRB formation rate provides a reasonable estimate.

Recently Frontera et al. (2016), building on the spectral model of the prompt emission of Titarchuk et al. (2012), gave a physical interpretation of the origin of the time resolved $L_{\text{iso}} - E_{\text{peak}}$ relation. The model consists of an expanding plasma shell, result of the star explosion, and a thermal bath of soft photons. Frontera et al. (2016) showed analytically that in the asymptotic case of the optical depth $\tau \gg 1$ the relation $\log L_{\text{iso}} - \log E_{\text{peak}}$ indeed has a slope of 1/2. This, in turn, is evidence for the physical origin of the Amati relation (see Sect. 3.5.2).

3.7. Comparisons between $E_{\text{peak}} - E_{\text{iso}}$ and $E_{\text{peak}} - L_{\text{peak}}$ correlation

For a more complete dissertation we compare the $E_{\text{peak}} - E_{\text{iso}}$ correlation with the $E_{\text{peak}} - L_{\text{peak}}$ correlation. To this end, Ghirlanda et al. (2005b) derived the $E_{\text{peak}} - L_{\text{peak}}$ relation with a sample of 22 GRBs with known z and well determined spectral properties. This relation has a slope of 0.51, similar to the one proposed by Yonetoku et al. (2004) with 12 GRBs, although its scatter is much larger than the one originally found.

Tsutsui et al. (2009) investigated these two relations using only data from the prompt phase of 33 low-redshift GRBs with $z \leq 1.6$. In both cases the correlation coefficient was high, but a significant scatter was also present. Next, a partial linear correlation degree, which is the degree of association between two random variables, was found to be $\rho_{L_{\text{peak}}, E_{\text{iso}}, E_{\text{peak}}} = 0.38$. Here, $\rho_{1,2,3}$ means the correlation coefficient between the first and the second parameter after fixing the third parameter. This fact indicates that two distance indicators may be independent from each other even if they are characterized by the same physical quantity, E_{peak} , and similar quantities, L_{peak} and E_{iso} . To correct the large dispersion of the Yonetoku correlation, Tsutsui et al. (2009) introduced a luminosity time constant T_L defined by $T_L = E_{\text{iso}}/L_{\text{peak}}$ as a third parameter and a new correlation was established in the form

$$\log L_{\text{peak}} = (-3.87 \pm 0.19) + (1.82 \pm 0.08) \log E_{\text{peak}} - (0.34 \pm 0.09) \log T_L, \quad (60)$$

with $r = 0.94$ and $P = 10^{-10}$. Here, L_{peak} is in units of $10^{52} \text{ erg s}^{-1}$, E_{peak} is in keV, and T_L in seconds. In this way the systematic errors were reduced by about 40%, and the plane represented by this correlation might be regarded as a “fundamental plane” of GRBs.

Later, Tsutsui et al. (2010) reconsidered the correlations among E_{peak} , L_{peak} and E_{iso} , using the database constructed by Yonetoku et al. (2010), which consisted of 109 GRBs with known redshifts, and E_{peak} , L_{peak} and E_{iso} well determined. The events are divided into two groups by their data quality. One (gold data set) consisted of GRBs with E_{peak} determined by the Band function with four free parameters. GRBs in the other group (bronze data set) had relatively poor energy spectra so that their E_{peak} were determined by the Band function with three free parameters (i.e., one spectral index was fixed) or by the cut-off power law (CPL) model with three free parameters. Using only the gold data set, the intrinsic dispersion, σ_{int} , in $\log L_{\text{peak}}$ is 0.13 for the $E_{\text{peak}} - T_L - L_{\text{peak}}$ correlation, and 0.22 for the $E_{\text{peak}} - L_{\text{peak}}$ correlation. In addition, GRBs in the bronze data set had systematically larger E_{peak} than expected by the correlations constructed with the gold data set. This indicates that the quality of the sample is an important issue for the scatter of correlations among E_{peak} , L_{peak} , and E_{iso} .

The difference between the $E_{\text{peak}} - L_{\text{peak}}$ correlation for LGRBs from (Ghirlanda et al. 2010) and the one from (Yonetoku et al. 2010) is due to the presence of GRB060218. In

the former, it was considered an ordinary LGRB, while in the latter, an outlier by a statistical argument. Because GRB060218 is located far from the $L_{\text{peak}} - E_{\text{peak}}$ correlation in (Yonetoku et al. 2010) (more than 8σ), it makes the best-fit line much steeper.

Regarding the high-energetic GRBs, Ghirlanda et al. (2010) considered 13 GRBs detected by *Fermi* up to the end of July 2009, and with known redshift. They found a tight relation:

$$\log E_{\text{peak}}^* \sim 0.4 \log L_{\text{iso}}, \quad (61)$$

with a scatter of $\sigma = 0.26$. A similarly tight relation exists between E_{peak}^* and E_{iso} :

$$\log E_{\text{peak}}^* \sim 0.5 \log E_{\text{iso}}. \quad (62)$$

The time integrated spectra of 8 *Fermi* GRBs with measured redshift were consistent with both the $E_{\text{peak}} - E_{\text{iso}}$ and the $E_{\text{peak}} - L_{\text{iso}}$ correlations defined by 100 pre-*Fermi* bursts.

Regarding the study of SGRBs within the context of these two correlations, Tsutsui et al. (2013) used 8 SGRBs out of 13 SGRB candidates to check whether the $E_{\text{peak}} - E_{\text{iso}}$ and $E_{\text{peak}} - L_{\text{peak}}$ correlations exist for SGRBs as well. It was found that the $E_{\text{peak}} - E_{\text{iso}}$ correlation seemed to hold in the form

$$\log E_{\text{iso}} = (51.42 \pm 0.15) + (1.58 \pm 0.28) \log E_{\text{peak}}^*, \quad (63)$$

with $r = 0.91$, $P = 1.5 \times 10^{-3}$, E_{iso} in erg s^{-1} and E_{peak}^* in units of 774.5 keV. They also found that the $E_{\text{peak}} - L_{\text{peak}}$ correlation with a functional form as in Eq. (59) is tighter than the $E_{\text{peak}} - E_{\text{iso}}$ one. Both correlations for SGRBs indicate that they are less luminous than LGRBs, for the same E_{peak} , by factors $\simeq 100$ (for $E_{\text{peak}} - E_{\text{iso}}$), and $\simeq 5$ (for $E_{\text{peak}} - L_{\text{peak}}$). It was the first time that the existence of distinct $E_{\text{peak}} - E_{\text{iso}}$ and $E_{\text{peak}} - L_{\text{peak}}$ correlations for SGRBs was argued.

3.8. The $L_{X,p} - T_p^*$ correlation and its physical interpretation

Using data gathered by *Swift*, Willingale et al. (2007) proposed a unique phenomenological function to estimate some relevant parameters of both the prompt and afterglow emission. Both components are well fitted by the same functional form:

$$f_i(t) = \begin{cases} F_i e^{\alpha_i(1-\frac{t}{T_i})} e^{-\frac{t}{t}}, & t < T_i, \\ F_i (\frac{t}{T_i})^{-\alpha_i} e^{-\frac{t}{t}}, & t \geq T_i. \end{cases} \quad (64)$$

The index i can take the values p or a to indicate the prompt and afterglow, respectively. The complete light curve, $f_{\text{tot}}(t) = f_p(t) + f_a(t)$, is described by two sets of four parameters

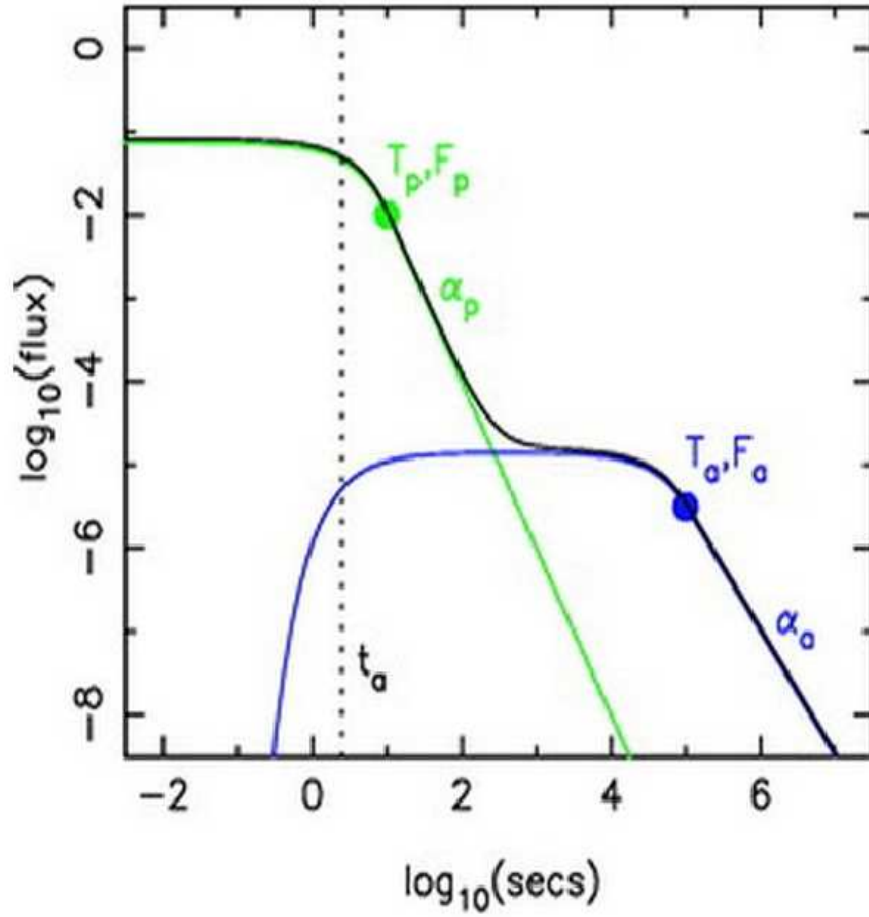


Fig. 13.— Functional form of the decay and the fitted parameters. The prompt component (green curve) has no rise because time zero is set at the peak. The afterglow component (blue curve) rises at time T_a as shown. (Figure after Willingale et al. (2007); see Fig. 1 therein. © AAS. Reproduced with permission.)

each: $\{T_i, F_i, \alpha_i, t_i\}$, where α_i is the temporal power law decay index, the time t_i is the initial rise timescale, F_i is the flux and T_i is the break time. Fig. 13 schematically illustrates this function.

Following the same approach as adopted in (Dainotti et al. 2008), Qi and Lu (2010) investigated the prompt emission properties of 107 GRB light curves detected by the XRT instrument onboard the *Swift* satellite in the X-ray energy band (0.3 – 10 keV). They found that there is a correlation between $L_{X,p}$ and T_p^* . Among the 107 GRBs, they used only 47, because some of the events did not have a firm redshift and some did not present reliable spectral parameters in the prompt decay phase. Among the 47 GRBs, only 37 had $T_p^* > 2$ s, and 3 of them had $T_p^* > 100$ s.

The functional form for this correlation could be written in the following way:

$$\log L_{X,p} = a + b \log T_p^*, \quad (65)$$

where $L_{X,p}$ is in erg s^{-1} , and T_p^* is in seconds. The fits were performed via the D’Agostini (2005) fitting method applied to the following data sets:

1. the total sample of 47 GRBs (see the left panel of Fig. 14),
2. 37 GRBs with $T_p^* > 2$ s (see the middle panel of Fig. 14),
3. 34 GRBs with $2 \text{ s} < T_p^* < 100 \text{ s}$ (see the right panel of Fig. 14).

The results of these fittings turned out to give different forms of Eq. (65). In case 1., $a = 50.91 \pm 0.23$ and $b = -0.89 \pm 0.19$ were obtained. The slope b is different in cases 2. and 3., $b = -1.73$ and $b = -0.74$, respectively. The best fit with the smallest σ_{int} comes from case 3. Remarkably, in this case the slope b is close to the slope $(-0.74_{-0.19}^{+0.20})$ of a similar $\log L_X - \log T_a^*$ relation (Dainotti et al. 2008).

Qi and Lu (2010) noticed a broken linear relation of the $L_{X,p} - T_p^*$ correlation. More specifically, an evidence of curvature appears in the middle panel of Fig. 14. One can see, from the left panel of Fig. 14, that if the best-fit line is extended to the range of $T_p^* < 2$ s, all the GRBs with $T_p^* < 2$ s are located below this line. However, the small sample of GRBs used in their analysis is still not sufficient to conclude whether the change in the slope is real or just a selection bias caused by outliers. If there is a change in the slope this may suggest that GRBs could be classified into two groups, long and short, based on their values of T_p^* instead of T_{90} , since T_p^* is an estimate of the GRB duration based on temporal features of the light curves, and T_{90} is a measure based on the energy. This idea has actually been proposed for the first time by O’Brien and Willingale (2007). It is worth noting that while

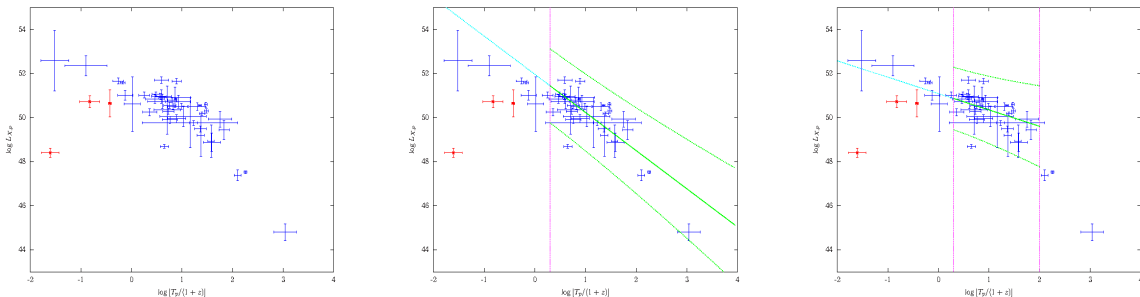


Fig. 14.— **Left panel:** $\log L_{X,p}$ (in erg s^{-1}) vs. $\log T_p^*$ (in s) for the whole sample of 47 GRBs. The red dots represent SGRBs (i.e., $T_{90} < 2\text{ s}$). (Figure after Qi and Lu (2010); see Fig. 1 therein. © AAS. Reproduced with permission.) **Middle panel:** best fit of the $\log L_{X,p}$ (in erg s^{-1}) vs. $\log T_p^*$ (in s) relation following Eq. (65) and the corresponding 2σ confidence region. Only GRBs with $T_p^* > 2\text{ s}$ are included in the fit. (Figure after Qi and Lu (2010); see Fig. 2 therein. © AAS. Reproduced with permission.) **Right panel:** Best fit of the $\log L_{X,p}$ (in erg s^{-1}) vs $\log T_p^*$ (in s) relation following Eq. (65) and the corresponding 2σ confidence region. In this case only the 34 GRBs with $2\text{ s} < T_p^* < 100\text{ s}$ are included in the fit. (Figure after Qi and Lu (2010); see Fig. 3 therein. © AAS. Reproduced with permission.)

T_{90} and T_p are both estimates of the GRB duration, the correlation does not hold if T_p is replaced with T_{90} . For an analysis of an extended sample and comparison of T_{45} versus T_p also, see (Dainotti et al. 2011b).

Regarding the physical interpretation, the change of the slope in the $L_{X,p} - T_p^*$ relation at different values of T_p^* in (Qi and Lu 2010) can be due to the presence of few GRBs with a large T_p^* , but it might also be due to different emission mechanisms. Unfortunately, the paucity of the sample prevents putting forward any conclusion due to the presence of (potential) outliers in the data set. A more detailed analysis is necessary to further validate this correlation and better understand its physical interpretation.

3.9. The $L_f - T_f$ correlation and its physical interpretation

In most GRBs a rapid decay phase (RDP) soon after the prompt emission is observed (Nousek et al. 2006), and this RDP appears continue smoothly after the prompt, both in terms of temporal and spectral variations (O’Brien et al. 2006). This indicates that the RDP could be the prompt emission’s tail and a number of models have been proposed to take it into account (see Zhang et al. 2007), in particular the high latitude emission (HLE). This model states that once the prompt emission from a spherical shell turns off at some radius, then the photons reach the observer from angles apparently larger (relative to the line of sight) due to the added path length caused by the curvature of the emitting region. The

Doppler factor of these late-arriving photons is smaller.

A successful attempt to individually fit all the distinct pulses in the prompt phase and in the late X-ray flares observed by the complete *Swift*/BAT+XRT light curves has been performed by Willingale et al. (2010) using a physically motivated pulse profile. This fitting is an improved procedure compared to the Willingale et al. (2007) one. The pulse profile has the following functional form:

$$P = \left\{ \left[\min \left(\frac{T - T_{\text{ej}}}{T_f}, 1 \right)^{\alpha+2} - \left(\frac{T_f - T_{\text{rise}}}{T_f} \right)^{\alpha+2} \right] \left[1 - \left(\frac{T_f - T_{\text{rise}}}{T_f} \right)^{\alpha+2} \right]^{-1} \right\} \left(\frac{T - T_{\text{ej}}}{T_f} \right)^{-1}, \quad (66)$$

where $T_0 = T_f - T_{\text{rise}}$ (with T_{rise} the rise time of the pulse) is the arrival time of the first photon emitted from the shell. It is assumed here that the emission comes from an ultra-relativistic thin shell spreading over a finite range of radii along the line of sight, in the observer frame measured with respect to the ejection time, T_{ej} . From these assumptions it is possible to model the rise of the pulse through α , T_{rise} and T_f (see also Fig. 1).

The combination of the pulse profile function $P(t, T_f, T_{\text{rise}})$ and the blue-shift of the spectral profile $B(x)$ produces the rise and fall of the pulse. $B(x)$ is approximated with the Band function in the form

$$B(x) = B_{\text{norm}} \times \begin{cases} x^{(\alpha-1)} e^{-x}, & x \leq \alpha - \beta \\ x^{(\beta-1)} (\alpha - \beta)^{(\alpha-\beta)} e^{-(\alpha-\beta)}, & x > \alpha - \beta \end{cases} \quad (67)$$

where $x = (E/E_f) [(T - T_{\text{ej}})/T_f]^{-1}$, with E_f the energy at the spectral break, and B_{norm} is the normalization.

Using this motivated pulse profile, Willingale et al. (2010) found that, within a sample of 12 GRBs observed by *Swift* in the BAT and XRT energy bands, L_f is anti-correlated with T_f^* in the following way:

$$\log L_f \sim -(2.0 \pm 0.2) \log T_f^*. \quad (68)$$

Therefore, high luminosity pulses occur shortly after ejection, while low luminosity pulses appear at later time (see the left panel of Fig. 15). Moreover, Willingale et al. (2010) also found a correlation between L_f and E_{peak} as shown in the right panel of Fig. 15. This is in agreement with the known correlation between the L_{peak} for the whole burst and the E_{peak} of the spectrum during the time T_{90} (Yonetoku et al. 2004; Tsutsui et al. 2013); for comparison with the $L_{\text{peak}} - E_{\text{peak}}$ correlation, see also Sect. 3.6.2.

In the 12 light curves considered by Willingale et al. (2010), 49 pulses were analysed. Although several pulses with a hard peak could not be correctly fitted, the overall fitting to

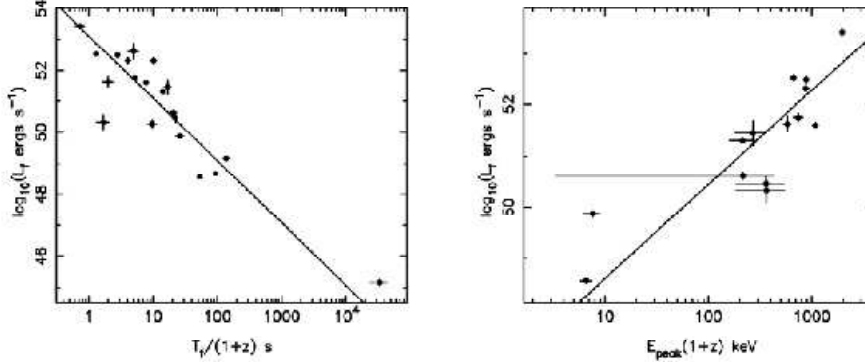


Fig. 15.— **Left panel:** L_f (in ergs s^{-1}) vs. T_f^* . **Right panel:** L_f (in ergs s^{-1}) vs. E_{peak} . (Figures after Willingale et al. (2010); see Fig. 16 therein.)

the RDP was satisfactory and the HLE model was shown to be able to take into account phase of the GRB emission. However, it is worth to mention the hard pulse in GRB061121 which requires a spectral index $\beta_S = 2.4$, larger than the value expected for synchrotron emission, i.e. $\beta_S = 1$.

Lee et al. (2000) and Quilligan et al. (2002) discussed analogous correlations, although these authors considered the width of a pulse rather than T_f , which is in fact closely correlated with pulse width. Many authors afterwards (Littlejohns et al. 2013; Bošnjak and Daigne 2014; Evans et al. 2014; Hakkila and Preece 2014; Laskar et al. 2014; Littlejohns and Butler 2014; Roychoudhury et al. 2014; Ceccobello and Kumar 2015; Kazanas et al. 2015; Laskar et al. 2015; Peng et al. 2015) have used the motivated pulse profile of Willingale et al. (2010) for various studies on the prompt emission properties of the pulses.

Regarding the physical interpretation, in (Willingale et al. 2010) the flux density of each prompt emission pulse is depicted by an analytical expression derived under the assumption that the radiation comes from a thin shell, as we have already described. The decay after the peak involves the HLE (Genet and Granot 2009) along the considered shell which is delayed and modified with a different Doppler factor due to the curvature of the surface (Ryde and Petrosian 2002; Dermer 2007).

4. Summary

In this work we have reviewed the bivariate correlations among a number of GRB prompt phase parameters and their characteristics. It is important to mention that several of these correlations have the problem of double truncation which affects the parameters. Some relations have also been tested to prove their intrinsic nature like the $E_{\text{peak}} - S_{\text{tot}}$, $E_{\text{peak}} - E_{\text{iso}}$ and $L_{\text{peak}} - E_{\text{peak}}$ relations. For the others we are not aware of their intrinsic forms and consequently how far the use of the observed relations can influence the evaluation of the theoretical models and the “best” cosmological settings. Therefore, the evaluation of the intrinsic correlations is crucial for the determination of the most plausible model to explain the prompt emission. In fact, though there are several theoretical interpretations describing each correlation, in many cases more than one is viable, thus showing that the emission processes that rule GRBs still need to be further investigated. These correlations might also serve as discriminating factors among different GRB classes, as several of them hold different forms for SGRBs and LGRBs, hence providing insight into the generating mechanisms. Hopefully those correlations could lead to new standard candles allowing to explore the high-redshift universe.

MT acknowledges support in a form of a special scholarship of Marian Smoluchowski Scientific Consortium Matter-Energy-Future from KNOW funding, grant number KNOW/48/SS/PC/2015. The work of R.D.V. was supported by the Polish National Science Centre through the grant DEC-2012/04/A/ST9/00083.

REFERENCES

- B. P. Abbott, R. Abbott, T. D. Abbott, M. R. Abernathy, F. Acernese, K. Ackley, C. Adams, T. Adams, P. Addesso, R. X. Adhikari, and et al. Observation of Gravitational Waves from a Binary Black Hole Merger. *Physical Review Letters*, 116(6):061102, February 2016. doi: 10.1103/PhysRevLett.116.061102.
- A. A. Abdo, M. Ackermann, M. Ajello, K. Asano, W. B. Atwood, M. Axelsson, L. Baldini, J. Ballet, G. Barbiellini, M. G. Baring, and et al. Fermi Observations of GRB 090902B: A Distinct Spectral Component in the Prompt and Delayed Emission. *ApJ*, 706:L138–L144, November 2009. doi: 10.1088/0004-637X/706/1/L138.
- M. Ackermann, K. Asano, W. B. Atwood, M. Axelsson, L. Baldini, J. Ballet, G. Barbiellini, M. G. Baring, D. Bastieri, K. Bechtol, and et al. Fermi Observations of GRB 090510: A Short-Hard Gamma-ray Burst with an Additional, Hard Power-law Component

- from 10 keV TO GeV Energies. *ApJ*, 716:1178–1190, June 2010. doi: 10.1088/0004-637X/716/2/1178.
- M. Ackermann, M. Ajello, K. Asano, M. Axelsson, L. Baldini, J. Ballet, G. Barbiellini, M. G. Baring, D. Bastieri, K. Bechtol, and et al. Detection of a Spectral Break in the Extra Hard Component of GRB 090926A. *ApJ*, 729:114, March 2011. doi: 10.1088/0004-637X/729/2/114.
- M. Ackermann, M. Ajello, A. Allafort, W. B. Atwood, L. Baldini, J. Ballet, G. Barbiellini, D. Bastieri, K. Bechtol, A. Belfiore, and et al. The First Fermi-LAT Catalog of Sources above 10 GeV. *ApJS*, 209:34, December 2013. doi: 10.1088/0067-0049/209/2/34.
- L. Amati. The $E_{p,i}$ - E_{iso} correlation in gamma-ray bursts: updated observational status, re-analysis and main implications. *MNRAS*, 372:233–245, October 2006. doi: 10.1111/j.1365-2966.2006.10840.x.
- L. Amati. COSMOLOGY WITH THE $E_{p,i}$ - E_{iso} CORRELATION OF GAMMA-RAY BURSTS. *International Journal of Modern Physics Conference Series*, 12:19–27, March 2012. doi: 10.1142/S2010194512006228.
- L. Amati and M. Della Valle. Measuring Cosmological Parameters with Gamma Ray Bursts. *International Journal of Modern Physics D*, 22:1330028, December 2013. doi: 10.1142/S0218271813300280.
- L. Amati, F. Frontera, M. Tavani, J. J. M. in’t Zand, A. Antonelli, E. Costa, M. Feroci, C. Guidorzi, J. Heise, N. Masetti, E. Montanari, L. Nicastro, E. Palazzi, E. Pian, L. Piro, and P. Soffitta. Intrinsic spectra and energetics of BeppoSAX Gamma-Ray Bursts with known redshifts. *A&A*, 390:81–89, July 2002. doi: 10.1051/0004-6361:20020722.
- L. Amati, F. Frontera, J. M. Castro Cerón, E. Costa, M. Feroci, G. Gandolfi, P. Giommi, C. Guidorzi, N. Masetti, E. Montanari, L. Piro, P. Soffitta, and J. J. M. in’t Zand. The Prompt and Afterglow Emission of GRB 001109 Measured by BeppoSAX. In G. R. Ricker and R. K. Vanderspek, editors, *Gamma-Ray Burst and Afterglow Astronomy 2001: A Workshop Celebrating the First Year of the HETE Mission*, volume 662 of *American Institute of Physics Conference Series*, pages 387–389, April 2003. doi: 10.1063/1.1579385.
- L. Amati, C. Guidorzi, F. Frontera, M. Della Valle, F. Finelli, R. Landi, and E. Montanari. Measuring the cosmological parameters with the $E_{p,i}$ - E_{iso} correlation of gamma-ray bursts. *MNRAS*, 391:577–584, December 2008. doi: 10.1111/j.1365-2966.2008.13943.x.

- L. Amati, F. Frontera, and C. Guidorzi. Extremely energetic Fermi gamma-ray bursts obey spectral energy correlations. *A&A*, 508:173–180, December 2009. doi: 10.1051/0004-6361/200912788.
- L. G. Balazs, A. Meszaros, and I. Horvath. Anisotropy of the sky distribution of gamma-ray bursts. *A&A*, 339:1–6, November 1998.
- D. Band, J. Matteson, L. Ford, B. Schaefer, D. Palmer, B. Teegarden, T. Cline, M. Briggs, W. Paciesas, G. Pendleton, G. Fishman, C. Kouveliotou, C. Meegan, R. Wilson, and P. Lestrade. BATSE observations of gamma-ray burst spectra. I - Spectral diversity. *ApJ*, 413:281–292, August 1993. doi: 10.1086/172995.
- R. Barkana and A. Loeb. Gamma-Ray Bursts versus Quasars: Ly α Signatures of Reionization versus Cosmological Infall. *ApJ*, 601:64–77, January 2004. doi: 10.1086/380435.
- R. Basak and A. R. Rao. Correlation between the Isotropic Energy and the Peak Energy at Zero Fluence for the Individual Pulses of Gamma-Ray Bursts: Toward a Universal Physical Correlation for the Prompt Emission. *ApJ*, 749:132, April 2012. doi: 10.1088/0004-637X/749/2/132.
- R. Basak and A. R. Rao. Pulse-wise Amati correlation in Fermi gamma-ray bursts. *MNRAS*, 436:3082–3088, December 2013. doi: 10.1093/mnras/stt1790.
- A. M. Beloborodov. Collisional mechanism for gamma-ray burst emission. *MNRAS*, 407:1033–1047, September 2010. doi: 10.1111/j.1365-2966.2010.16770.x.
- E. Berger. Short-Duration Gamma-Ray Bursts. *ARA&A*, 52:43–105, August 2014. doi: 10.1146/annurev-astro-081913-035926.
- A. Bernui, I. S. Ferreira, and C. A. Wuensche. On the Large-Scale Angular Distribution of Short Gamma-Ray Bursts. *ApJ*, 673:968–971, February 2008. doi: 10.1086/524678.
- P. R. Bevington and D. K. Robinson. *Data reduction and error analysis for the physical sciences*. McGraw-Hill, 2003.
- J. S. Bloom, D. A. Frail, and R. Sari. The Prompt Energy Release of Gamma-Ray Bursts using a Cosmological k-Correction. *AJ*, 121:2879–2888, June 2001. doi: 10.1086/321093.
- M. Boër, B. Gendre, and G. Stratta. Are Ultra-long Gamma-Ray Bursts Different? *ApJ*, 800:16, February 2015. doi: 10.1088/0004-637X/800/1/16.

- L. Boronovo and F. Ryde. On the Hardness-Intensity Correlation in Gamma-Ray Burst Pulses. *ApJ*, 548:770–786, February 2001. doi: 10.1086/319008.
- Ž. Bošnjak and F. Daigne. Spectral evolution in gamma-ray bursts: Predictions of the internal shock model and comparison to observations. *A&A*, 568:A45, August 2014. doi: 10.1051/0004-6361/201322341.
- M. S. Briggs, W. S. Paciesas, G. N. Pendleton, C. A. Meegan, G. J. Fishman, J. M. Horack, M. N. Brock, C. Kouveliotou, D. H. Hartmann, and J. Hakkila. BATSE Observations of the Large-Scale Isotropy of Gamma-Ray Bursts. *ApJ*, 459:40, March 1996. doi: 10.1086/176867.
- O. Bromberg, E. Nakar, T. Piran, and R. Sari. Short versus Long and Collapsars versus Non-collapsars: A Quantitative Classification of Gamma-Ray Bursts. *ApJ*, 764:179, February 2013. doi: 10.1088/0004-637X/764/2/179.
- V. Bromm and A. Loeb. High-Redshift Gamma-Ray Bursts from Population III Progenitors. *ApJ*, 642:382–388, May 2006. doi: 10.1086/500799.
- C. Ceccobello and P. Kumar. Inverse-Compton drag on a highly magnetized GRB jet in stellar envelope. *MNRAS*, 449:2566–2575, May 2015. doi: 10.1093/mnras/stv457.
- A. C. Collazzi, B. E. Schaefer, and J. A. Moree. The Total Errors in Measuring E_{peak} for Gamma-ray Bursts. *ApJ*, 729:89, March 2011. doi: 10.1088/0004-637X/729/2/89.
- V. Connaughton, E. Burns, A. Goldstein, M. S. Briggs, B.-B. Zhang, C. M. Hui, P. Jenke, J. Racusin, C. A. Wilson-Hodge, P. N. Bhat, E. Bissaldi, W. Cleveland, G. Fitzpatrick, M. M. Giles, M. H. Gibby, J. Greiner, A. von Kienlin, R. M. Kippen, S. McBreen, B. Mailyan, C. A. Meegan, W. S. Paciesas, R. D. Preece, O. Roberts, L. Sparke, M. Stanbro, K. Toelge, P. Veres, H.-F. Yu, and o. authors. Fermi GBM Observations of LIGO Gravitational Wave event GW150914. *ArXiv e-prints*, February 2016.
- E. Costa, F. Frontera, J. Heise, M. Feroci, J. in’t Zand, F. Fiore, M. N. Cinti, D. Dal Fiume, L. Nicastro, M. Orlandini, E. Palazzi, M. Rapisarda, G. Zavattini, R. Jager, A. Parmar, A. Owens, S. Molendi, G. Cusumano, M. C. Maccarone, S. Giarrusso, A. Coletta, L. A. Antonelli, P. Giommi, J. M. Muller, L. Piro, and R. C. Butler. Discovery of an X-ray afterglow associated with the γ -ray burst of 28 February 1997. *Nature*, 387:783–785, June 1997. doi: 10.1038/42885.
- A. Cucchiara, A. J. Levan, D. B. Fox, N. R. Tanvir, T. N. Ukwatta, E. Berger, T. Krühler, A. Küpcü Yoldaş, X. F. Wu, K. Toma, J. Greiner, F. E. Olivares, A. Rowlinson,

- L. Amati, T. Sakamoto, K. Roth, A. Stephens, A. Fritz, J. P. U. Fynbo, J. Hjorth, D. Malesani, P. Jakobsson, K. Wiersema, P. T. O’Brien, A. M. Soderberg, R. J. Foley, A. S. Fruchter, J. Rhoads, R. E. Rutledge, B. P. Schmidt, M. A. Dopita, P. Podsiadlowski, R. Willingale, C. Wolf, S. R. Kulkarni, and P. D’Avanzo. A Photometric Redshift of $z \sim 9.4$ for GRB 090429B. *ApJ*, 736:7, July 2011. doi: 10.1088/0004-637X/736/1/7.
- G. D’Agostini. Fits, and especially linear fits, with errors on both axes, extra variance of the data points and other complications. *ArXiv Physics e-prints*, November 2005.
- F. Daigne and R. Mochkovitch. The physics of pulses in gamma-ray bursts: emission processes, temporal profiles and time-lags. *MNRAS*, 342:587–592, June 2003. doi: 10.1046/j.1365-8711.2003.06575.x.
- M. Dainotti, V. Petrosian, R. Willingale, P. O’Brien, M. Ostrowski, and S. Nagataki. Luminosity-time and luminosity-luminosity correlations for GRB prompt and afterglow plateau emissions. *MNRAS*, 451:3898–3908, August 2015. doi: 10.1093/mnras/stv1229.
- M. G. Dainotti, V. F. Cardone, and S. Capozziello. A time-luminosity correlation for γ -ray bursts in the X-rays. *MNRAS*, 391:L79–L83, November 2008. doi: 10.1111/j.1745-3933.2008.00560.x.
- M. G. Dainotti, R. Willingale, S. Capozziello, V. Fabrizio Cardone, and M. Ostrowski. Discovery of a Tight Correlation for Gamma-ray Burst Afterglows with ”Canonical” Light Curves. *ApJ*, 722:L215–L219, October 2010. doi: 10.1088/2041-8205/722/2/L215.
- M. G. Dainotti, V. Fabrizio Cardone, S. Capozziello, M. Ostrowski, and R. Willingale. Study of Possible Systematics in the L^*_X - T^*_a Correlation of Gamma-ray Bursts. *ApJ*, 730:135, April 2011a. doi: 10.1088/0004-637X/730/2/135.
- M. G. Dainotti, M. Ostrowski, and R. Willingale. Towards a standard gamma-ray burst: tight correlations between the prompt and the afterglow plateau phase emission. *MNRAS*, 418:2202–2206, December 2011b. doi: 10.1111/j.1365-2966.2011.19433.x.
- M. G. Dainotti, V. F. Cardone, E. Piedipalumbo, and S. Capozziello. Slope evolution of GRB correlations and cosmology. *MNRAS*, 436:82–88, November 2013. doi: 10.1093/mnras/stt1516.

- R. S. de Souza, N. Yoshida, and K. Ioka. Populations III.1 and III.2 gamma-ray bursts: constraints on the event rate for future radio and X-ray surveys. *A&A*, 533:A32, September 2011. doi: 10.1051/0004-6361/201117242.
- M. Della Valle, D. Malesani, S. Benetti, G. Chincarini, L. Stella, and G. Tagliaferri. Supernova 2005nc and GRB 050525A. *IAU Circ.*, 8696:1, March 2006.
- C. D. Dermer. Rapid X-Ray Declines and Plateaus in Swift GRB Light Curves Explained by a Highly Radiative Blast Wave. *ApJ*, 664:384–396, July 2007. doi: 10.1086/518996.
- D. Eichler, M. Livio, T. Piran, and D. N. Schramm. Nucleosynthesis, neutrino bursts and gamma-rays from coalescing neutron stars. *Nature*, 340:126–128, July 1989. doi: 10.1038/340126a0.
- P. A. Evans, R. Willingale, J. P. Osborne, P. T. O’Brien, N. R. Tanvir, D. D. Frederiks, V. D. Pal’shin, D. S. Svinkin, A. Lien, J. Cummings, S. Xiong, B.-B. Zhang, D. Götz, V. Savchenko, H. Negoro, S. Nakahira, K. Suzuki, K. Wiersema, R. L. C. Starling, A. J. Castro-Tirado, A. P. Beardmore, R. Sánchez-Ramírez, J. Gorosabel, S. Jeong, J. A. Kennea, D. N. Burrows, and N. Gehrels. GRB 130925A: an ultralong gamma ray burst with a dust-echo afterglow, and implications for the origin of the ultralong GRBs. *MNRAS*, 444:250–267, October 2014. doi: 10.1093/mnras/stu1459.
- P. A. Evans, J. A. Kennea, S. D. Barthelmy, A. P. Beardmore, D. N. Burrows, S. Campana, S. B. Cenko, N. Gehrels, P. Giommi, C. Gronwall, F. E. Marshall, D. Malesani, C. B. Markwardt, B. Mingo, J. A. Nousek, P. T. O’Brien, J. P. Osborne, C. Pagani, K. L. Page, D. M. Palmer, M. Perri, J. L. Racusin, M. H. Siegel, B. Sbarufatti, and G. Tagliaferri. Swift follow-up of the Gravitational Wave source GW150914. *MNRAS*, April 2016. doi: 10.1093/mnrasl/slw065.
- Y.-Z. Fan. The spectrum of γ -ray burst: a clue. *MNRAS*, 403:483–490, March 2010. doi: 10.1111/j.1365-2966.2009.16134.x.
- E. E. Fenimore and E. Ramirez-Ruiz. Redshifts For 220 BATSE Gamma-Ray Bursts Determined by Variability and the Cosmological Consequences. *ArXiv Astrophysics e-prints*, April 2000.
- E. E. Fenimore, C. D. Madras, and S. Nayakshin. Expanding Relativistic Shells and Gamma-Ray Burst Temporal Structure. *ApJ*, 473:998, December 1996. doi: 10.1086/178210.
- G. J. Fishman and C. A. Meegan. Gamma-Ray Bursts. *ARA&A*, 33:415–458, 1995. doi: 10.1146/annurev.aa.33.090195.002215.

- G. J. Fishman, C. A. Meegan, R. B. Wilson, M. N. Brock, J. M. Horack, C. Kouveliotou, S. Howard, W. S. Paciesas, M. S. Briggs, G. N. Pendleton, T. M. Koshut, R. S. Mallozzi, M. Stollberg, and J. P. Lestrade. The first BATSE gamma-ray burst catalog. *ApJS*, 92:229–283, May 1994. doi: 10.1086/191968.
- D. A. Frail, S. R. Kulkarni, R. Sari, G. B. Taylor, D. S. Shepherd, J. S. Bloom, C. H. Young, L. Nicastro, and N. Masetti. The Radio Afterglow from GRB 980519: A Test of the Jet and Circumstellar Models. *ApJ*, 534:559–564, May 2000. doi: 10.1086/308802.
- D. L. Freedman and E. Waxman. On the Energy of Gamma-Ray Bursts. *ApJ*, 547:922–928, February 2001. doi: 10.1086/318386.
- F. Frontera, L. Amati, E. Costa, J. M. Muller, E. Pian, L. Piro, P. Soffitta, M. Tavani, A. Castro-Tirado, D. Dal Fiume, M. Feroci, J. Heise, N. Masetti, L. Nicastro, M. Orlandini, E. Palazzi, and R. Sari. Prompt and Delayed Emission Properties of Gamma-Ray Bursts Observed with BeppoSAX. *ApJS*, 127:59–78, March 2000. doi: 10.1086/313316.
- F. Frontera, L. Amati, C. Guidorzi, R. Landi, and J. in’t Zand. Broadband Time-resolved $E_{p,i}$ - L_{iso} Correlation in Gamma-Ray Bursts. *ApJ*, 754:138, August 2012. doi: 10.1088/0004-637X/754/2/138.
- F. Frontera, L. Amati, R. Farinelli, S. Dichiara, C. Guidorzi, R. Landi, and L. Titarchuk. Possible physical explanation of the intrinsic $E_{p,i}$ -”intensity” correlation commonly used to ”standardize” GRBs. *International Journal of Modern Physics D*, 25:1630014, March 2016. doi: 10.1142/S0218271816300147.
- J. P. U. Fynbo, D. Watson, C. C. Thöne, J. Sollerman, J. S. Bloom, T. M. Davis, J. Hjorth, P. Jakobsson, U. G. Jørgensen, J. F. Graham, A. S. Fruchter, D. Bersier, L. Kewley, A. Cassan, J. M. Castro Cerón, S. Foley, J. Gorosabel, T. C. Hinse, K. D. Horne, B. L. Jensen, S. Klose, D. Kocevski, J.-B. Marquette, D. Perley, E. Ramirez-Ruiz, M. D. Stritzinger, P. M. Vreeswijk, R. A. M. Wijers, K. G. Woller, D. Xu, and M. Zub. No supernovae associated with two long-duration γ -ray bursts. *Nature*, 444:1047–1049, December 2006. doi: 10.1038/nature05375.
- H. Gao, Y. Lu, and S. N. Zhang. A New Class of Gamma-ray Bursts from Stellar Disruptions by Intermediate-mass Black Holes. *ApJ*, 717:268–276, July 2010. doi: 10.1088/0004-637X/717/1/268.
- N. Gehrels and S. Razzaque. Gamma-ray bursts in the Swift-Fermi era. *Frontiers of Physics*, 8:661–678, December 2013. doi: 10.1007/s11467-013-0282-3.

- N. Gehrels, G. Chincarini, P. Giommi, K. O. Mason, J. A. Nousek, A. A. Wells, N. E. White, S. D. Barthelmy, D. N. Burrows, L. R. Cominsky, K. C. Hurley, F. E. Marshall, P. Mészáros, P. W. A. Roming, L. Angelini, L. M. Barbier, T. Belloni, S. Campana, P. A. Caraveo, M. M. Chester, O. Citterio, T. L. Cline, M. S. Cropper, J. R. Cummings, A. J. Dean, E. D. Feigelson, E. E. Fenimore, D. A. Frail, A. S. Fruchter, G. P. Garmire, K. Gendreau, G. Ghisellini, J. Greiner, J. E. Hill, S. D. Hunsberger, H. A. Krimm, S. R. Kulkarni, P. Kumar, F. Lebrun, N. M. Lloyd-Ronning, C. B. Markwardt, B. J. Mattson, R. F. Mushotzky, J. P. Norris, J. Osborne, B. Paczynski, D. M. Palmer, H.-S. Park, A. M. Parsons, J. Paul, M. J. Rees, C. S. Reynolds, J. E. Rhoads, T. P. Sasseen, B. E. Schaefer, A. T. Short, A. P. Smale, I. A. Smith, L. Stella, G. Tagliaferri, T. Takahashi, M. Tashiro, L. K. Townsley, J. Tueller, M. J. L. Turner, M. Vietri, W. Voges, M. J. Ward, R. Willingale, F. M. Zerbi, and W. W. Zhang. The Swift Gamma-Ray Burst Mission. *ApJ*, 611:1005–1020, August 2004. doi: 10.1086/422091.
- N. Gehrels, J. P. Norris, S. D. Barthelmy, J. Granot, Y. Kaneko, C. Kouveliotou, C. B. Markwardt, P. Mészáros, E. Nakar, J. A. Nousek, P. T. O’Brien, M. Page, D. M. Palmer, A. M. Parsons, P. W. A. Roming, T. Sakamoto, C. L. Sarazin, P. Schady, M. Stamatikos, and S. E. Woosley. A new γ -ray burst classification scheme from GRB060614. *Nature*, 444:1044–1046, December 2006. doi: 10.1038/nature05376.
- F. Genet and J. Granot. Realistic analytic model for the prompt and high-latitude emission in GRBs. *MNRAS*, 399:1328–1346, November 2009. doi: 10.1111/j.1365-2966.2009.15355.x.
- G. Ghirlanda, A. Celotti, and G. Ghisellini. Extremely hard GRB spectra prune down the forest of emission models. *A&A*, 406:879–892, August 2003. doi: 10.1051/0004-6361:20030803.
- G. Ghirlanda, G. Ghisellini, and A. Celotti. The spectra of short gamma-ray bursts. *A&A*, 422:L55–L58, July 2004a. doi: 10.1051/0004-6361:20048008.
- G. Ghirlanda, G. Ghisellini, and D. Lazzati. The Collimation-corrected Gamma-Ray Burst Energies Correlate with the Peak Energy of Their νF_ν Spectrum. *ApJ*, 616:331–338, November 2004b. doi: 10.1086/424913.
- G. Ghirlanda, G. Ghisellini, and C. Firmani. Probing the existence of the E_{peak} - E_{iso} correlation in long gamma ray bursts. *MNRAS*, 361:L10–L14, July 2005a. doi: 10.1111/j.1745-3933.2005.00053.x.

- G. Ghirlanda, G. Ghisellini, C. Firmani, A. Celotti, and Z. Bosnjak. The peak luminosity-peak energy correlation in gamma-ray bursts. *MNRAS*, 360:L45–L49, June 2005b. doi: 10.1111/j.1745-3933.2005.00043.x.
- G. Ghirlanda, L. Nava, G. Ghisellini, and C. Firmani. Confirming the γ -ray burst spectral-energy correlations in the era of multiple time breaks. *A&A*, 466:127–136, April 2007. doi: 10.1051/0004-6361:20077119.
- G. Ghirlanda, L. Nava, G. Ghisellini, C. Firmani, and J. I. Cabrera. The E_{peak} - E_{iso} plane of long gamma-ray bursts and selection effects. *MNRAS*, 387:319–330, June 2008. doi: 10.1111/j.1365-2966.2008.13232.x.
- G. Ghirlanda, L. Nava, and G. Ghisellini. Spectral-luminosity relation within individual Fermi gamma rays bursts. *A&A*, 511:A43, February 2010. doi: 10.1051/0004-6361/200913134.
- G. Ghirlanda, G. Ghisellini, L. Nava, and D. Burlon. Spectral evolution of Fermi/GBM short gamma-ray bursts. *MNRAS*, 410:L47–L51, January 2011. doi: 10.1111/j.1745-3933.2010.00977.x.
- G. Ghirlanda, G. Ghisellini, R. Salvaterra, L. Nava, D. Burlon, G. Tagliaferri, S. Campana, P. D’Avanzo, and A. Melandri. The faster the narrower: characteristic bulk velocities and jet opening angles of gamma-ray bursts. *MNRAS*, 428:1410–1423, January 2013. doi: 10.1093/mnras/sts128.
- A. Goldstein, R. D. Preece, and M. S. Briggs. A New Discriminator for Gamma-ray Burst Classification: The E_{peak} -fluence Energy Ratio. *ApJ*, 721:1329–1332, October 2010. doi: 10.1088/0004-637X/721/2/1329.
- S. V. Golenetskii, E. P. Mazets, R. L. Aptekar, and V. N. Ilinskii. Correlation between luminosity and temperature in gamma-ray burst sources. *Nature*, 306:451–453, December 1983. doi: 10.1038/306451a0.
- J. Granot, T. Piran, and R. Sari. Images and Spectra from the Interior of a Relativistic Fireball. *ApJ*, 513:679–689, March 1999. doi: 10.1086/306884.
- J. Greiner, P. A. Mazzali, D. A. Kann, T. Krühler, E. Pian, S. Prentice, F. Olivares E., A. Rossi, S. Klose, S. Taubenberger, F. Knust, P. M. J. Afonso, C. Ashall, J. Bolmer, C. Delvaux, R. Diehl, J. Elliott, R. Filgas, J. P. U. Fynbo, J. F. Graham, A. N. Guehbenzu, S. Kobayashi, G. Leloudas, S. Savaglio, P. Schady, S. Schmidl, T. Schweyer,

- V. Sudilovsky, M. Tanga, A. C. Updike, H. van Eerten, and K. Varela. A very luminous magnetar-powered supernova associated with an ultra-long γ -ray burst. *Nature*, 523:189–192, July 2015. doi: 10.1038/nature14579.
- D. Grupe, J. A. Nousek, P. Veres, B.-B. Zhang, and N. Gehrels. Evidence for New Relations between Gamma-Ray Burst Prompt and X-Ray Afterglow Emission from 9 Years of Swift. *ApJS*, 209:20, December 2013. doi: 10.1088/0067-0049/209/2/20.
- C. Guidorzi. Testing the gamma-ray burst variability/peak luminosity correlation using the pseudo-redshifts of a large sample of BATSE gamma-ray bursts. *MNRAS*, 364:163–168, November 2005. doi: 10.1111/j.1365-2966.2005.09545.x.
- C. Guidorzi, F. Frontera, E. Montanari, F. Rossi, L. Amati, A. Gomboc, K. Hurley, and C. G. Mundell. The gamma-ray burst variability-peak luminosity correlation: new results. *MNRAS*, 363:315–325, October 2005. doi: 10.1111/j.1365-2966.2005.09450.x.
- C. Guidorzi, F. Frontera, E. Montanari, F. Rossi, L. Amati, A. Gomboc, and C. G. Mundell. The slope of the gamma-ray burst variability/peak luminosity correlation. *MNRAS*, 371:843–851, September 2006. doi: 10.1111/j.1365-2966.2006.10717.x.
- S. Guiriec, M. S. Briggs, V. Connaughton, E. Kara, F. Daigne, C. Kouveliotou, A. J. van der Horst, W. Paciesas, C. A. Meegan, P. N. Bhat, S. Foley, E. Bissaldi, M. Burgess, V. Chaplin, R. Diehl, G. Fishman, M. Gibby, M. M. Giles, A. Goldstein, J. Greiner, D. Gruber, A. von Kienlin, M. Kippen, S. McBreen, R. Preece, A. Rau, D. Tierney, and C. Wilson-Hodge. Time-resolved Spectroscopy of the Three Brightest and Hardest Short Gamma-ray Bursts Observed with the Fermi Gamma-ray Burst Monitor. *ApJ*, 725:225–241, December 2010. doi: 10.1088/0004-637X/725/1/225.
- S. Guiriec, V. Connaughton, M. S. Briggs, M. Burgess, F. Ryde, F. Daigne, P. Mészáros, A. Goldstein, J. McEnery, N. Omodei, P. N. Bhat, E. Bissaldi, A. Camero-Arranz, V. Chaplin, R. Diehl, G. Fishman, S. Foley, M. Gibby, M. M. Giles, J. Greiner, D. Gruber, A. von Kienlin, M. Kippen, C. Kouveliotou, S. McBreen, C. A. Meegan, W. Paciesas, R. Preece, A. Rau, D. Tierney, A. J. van der Horst, and C. Wilson-Hodge. Detection of a Thermal Spectral Component in the Prompt Emission of GRB 100724B. *ApJ*, 727:L33, February 2011. doi: 10.1088/2041-8205/727/2/L33.
- S. Guiriec, F. Daigne, R. Hascoët, G. Vianello, F. Ryde, R. Mochkovitch, C. Kouveliotou, S. Xiong, P. N. Bhat, S. Foley, D. Gruber, J. M. Burgess, S. McGlynn, J. McEnery, and N. Gehrels. Evidence for a Photospheric Component in the Prompt Emission of the Short GRB 120323A and Its Effects on the GRB Hardness-Luminosity Relation. *ApJ*, 770:32, June 2013. doi: 10.1088/0004-637X/770/1/32.

- S. Guiriec, C. Kouveliotou, F. Daigne, B. Zhang, R. Hascoët, R. S. Nemmen, D. J. Thompson, P. N. Bhat, N. Gehrels, M. M. Gonzalez, Y. Kaneko, J. McEnery, R. Mochkovitch, J. L. Racusin, F. Ryde, J. R. Sacahui, and A. M. Ünsal. Toward a Better Understanding of the GRB Phenomenon: a New Model for GRB Prompt Emission and its Effects on the New L_i^{NT} - $E_{peak,i}^{rest,NT}$ Relation. *ApJ*, 807:148, July 2015a. doi: 10.1088/0004-637X/807/2/148.
- S. Guiriec, R. Mochkovitch, T. Piran, F. Daigne, C. Kouveliotou, J. Racusin, N. Gehrels, and J. McEnery. GRB 131014A: A Laboratory for Studying the Thermal-like and Non-thermal Emissions in Gamma-Ray Bursts, and the New L_i^{nTh} - $E_{peak,i}^{nTh,rest}$ Relation. *ApJ*, 814:10, November 2015b. doi: 10.1088/0004-637X/814/1/10.
- S. Guiriec, M. M. Gonzalez, J. R. Sacahui, C. Kouveliotou, N. Gehrels, and J. McEnery. CGRO/BATSE Data Support the New Paradigm for GRB Prompt Emission and the New L_i^{nTh} - $E_{peak,i}^{nTh,rest}$ Relation. *ApJ*, 819:79, March 2016. doi: 10.3847/0004-637X/819/1/79.
- J. Hakkila and R. D. Preece. Gamma-Ray Burst Pulse Shapes: Evidence for Embedded Shock Signatures? *ApJ*, 783:88, March 2014. doi: 10.1088/0004-637X/783/2/88.
- J. Hakkila, T. W. Giblin, J. P. Norris, P. C. Fragile, and J. T. Bonnell. Correlations between Lag, Luminosity, and Duration in Gamma-Ray Burst Pulses. *ApJ*, 677:L81, April 2008. doi: 10.1086/588094.
- R. Hascoët, F. Daigne, and R. Mochkovitch. Prompt thermal emission in gamma-ray bursts. *A&A*, 551:A124, March 2013. doi: 10.1051/0004-6361/201220023.
- J. Heise, J. I. Zand, R. M. Kippen, and P. M. Woods. X-Ray Flashes and X-Ray Rich Gamma Ray Bursts. In E. Costa, F. Frontera, and J. Hjorth, editors, *Gamma-ray Bursts in the Afterglow Era*, page 16, 2001. doi: 10.1007/10853853\4.
- V. Heussaff, J.-L. Atteia, and Y. Zolnierowski. The E_{peak} - E_{iso} relation revisited with Fermi GRBs. Resolving a long-standing debate? *A&A*, 557:A100, September 2013. doi: 10.1051/0004-6361/201321528.
- J. Hjorth, J. Sollerman, P. Møller, J. P. U. Fynbo, S. E. Woosley, C. Kouveliotou, N. R. Tanvir, J. Greiner, M. I. Andersen, A. J. Castro-Tirado, J. M. Castro Cerón, A. S. Fruchter, J. Gorosabel, P. Jakobsson, L. Kaper, S. Klose, N. Masetti, H. Pedersen, K. Pedersen, E. Pian, E. Palazzi, J. E. Rhoads, E. Rol, E. P. J. van den Heuvel, P. M. Vreeswijk, D. Watson, and R. A. M. J. Wijers. A very energetic supernova associated with the γ -ray burst of 29 March 2003. *Nature*, 423:847–850, June 2003. doi: 10.1038/nature01750.

- I. Horváth. A Third Class of Gamma-Ray Bursts? *ApJ*, 508:757–759, December 1998. doi: 10.1086/306416.
- I. Horváth. A further study of the BATSE Gamma-Ray Burst duration distribution. *A&A*, 392:791–793, September 2002. doi: 10.1051/0004-6361:20020808.
- I. Horváth. Classification of BeppoSAX’s gamma-ray bursts. *Ap&SS*, 323:83–86, September 2009. doi: 10.1007/s10509-009-0039-1.
- I. Horváth, L. G. Balázs, Z. Bagoly, F. Ryde, and A. Mészáros. A new definition of the intermediate group of gamma-ray bursts. *A&A*, 447:23–30, February 2006. doi: 10.1051/0004-6361:20041129.
- I. Horváth, L. G. Balázs, Z. Bagoly, and P. Veres. Classification of Swift’s gamma-ray bursts. *A&A*, 489:L1–L4, October 2008. doi: 10.1051/0004-6361:200810269.
- I. Horváth, Z. Bagoly, L. G. Balázs, A. de Ugarte Postigo, P. Veres, and A. Mészáros. Detailed Classification of Swift’s Gamma-ray Bursts. *ApJ*, 713:552–557, April 2010. doi: 10.1088/0004-637X/713/1/552.
- D. Huja, A. Mészáros, and J. Řípa. A comparison of the gamma-ray bursts detected by BATSE and Swift. *A&A*, 504:67–71, September 2009. doi: 10.1051/0004-6361/200809802.
- S. Inoue, K. Omukai, and B. Ciardi. The radio to infrared emission of very high redshift gamma-ray bursts: probing early star formation through molecular and atomic absorption lines. *MNRAS*, 380:1715–1728, October 2007. doi: 10.1111/j.1365-2966.2007.12234.x.
- K. Ioka and P. Mészáros. Radio Afterglows of Gamma-Ray Bursts and Hypernovae at High Redshift and Their Potential for 21 Centimeter Absorption Studies. *ApJ*, 619:684–696, February 2005. doi: 10.1086/426785.
- K. Ioka and T. Nakamura. Peak Luminosity-Spectral Lag Relation Caused by the Viewing Angle of the Collimated Gamma-Ray Bursts. *ApJ*, 554:L163–L167, June 2001. doi: 10.1086/321717.
- H. Ito, S. Nagataki, M. Ono, S.-H. Lee, J. Mao, S. Yamada, A. Pe’er, A. Mizuta, and S. Harikae. Photospheric Emission from Stratified Jets. *ApJ*, 777:62, November 2013. doi: 10.1088/0004-637X/777/1/62.

- D. Kazanas, J. L. Racusin, J. Sultana, and A. Mastichiadis. The Statistics of the Prompt-to-Afterglow GRB Flux Ratios and the Supercritical Pile GRB Model. *ArXiv e-prints*, January 2015.
- M. Kendall and A. Stuart. *The advanced theory of statistics. Vol.2: Inference and relationship*. London: Griffin, 1973, 3rd ed., 1973.
- M. G. Kendall. A new measure of rank correlation. *Biometrika*, 30(1-2):81–93, 1938. doi: 10.1093/biomet/30.1-2.81. URL <http://biomet.oxfordjournals.org/content/30/1-2/81.short>.
- R. M. Kippen, P. M. Woods, J. Heise, J. I. Zand, R. D. Preece, and M. S. Briggs. BATSE Observations of Fast X-Ray Transients Detected by BeppoSAX-WFC. In E. Costa, F. Frontera, and J. Hjorth, editors, *Gamma-ray Bursts in the Afterglow Era*, page 22, 2001. doi: 10.1007/10853853\5.
- M. D. Kistler, H. Yüksel, J. F. Beacom, A. M. Hopkins, and J. S. B. Wyithe. The Star Formation Rate in the Reionization Era as Indicated by Gamma-Ray Bursts. *ApJ*, 705:L104–L108, November 2009. doi: 10.1088/0004-637X/705/2/L104.
- R. W. Klebesadel, I. B. Strong, and R. A. Olson. Observations of Gamma-Ray Bursts of Cosmic Origin. *ApJ*, 182:L85, June 1973. doi: 10.1086/181225.
- D. Kocevski and E. Liang. The Connection between Spectral Evolution and Gamma-Ray Burst Lag. *ApJ*, 594:385–389, September 2003. doi: 10.1086/376868.
- C. Koen and A. Bere. On multiple classes of gamma-ray bursts, as deduced from autocorrelation functions or bivariate duration/hardness ratio distributions. *MNRAS*, 420:405–415, February 2012. doi: 10.1111/j.1365-2966.2011.20045.x.
- C. Kouveliotou, C. A. Meegan, G. J. Fishman, N. P. Bhat, M. S. Briggs, T. M. Koshut, W. S. Paciesas, and G. N. Pendleton. Identification of two classes of gamma-ray bursts. *ApJ*, 413:L101–L104, August 1993. doi: 10.1086/186969.
- P. Kumar and B. Zhang. The physics of gamma-ray bursts and relativistic jets. *Phys. Rep.*, 561:1–109, February 2015. doi: 10.1016/j.physrep.2014.09.008.
- D. Q. Lamb, T. Q. Donaghy, and C. Graziani. A unified jet model of X-ray flashes and γ -ray bursts. *New A Rev.*, 48:459–464, April 2004. doi: 10.1016/j.newar.2003.12.030.
- T. Laskar, E. Berger, N. Tanvir, B. A. Zauderer, R. Margutti, A. Levan, D. Perley, W.-f. Fong, K. Wiersema, K. Menten, and M. Hrudkova. GRB 120521C at $z \sim 6$ and the

- Properties of High-redshift γ -Ray Bursts. *ApJ*, 781:1, January 2014. doi: 10.1088/0004-637X/781/1/1.
- T. Laskar, E. Berger, R. Margutti, D. Perley, B. A. Zauderer, R. Sari, and W.-f. Fong. Energy Injection in Gamma-ray Burst Afterglows. *ArXiv e-prints*, April 2015.
- A. Lee, E. D. Bloom, and V. Petrosian. Properties of Gamma-Ray Burst Time Profiles Using Pulse Decomposition Analysis. *ApJS*, 131:1–19, November 2000. doi: 10.1086/317364.
- T. T. Lee and V. Petrosian. Distributions of Peak Flux and Duration for Gamma-Ray Bursts. *ApJ*, 470:479, October 1996. doi: 10.1086/177879.
- W. H. Lei, D. X. Wang, L. Zhang, Z. M. Gan, Y. C. Zou, and Y. Xie. Magnetically Torqued Neutrino-dominated Accretion Flows for Gamma-ray Bursts. *ApJ*, 700:1970–1976, August 2009. doi: 10.1088/0004-637X/700/2/1970.
- A. J. Levan. Swift discoveries of new populations of extremely long duration high energy transient. *Journal of High Energy Astrophysics*, 7:44–55, September 2015. doi: 10.1016/j.jheap.2015.05.004.
- A. J. Levan, N. R. Tanvir, R. L. C. Starling, K. Wiersema, K. L. Page, D. A. Perley, S. Schulze, G. A. Wynn, R. Chornock, J. Hjorth, S. B. Cenko, A. S. Fruchter, P. T. O’Brien, G. C. Brown, R. L. Tunnicliffe, D. Malesani, P. Jakobsson, D. Watson, E. Berger, D. Bersier, B. E. Cobb, S. Covino, A. Cucchiara, A. de Ugarte Postigo, D. B. Fox, A. Gal-Yam, P. Goldoni, J. Gorosabel, L. Kaper, T. Krühler, R. Karjalainen, J. P. Osborne, E. Pian, R. Sánchez-Ramírez, B. Schmidt, I. Skillen, G. Tagliferri, C. Thöne, O. Vaduvescu, R. A. M. J. Wijers, and B. A. Zauderer. A New Population of Ultra-long Duration Gamma-Ray Bursts. *ApJ*, 781:13, January 2014. doi: 10.1088/0004-637X/781/1/13.
- L.-X. Li and B. Paczyński. Improved correlation between the variability and peak luminosity of gamma-ray bursts. *MNRAS*, 366:219–226, February 2006. doi: 10.1111/j.1365-2966.2005.09836.x.
- X. Li, F.-W. Zhang, Q. Yuan, Z.-P. Jin, Y.-Z. Fan, S.-M. Liu, and D.-M. Wei. Implication of the association between GBM transient 150914 and LIGO Gravitational Wave event GW150914. *ArXiv e-prints*, February 2016.
- E. Liang and V. Kargatis. Dependence of the spectral evolution of γ -ray bursts on their photon fluence. *Nature*, 381:49–51, May 1996. doi: 10.1038/381049a0.

- E. Liang and B. Zhang. Model-independent Multivariable Gamma-Ray Burst Luminosity Indicator and Its Possible Cosmological Implications. *ApJ*, 633:611–623, November 2005. doi: 10.1086/491594.
- E. W. Liang, Z. G. Dai, and X. F. Wu. The Luminosity- E_p Relation within Gamma-Ray Bursts and the Implications for Fireball Models. *ApJ*, 606:L29–L32, May 2004. doi: 10.1086/421047.
- E.-W. Liang, J. L. Racusin, B. Zhang, B.-B. Zhang, and D. N. Burrows. A Comprehensive Analysis of Swift XRT Data. III. Jet Break Candidates in X-Ray and Optical Afterglow Light Curves. *ApJ*, 675:528–552, March 2008. doi: 10.1086/524701.
- E.-W. Liang, S.-X. Yi, J. Zhang, H.-J. Lü, B.-B. Zhang, and B. Zhang. Constraining Gamma-ray Burst Initial Lorentz Factor with the Afterglow Onset Feature and Discovery of a Tight Γ_0 - $E_{\text{gamma,iso}}$ Correlation. *ApJ*, 725:2209–2224, December 2010. doi: 10.1088/0004-637X/725/2/2209.
- H.-N. Lin, X. Li, S. Wang, and Z. Chang. Are long gamma-ray bursts standard candles? *MNRAS*, 453:128–132, October 2015. doi: 10.1093/mnras/stv1624.
- H.-N. Lin, X. Li, and Z. Chang. Effect of GRB spectra on the empirical luminosity correlations and the GRB Hubble diagram. *MNRAS*, April 2016. doi: 10.1093/mnras/stw817.
- Y. Lithwick and R. Sari. Lower Limits on Lorentz Factors in Gamma-Ray Bursts. *ApJ*, 555: 540–545, July 2001. doi: 10.1086/321455.
- O. M. Littlejohns and N. R. Butler. Investigating signatures of cosmological time dilation in duration measures of prompt gamma-ray burst light curves. *MNRAS*, 444:3948–3960, November 2014. doi: 10.1093/mnras/stu1767.
- O. M. Littlejohns, N. R. Tanvir, R. Willingale, P. A. Evans, P. T. O’Brien, and A. J. Levan. Are gamma-ray bursts the same at high redshift and low redshift? *MNRAS*, 436: 3640–3655, December 2013. doi: 10.1093/mnras/stt1841.
- N. M. Lloyd and V. Petrosian. Distribution of Spectral Characteristics and the Cosmological Evolution of Gamma-Ray Bursts. *ApJ*, 511:550–561, February 1999. doi: 10.1086/306719.
- N. M. Lloyd, V. Petrosian, and R. S. Mallozzi. Cosmological versus Intrinsic: The Correlation between Intensity and the Peak of the νF Spectrum of Gamma-Ray Bursts. *ApJ*, 534: 227–238, May 2000a. doi: 10.1086/308742.

- N. M. Lloyd, V. Petrosian, and R. D. Preece. Synchrotron emission as the source of GRB spectra, Part II: Observations. In R. M. Kippen, R. S. Mallozzi, and G. J. Fishman, editors, *Gamma-ray Bursts, 5th Huntsville Symposium*, volume 526 of *American Institute of Physics Conference Series*, pages 155–159, September 2000b. doi: 10.1063/1.1361525.
- N. M. Lloyd-Ronning and V. Petrosian. Interpreting the Behavior of Time-resolved Gamma-Ray Burst Spectra. *ApJ*, 565:182–194, January 2002. doi: 10.1086/324484.
- N. M. Lloyd-Ronning and E. Ramirez-Ruiz. On the Spectral Energy Dependence of Gamma-Ray Burst Variability. *ApJ*, 576:101–106, September 2002. doi: 10.1086/341723.
- A. Loeb. Electromagnetic Counterparts to Black Hole Mergers Detected by LIGO. *ApJ*, 819:L21, March 2016. doi: 10.3847/2041-8205/819/2/L21.
- J. Lü, Y.-C. Zou, W.-H. Lei, B. Zhang, Q. Wu, D.-X. Wang, E.-W. Liang, and H.-J. Lü. Lorentz-factor-Isotropic-luminosity/Energy Correlations of Gamma-Ray Bursts and Their Interpretation. *ApJ*, 751:49, May 2012a. doi: 10.1088/0004-637X/751/1/49.
- J. Lü, Y.-C. Zou, W.-H. Lei, B. Zhang, Q. Wu, D.-X. Wang, E.-W. Liang, and H.-J. Lü. Lorentz-factor-Isotropic-luminosity/Energy Correlations of Gamma-Ray Bursts and Their Interpretation. *ApJ*, 751:49, May 2012b. doi: 10.1088/0004-637X/751/1/49.
- R. Lu and E. Liang. Luminosity-peak energy relation in the decay phases of gamma-ray burst pulses. *Science China Physics, Mechanics, and Astronomy*, 53:163–170, January 2010. doi: 10.1007/s11433-010-0086-1.
- R.-J. Lu, J.-J. Wei, E.-W. Liang, B.-B. Zhang, H.-J. Lü, L.-Z. Lü, W.-H. Lei, and B. Zhang. A Comprehensive Analysis of Fermi Gamma-Ray Burst Data. II. E_p Evolution Patterns and Implications for the Observed Spectrum-Luminosity Relations. *ApJ*, 756:112, September 2012. doi: 10.1088/0004-637X/756/2/112.
- M. Lyutikov. Fermi GBM signal contemporaneous with GW150914 - an unlikely association. *ArXiv e-prints*, February 2016.
- M. Magliocchetti, G. Ghirlanda, and A. Celotti. Evidence for anisotropy in the distribution of short-lived gamma-ray bursts. *MNRAS*, 343:255–258, July 2003. doi: 10.1046/j.1365-8711.2003.06657.x.
- D. Malesani, G. Tagliaferri, G. Chincarini, S. Covino, M. Della Valle, D. Fugazza, P. A. Mazzali, F. M. Zerbi, P. D’Avanzo, S. Kalogerakos, A. Simoncelli, L. A. Antonelli, L. Burderi, S. Campana, A. Cucchiara, F. Fiore, G. Ghirlanda, P. Goldoni, D. Götz,

- S. Mereghetti, I. F. Mirabel, P. Romano, L. Stella, T. Minezaki, Y. Yoshii, and K. Nomoto. SN 2003lw and GRB 031203: A Bright Supernova for a Faint Gamma-Ray Burst. *ApJ*, 609:L5–L8, July 2004. doi: 10.1086/422684.
- R. S. Mallozzi, W. S. Paciesas, G. N. Pendleton, M. S. Briggs, R. D. Preece, C. A. Meegan, and G. J. Fishman. The ν F ν Peak Energy Distributions of Gamma-Ray Bursts Observed by BATSE. *ApJ*, 454:597, December 1995. doi: 10.1086/176513.
- R. S. Mallozzi, G. N. Pendleton, W. S. Paciesas, R. D. Preece, and M. S. Briggs. Gamma-ray burst spectra and the hardness-intensity correlation. In C. A. Meegan, R. D. Preece, and T. M. Koshut, editors, *Gamma-Ray Bursts, 4th Huntsville Symposium*, volume 428 of *American Institute of Physics Conference Series*, pages 273–277, May 1998. doi: 10.1063/1.55334.
- R. Margutti, C. Guidorzi, G. Chincarini, M. G. Bernardini, F. Genet, J. Mao, and F. Pasotti. Lag-luminosity relation in γ -ray burst X-ray flares: a direct link to the prompt emission. *MNRAS*, 406:2149–2167, August 2010. doi: 10.1111/j.1365-2966.2010.16824.x.
- E. P. Mazets, S. V. Golenetskii, V. N. Ilinskii, V. N. Panov, R. L. Aptekar, I. A. Gurian, M. P. Proskura, I. A. Sokolov, Z. I. Sokolova, and T. V. Kharitonova. Catalog of cosmic gamma-ray bursts from the KONUS experiment data. I. *Ap&SS*, 80:3–83, November 1981. doi: 10.1007/BF00649140.
- C. A. Meegan, G. J. Fishman, R. B. Wilson, J. M. Horack, M. N. Brock, W. S. Paciesas, G. N. Pendleton, and C. Kouveliotou. Spatial distribution of gamma-ray bursts observed by BATSE. *Nature*, 355:143–145, January 1992. doi: 10.1038/355143a0.
- A. Melandri, C. G. Mundell, S. Kobayashi, C. Guidorzi, A. Gomboc, I. A. Steele, R. J. Smith, D. Bersier, C. J. Mottram, D. Carter, M. F. Bode, P. T. O’Brien, N. R. Tanvir, E. Rol, and R. Chapman. The Early-Time Optical Properties of Gamma-Ray Burst Afterglows. *ApJ*, 686:1209–1230, October 2008. doi: 10.1086/591243.
- S. Mendoza, J. C. Hidalgo, D. Olvera, and J. I. Cabrera. Internal shocks in relativistic jets with time-dependent sources. *MNRAS*, 395:1403–1408, May 2009. doi: 10.1111/j.1365-2966.2009.14483.x.
- A. Mészáros and J. Štoček. Anisotropy in the angular distribution of the long gamma-ray bursts? *A&A*, 403:443–448, May 2003. doi: 10.1051/0004-6361:20030328.
- A. Mészáros, Z. Bagoly, I. Horváth, L. G. Balázs, and R. Vavrek. A Remarkable Angular Distribution of the Intermediate Subclass of Gamma-Ray Bursts. *ApJ*, 539:98–101, August 2000a. doi: 10.1086/309193.

- A. Mészáros, Z. Bagoly, and R. Vavrek. On the existence of the intrinsic anisotropies in the angular distributions of gamma-ray bursts. *A&A*, 354:1–6, February 2000b.
- A. Mészáros, L. G. Balázs, Z. Bagoly, and P. Veres. Impact on Cosmology of the Celestial Anisotropy of the Short Gamma-Ray Bursts. *Baltic Astronomy*, 18:293–296, 2009.
- P. Mészáros. Theoretical models of gamma-ray bursts. In C. A. Meegan, R. D. Preece, and T. M. Koshut, editors, *Gamma-Ray Bursts, 4th Hunstville Symposium*, volume 428 of *American Institute of Physics Conference Series*, pages 647–656, May 1998. doi: 10.1063/1.55394.
- P. Mészáros. Gamma-ray bursts. *Reports on Progress in Physics*, 69:2259–2321, August 2006a. doi: 10.1088/0034-4885/69/8/R01.
- P. Mészáros. Gamma-ray bursts. *Reports on Progress in Physics*, 69:2259–2321, August 2006b. doi: 10.1088/0034-4885/69/8/R01.
- P. Mészáros and M. J. Rees. Gamma-ray bursts. In A. Ashtekar, B. Berger, J. Isenberg, and M. A. H MacCallum, editors, *General Relativity and Gravitation: A Centennial Perspective*, Cambridge Univ. Press, Cambridge, pages 148–161, June 2015.
- M. R. Metzger, S. G. Djorgovski, S. R. Kulkarni, C. C. Steidel, K. L. Adelberger, D. A. Frail, E. Costa, and F. Frontera. Spectral constraints on the redshift of the optical counterpart to the γ -ray burst of 8 May 1997. *Nature*, 387:878–880, June 1997. doi: 10.1038/43132.
- R. Mochkovitch and L. Nava. The $E_p - E_{\text{iso}}$ relation and the internal shock model. *A&A*, 577:A31, May 2015. doi: 10.1051/0004-6361/201424490.
- B. J. Morsony, J. C. Workman, and D. M. Ryan. Modeling the Afterglow of GW150914-GBM. *ArXiv e-prints*, February 2016.
- S. Mukherjee, E. D. Feigelson, G. Jogesh Babu, F. Murtagh, C. Fraley, and A. Raftery. Three Types of Gamma-Ray Bursts. *ApJ*, 508:314–327, November 1998. doi: 10.1086/306386.
- E. Nakar. Short-hard gamma-ray bursts. *Phys. Rep.*, 442:166–236, April 2007. doi: 10.1016/j.physrep.2007.02.005.
- E. Nakar and T. Piran. Outliers to the peak energy-isotropic energy relation in gamma-ray bursts. *MNRAS*, 360:L73–L76, June 2005. doi: 10.1111/j.1745-3933.2005.00049.x.

- R. Narayan, B. Paczynski, and T. Piran. Gamma-ray bursts as the death throes of massive binary stars. *ApJ*, 395:L83–L86, August 1992. doi: 10.1086/186493.
- P. Narayana Bhat, C. A. Meegan, A. von Kienlin, W. S. Paciesas, M. S. Briggs, J. M. Burgess, E. Burns, V. Chaplin, W. H. Cleveland, A. C. Collazzi, V. Connaughton, A. M. Diekmann, G. Fitzpatrick, M. H. Gibby, M. M. Giles, A. M. Goldstein, J. Greiner, P. A. Jenke, R. M. Kippen, C. Kouveliotou, B. Mailyan, S. McBreen, V. Pelassa, R. D. Preece, O. J. Roberts, L. S. Sparke, M. Stanbro, P. Veres, C. A. Wilson-Hodge, S. Xiong, G. Younes, H.-F. Yu, and B. Zhang. The Third Fermi GBM Gamma-Ray Burst Catalog: The First Six Years. *ApJS*, 223:28, April 2016. doi: 10.3847/0067-0049/223/2/28.
- L. Nava, G. Ghisellini, G. Ghirlanda, F. Tavecchio, and C. Firmani. On the interpretation of spectral-energy correlations in long gamma-ray bursts. *A&A*, 450:471–481, May 2006. doi: 10.1051/0004-6361:20054211.
- L. Nava, R. Salvaterra, G. Ghirlanda, G. Ghisellini, S. Campana, S. Covino, G. Cusumano, P. D’Avanzo, V. D’Elia, D. Fugazza, A. Melandri, B. Sbarufatti, S. D. Vergani, and G. Tagliaferri. A complete sample of bright Swift long gamma-ray bursts: testing the spectral-energy correlations. *MNRAS*, 421:1256–1264, April 2012. doi: 10.1111/j.1365-2966.2011.20394.x.
- J. P. Norris and J. T. Bonnell. Short Gamma-Ray Bursts with Extended Emission. *ApJ*, 643:266–275, May 2006. doi: 10.1086/502796.
- J. P. Norris, R. J. Nemiroff, J. T. Bonnell, J. D. Scargle, C. Kouveliotou, W. S. Paciesas, C. A. Meegan, and G. J. Fishman. Attributes of Pulses in Long Bright Gamma-Ray Bursts. *ApJ*, 459:393, March 1996. doi: 10.1086/176902.
- J. P. Norris, G. F. Marani, and J. T. Bonnell. Connection between Energy-dependent Lags and Peak Luminosity in Gamma-Ray Bursts. *ApJ*, 534:248–257, May 2000. doi: 10.1086/308725.
- J. A. Nousek, C. Kouveliotou, D. Grupe, K. L. Page, J. Granot, E. Ramirez-Ruiz, S. K. Patel, D. N. Burrows, V. Mangano, S. Barthelmy, A. P. Beardmore, S. Campana, M. Capalbi, G. Chincarini, G. Cusumano, A. D. Falcone, N. Gehrels, P. Giommi, M. R. Goad, O. Godet, C. P. Hurkett, J. A. Kennea, A. Moretti, P. T. O’Brien, J. P. Osborne, P. Romano, G. Tagliaferri, and A. A. Wells. Evidence for a Canonical Gamma-Ray Burst Afterglow Light Curve in the Swift XRT Data. *ApJ*, 642:389–400, May 2006. doi: 10.1086/500724.

- S. R. Oates, M. J. Page, P. Schady, M. de Pasquale, P. A. Evans, K. L. Page, M. M. Chester, P. A. Curran, T. S. Koch, N. P. M. Kuin, P. W. A. Roming, M. H. Siegel, S. Zane, and J. A. Nousek. A statistical comparison of the optical/UV and X-ray afterglows of gamma-ray bursts using the Swift Ultraviolet Optical and X-ray Telescopes. *MNRAS*, 412:561–579, March 2011. doi: 10.1111/j.1365-2966.2010.17928.x.
- P. T. O’Brien and R. Willingale. Using Swift observations of prompt and afterglow emission to classify GRBs. *Royal Society of London Philosophical Transactions Series A*, 365: 1179–1188, May 2007. doi: 10.1098/rsta.2006.1984.
- P. T. O’Brien, R. Willingale, J. Osborne, M. R. Goad, K. L. Page, S. Vaughan, E. Rol, A. Beardmore, O. Godet, C. P. Hurkett, A. Wells, B. Zhang, S. Kobayashi, D. N. Burrows, J. A. Nousek, J. A. Kennea, A. Falcone, D. Grupe, N. Gehrels, S. Barthelmy, J. Cannizzo, J. Cummings, J. E. Hill, H. Krimm, G. Chincarini, G. Tagliaferri, S. Campana, A. Moretti, P. Giommi, M. Perri, V. Mangano, and V. LaParola. The Early X-Ray Emission from GRBs. *ApJ*, 647:1213–1237, August 2006. doi: 10.1086/505457.
- B. Paczynski. On the Galactic origin of gamma-ray bursts. *Acta Astron.*, 41:157–166, 1991a.
- B. Paczynski. Cosmological gamma-ray bursts. *Acta Astron.*, 41:257–267, 1991b.
- A. Panaitescu. An external-shock origin of the relation for gamma-ray bursts. *MNRAS*, 393: 1010–1015, March 2009. doi: 10.1111/j.1365-2966.2008.14240.x.
- A. Panaitescu and P. Kumar. Properties of Relativistic Jets in Gamma-Ray Burst Afterglows. *ApJ*, 571:779–789, June 2002. doi: 10.1086/340094.
- Z. Y. Peng, Y. Yin, T. F. Yi, Y. Y. Bao, and H. Wu. A comprehensive comparative study of temporal properties between X-ray flares and GRB pulses. *Ap&SS*, 355:95–103, January 2015. doi: 10.1007/s10509-014-2149-7.
- D. A. Perley, N. R. Tanvir, J. Hjorth, T. Laskar, E. Berger, R. Chary, A. de Ugarte Postigo, J. P. U. Fynbo, T. Krühler, A. J. Levan, M. J. Michałowski, and S. Schulze. The Swift GRB Host Galaxy Legacy Survey - II. Rest-Frame NIR Luminosity Distribution and Evidence for a Near-Solar Metallicity Threshold. *ArXiv e-prints*, April 2015.
- R. Perna, D. Lazzati, and B. Giacomazzo. Short Gamma-Ray Bursts from the Merger of Two Black Holes. *ApJ*, 821:L18, April 2016. doi: 10.3847/2041-8205/821/1/L18.
- T. Piran. The physics of gamma-ray bursts. *Reviews of Modern Physics*, 76:1143–1210, October 2004. doi: 10.1103/RevModPhys.76.1143.

- C. Porciani and P. Madau. On the Association of Gamma-Ray Bursts with Massive Stars: Implications for Number Counts and Lensing Statistics. *ApJ*, 548:522–531, February 2001. doi: 10.1086/319027.
- R. D. Preece, M. S. Briggs, R. S. Mallozzi, G. N. Pendleton, W. S. Paciesas, and D. L. Band. The BATSE Gamma-Ray Burst Spectral Catalog. I. High Time Resolution Spectroscopy of Bright Bursts Using High Energy Resolution Data. *ApJS*, 126:19–36, January 2000. doi: 10.1086/313289.
- S. Qi and T. Lu. A New Luminosity Relation for Gamma-ray Bursts and its Implication. *ApJ*, 717:1274–1278, July 2010. doi: 10.1088/0004-637X/717/2/1274.
- Y.-P. Qin and Z.-F. Chen. Statistical classification of gamma-ray bursts based on the Amati relation. *MNRAS*, 430:163–173, March 2013. doi: 10.1093/mnras/sts547.
- F. Quilligan, B. McBreen, L. Hanlon, S. McBreen, K. J. Hurley, and D. Watson. Temporal properties of gamma ray bursts as signatures of jets from the central engine. *A&A*, 385:377–398, April 2002. doi: 10.1051/0004-6361:20020038.
- E. Ramirez-Ruiz. Photospheric signatures imprinted on the γ -ray burst spectra. *MNRAS*, 363:L61–L65, October 2005. doi: 10.1111/j.1745-3933.2005.00089.x.
- M. J. Rees and P. Mészáros. Dissipative Photosphere Models of Gamma-Ray Bursts and X-Ray Flashes. *ApJ*, 628:847–852, August 2005. doi: 10.1086/430818.
- D. E. Reichart and M. C. Nysewander. GRB Variability-Luminosity Correlation Confirmed. *ArXiv Astrophysics e-prints*, August 2005.
- D. E. Reichart, D. Q. Lamb, E. E. Fenimore, E. Ramirez-Ruiz, T. L. Cline, and K. Hurley. A Possible Cepheid-like Luminosity Estimator for the Long Gamma-Ray Bursts. *ApJ*, 552:57–71, May 2001. doi: 10.1086/320434.
- J. E. Rhoads. How to Tell a Jet from a Balloon: A Proposed Test for Beaming in Gamma-Ray Bursts. *ApJ*, 487:L1–L4, September 1997. doi: 10.1086/310876.
- D. Rizzuto, C. Guidorzi, P. Romano, S. Covino, S. Campana, M. Capalbi, G. Chincarini, G. Cusumano, D. Fugazza, V. Mangano, A. Moretti, M. Perri, and G. Tagliaferri. Testing the gamma-ray burst variability/peak luminosity correlation on a Swift homogeneous sample. *MNRAS*, 379:619–628, August 2007. doi: 10.1111/j.1365-2966.2007.11880.x.

- S. A. Rodney, A. G. Riess, D. M. Scolnic, D. O. Jones, S. Hemmati, A. Molino, C. McCully, B. Mobasher, L.-G. Strolger, O. Graur, B. Hayden, and S. Casertano. Two SNe Ia at Redshift ~ 2 : Improved Classification and Redshift Determination with Medium-band Infrared Imaging. *AJ*, 150:156, November 2015. doi: 10.1088/0004-6256/150/5/156.
- A. Roychoudhury, S. K. Sarkar, and A. Bhadra. Spectral Lag Features of GRB 060814 from Swift BAT and Suzaku Observations. *ApJ*, 782:105, February 2014. doi: 10.1088/0004-637X/782/2/105.
- G. Ryan, H. van Eerten, A. MacFadyen, and B.-B. Zhang. Gamma-Ray Bursts are Observed Off-axis. *ApJ*, 799:3, January 2015. doi: 10.1088/0004-637X/799/1/3.
- F. Ryde. Is Thermal Emission in Gamma-Ray Bursts Ubiquitous? *ApJ*, 625:L95–L98, June 2005. doi: 10.1086/431239.
- F. Ryde and V. Petrosian. Gamma-Ray Burst Spectra and Light Curves as Signatures of a Relativistically Expanding Plasma. *ApJ*, 578:290–303, October 2002. doi: 10.1086/342271.
- F. Ryde and R. Svensson. On the Variety of the Spectral and Temporal Behavior of Long Gamma-Ray Burst Pulses. *ApJ*, 566:210–228, February 2002. doi: 10.1086/337962.
- E. S. Rykoff, F. Aharonian, C. W. Akerlof, M. C. B. Ashley, S. D. Barthelmy, H. A. Flewelling, N. Gehrels, E. Göğüş, T. Güver, Ü. Kiziloğlu, H. A. Krimm, T. A. McKay, M. Özel, A. Phillips, R. M. Quimby, G. Rowell, W. Rujopakarn, B. E. Schaefer, D. A. Smith, W. T. Vestrand, J. C. Wheeler, J. Wren, F. Yuan, and S. A. Yost. Looking Into the Fireball: ROTSE-III and Swift Observations of Early Gamma-ray Burst Afterglows. *ApJ*, 702:489–505, September 2009. doi: 10.1088/0004-637X/702/1/489.
- T. Sakamoto, D. Q. Lamb, C. Graziani, T. Q. Donaghy, M. Suzuki, G. Ricker, J.-L. Atteia, N. Kawai, A. Yoshida, Y. Shirasaki, T. Tamagawa, K. Torii, M. Matsuoka, E. E. Fenimore, M. Galassi, T. Tavenner, J. Doty, R. Vanderspek, G. B. Crew, J. Villasenor, N. Butler, G. Prigozhin, J. G. Jernigan, C. Barraud, M. Boer, J.-P. Dezalay, J.-F. Olive, K. Hurley, A. Levine, G. Monnelly, F. Martel, E. Morgan, S. E. Woosley, T. Cline, J. Braga, R. Manchanda, G. Pizzichini, K. Takagishi, and M. Yamauchi. High Energy Transient Explorer 2 Observations of the Extremely Soft X-Ray Flash XRF 020903. *ApJ*, 602:875–885, February 2004. doi: 10.1086/381232.
- T. Sakamoto, J. E. Hill, R. Yamazaki, L. Angelini, H. A. Krimm, G. Sato, S. Swindell, K. Takami, and J. P. Osborne. Evidence of Exponential Decay Emission in the Swift Gamma-Ray Bursts. *ApJ*, 669:1115–1129, November 2007. doi: 10.1086/521640.

- J. D. Salmonson. On the Kinematic Origin of the Luminosity-Pulse Lag Relationship in Gamma-Ray Bursts. *ApJ*, 544:L115–L117, December 2000. doi: 10.1086/317305.
- J. D. Salmonson and T. J. Galama. Discovery of a Tight Correlation between Pulse Lag/Luminosity and Jet-Break Times: A Connection between Gamma-Ray Bursts and Afterglow Properties. *ApJ*, 569:682–688, April 2002. doi: 10.1086/339391.
- R. Salvaterra. High redshift Gamma-Ray Bursts. *Journal of High Energy Astrophysics*, 7: 35–43, September 2015. doi: 10.1016/j.jheap.2015.03.001.
- R. Sari and T. Piran. GRB 990123: The Optical Flash and the Fireball Model. *ApJ*, 517: L109–L112, June 1999. doi: 10.1086/312039.
- R. Sari, T. Piran, and J. P. Halpern. Jets in Gamma-Ray Bursts. *ApJ*, 519:L17–L20, July 1999. doi: 10.1086/312109.
- V. Savchenko, C. Ferrigno, S. Mereghetti, L. Natalucci, A. Bazzano, E. Bozzo, S. Brandt, T. J.-L. Courvoisier, R. Diehl, L. Hanlon, A. von Kienlin, E. Kuulkers, P. Laurent, F. Lebrun, J. P. Roques, P. Ubertini, and G. Weidenspointner. INTEGRAL Upper Limits on Gamma-Ray Emission Associated with the Gravitational Wave Event GW150914. *ApJ*, 820:L36, April 2016. doi: 10.3847/2041-8205/820/2/L36.
- B. Schaefer. Four luminosity indicators for gamma-ray bursts. In *34th COSPAR Scientific Assembly*, volume 34 of *COSPAR Meeting*, page 1141, 2002.
- B. E. Schaefer. Explaining the Gamma-Ray Burst E_{peak} Distribution. *ApJ*, 583:L71–L74, February 2003a. doi: 10.1086/368106.
- B. E. Schaefer. Gamma-Ray Burst Hubble Diagram to $z=4.5$. *ApJ*, 583:L67–L70, February 2003b. doi: 10.1086/368104.
- B. E. Schaefer. Explaining the Gamma-Ray Burst Lag/Luminosity Relation. *ApJ*, 602: 306–311, February 2004. doi: 10.1086/380898.
- B. E. Schaefer. The Hubble Diagram to Redshift > 6 from 69 Gamma-Ray Bursts. *ApJ*, 660:16–46, May 2007. doi: 10.1086/511742.
- B. E. Schaefer, M. Deng, and D. L. Band. Redshifts and Luminosities for 112 Gamma-Ray Bursts. *ApJ*, 563:L123–L127, December 2001. doi: 10.1086/338651.
- B.E. Schaefer. Gamma-ray bursts: The brightest explosions in the universe, 2002.

- S. Schulze, D. Malesani, A. Cucchiara, N. R. Tanvir, T. Krühler, A. de Ugarte Postigo, G. Leloudas, J. Lyman, D. Bersier, K. Wiersema, D. A. Perley, P. Schady, J. Gorosabel, J. P. Anderson, A. J. Castro-Tirado, S. B. Cenko, A. De Cia, L. E. Ellerbroek, J. P. U. Fynbo, J. Greiner, J. Hjorth, D. A. Kann, L. Kaper, S. Klose, A. J. Levan, S. Martín, P. T. O’Brien, K. L. Page, G. Pignata, S. Rapaport, R. Sánchez-Ramírez, J. Sollerman, I. A. Smith, M. Sparre, C. C. Thöne, D. J. Watson, D. Xu, F. E. Bauer, M. Bayliss, G. Björnsson, M. Bremer, Z. Cano, S. Covino, V. D’Elia, D. A. Frail, S. Geier, P. Goldoni, O. E. Hartoog, P. Jakobsson, H. Korhonen, K. Y. Lee, B. Milvang-Jensen, M. Nardini, A. Nicuesa Guelbenzu, M. Oguri, S. B. Pandey, G. Petitpas, A. Rossi, A. Sandberg, S. Schmidl, G. Tagliaferri, R. P. J. Tilanus, J. M. Winters, D. Wright, and E. Wuyts. GRB 120422A/SN 2012bz: Bridging the gap between low- and high-luminosity gamma-ray bursts. *A&A*, 566:A102, June 2014. doi: 10.1051/0004-6361/201423387.
- M. Sparre, J. Sollerman, J. P. U. Fynbo, D. Malesani, P. Goldoni, A. de Ugarte Postigo, S. Covino, V. D’Elia, H. Flores, F. Hammer, J. Hjorth, P. Jakobsson, L. Kaper, G. Leloudas, A. J. Levan, B. Milvang-Jensen, S. Schulze, G. Tagliaferri, N. R. Tanvir, D. J. Watson, K. Wiersema, and R. A. M. J. Wijers. Spectroscopic Evidence for SN 2010ma Associated with GRB 101219B. *ApJ*, 735:L24, July 2011. doi: 10.1088/2041-8205/735/1/L24.
- C. Spearman. The proof and measurement of association between two things. *The American Journal of Psychology*, 15(1):72–101, 1904. ISSN 00029556. URL <http://www.jstor.org/stable/1412159>.
- B. E. Stern and R. Svensson. Evidence for ”Chain Reaction” in the Time Profiles of Gamma-Ray Bursts. *ApJ*, 469:L109, October 1996. doi: 10.1086/310267.
- G. Stratta, D. Guetta, V. D’Elia, M. Perri, S. Covino, and L. Stella. Evidence for an anti-correlation between the duration of the shallow decay phase of GRB X-ray afterglows and redshift. *A&A*, 494:L9–L12, February 2009. doi: 10.1051/0004-6361:200811335.
- J. Sultana, D. Kazanas, and K. Fukumura. Luminosity Correlations for Gamma-Ray Bursts and Implications for Their Prompt and Afterglow Emission Mechanisms. *ApJ*, 758:32, October 2012. doi: 10.1088/0004-637X/758/1/32.
- M. Tarnopolski. Testing the anisotropy in the angular distribution of *Fermi*/GBM gamma-ray bursts. *ArXiv e-prints*, December 2015a.
- M. Tarnopolski. Analysis of Fermi gamma-ray burst duration distribution. *A&A*, 581:A29, September 2015b. doi: 10.1051/0004-6361/201526415.

- M. Tarnopolski. On the limit between short and long GRBs. *Ap&SS*, 359:20, September 2015c. doi: 10.1007/s10509-015-2473-6.
- M. Tarnopolski. Analysis of gamma-ray burst duration distribution using mixtures of skewed distributions. *MNRAS*, 458:2024–2031, May 2016a. doi: 10.1093/mnras/stw429.
- M. Tarnopolski. Analysis of the observed and intrinsic durations of gamma-ray bursts with known redshift. *Ap&SS*, 361:125, March 2016b. doi: 10.1007/s10509-016-2687-2.
- M. Tarnopolski. Analysis of the observed and intrinsic durations of Swift/BAT gamma-ray bursts. *New A*, 46:54–59, July 2016c. doi: 10.1016/j.newast.2015.12.006.
- L. Titarchuk, R. Farinelli, F. Frontera, and L. Amati. An Upscattering Spectral Formation Model for the Prompt Emission of Gamma-Ray Bursts. *ApJ*, 752:116, June 2012. doi: 10.1088/0004-637X/752/2/116.
- T. Totani. Cosmological Gamma-Ray Bursts and Evolution of Galaxies. *ApJ*, 486:L71–L74, September 1997. doi: 10.1086/310853.
- R. Tsutsui, T. Nakamura, D. Yonetoku, T. Murakami, S. Tanabe, and Y. Kodama. Redshift Dependent Lag-Luminosity Relation in 565 BASTE Gamma Ray Bursts. In M. Galassi, D. Palmer, and E. Fenimore, editors, *American Institute of Physics Conference Series*, volume 1000 of *American Institute of Physics Conference Series*, pages 28–31, May 2008. doi: 10.1063/1.2943466.
- R. Tsutsui, T. Nakamura, D. Yonetoku, T. Murakami, Y. Kodama, and K. Takahashi. Cosmological constraints from calibrated Yonetoku and Amati relation suggest fundamental plane of gamma-ray bursts. *J. Cosmology Astropart. Phys.*, 8:015, August 2009. doi: 10.1088/1475-7516/2009/08/015.
- R. Tsutsui, T. Nakamura, D. Yonetoku, T. Murakami, and K. Takahashi. Intrinsic Dispersion of Correlations among E_p , L_p , and E_{iso} of Gamma Ray Bursts depends on the quality of Data Set. *ArXiv e-prints*, December 2010.
- R. Tsutsui, D. Yonetoku, T. Nakamura, K. Takahashi, and Y. Morihara. Possible existence of the E_p - L_p and E_p - E_{iso} correlations for short gamma-ray bursts with a factor 5-100 dimmer than those for long gamma-ray bursts. *MNRAS*, 431:1398–1404, May 2013. doi: 10.1093/mnras/stt262.
- Z. L. Uhm and B. Zhang. Toward an Understanding of GRB Prompt Emission Mechanism. I. The Origin of Spectral Lags. *ApJ*, 825:97, July 2016. doi: 10.3847/0004-637X/825/2/97.

- T. N. Ukwatta, M. Stamatikos, K. S. Dhuga, T. Sakamoto, S. D. Barthelmy, A. Eskandarian, N. Gehrels, L. C. Maximon, J. P. Norris, and W. C. Parke. Spectral Lags and the Lag-Luminosity Relation: An Investigation with Swift BAT Gamma-ray Bursts. *ApJ*, 711:1073–1086, March 2010. doi: 10.1088/0004-637X/711/2/1073.
- T. N. Ukwatta, K. S. Dhuga, M. Stamatikos, C. D. Dermer, T. Sakamoto, E. Sonbas, W. C. Parke, L. C. Maximon, J. T. Linnemann, P. N. Bhat, A. Eskandarian, N. Gehrels, A. U. Abeysekara, K. Tollefson, and J. P. Norris. The lag-luminosity relation in the GRB source frame: an investigation with Swift BAT bursts. *MNRAS*, 419:614–623, January 2012. doi: 10.1111/j.1365-2966.2011.19723.x.
- J. Řípa, A. Mészáros, C. Wigger, D. Huja, R. Hudec, and W. Hajdas. Search for gamma-ray burst classes with the RHESSI satellite. *A&A*, 498:399–406, May 2009. doi: 10.1051/0004-6361/200810913.
- J. van Paradijs, P. J. Groot, T. Galama, C. Kouveliotou, R. G. Strom, J. Telting, R. G. M. Rutten, G. J. Fishman, C. A. Meegan, M. Pettini, N. Tanvir, J. Bloom, H. Pedersen, H. U. Nørdgaard-Nielsen, M. Linden-Vørnle, J. Melnick, G. van der Steene, M. Bremer, R. Naber, J. Heise, J. in’t Zand, E. Costa, M. Feroci, L. Piro, F. Frontera, G. Zavattini, L. Nicastro, E. Palazzi, K. Bennett, L. Hanlon, and A. Parmar. Transient optical emission from the error box of the γ -ray burst of 28 February 1997. *Nature*, 386:686–689, April 1997. doi: 10.1038/386686a0.
- R. Vavrek, L. G. Balázs, A. Mészáros, I. Horváth, and Z. Bagoly. Testing the randomness in the sky-distribution of gamma-ray bursts. *MNRAS*, 391:1741–1748, December 2008. doi: 10.1111/j.1365-2966.2008.13635.x.
- P. Veres, Z. Bagoly, I. Horváth, A. Mészáros, and L. G. Balázs. A Distinct Peak-flux Distribution of the Third Class of Gamma-ray Bursts: A Possible Signature of X-ray Flashes? *ApJ*, 725:1955–1964, December 2010. doi: 10.1088/0004-637X/725/2/1955.
- F. J. Virgili, C. G. Mundell, V. Pal’shin, C. Guidorzi, R. Margutti, A. Melandri, R. Harrison, S. Kobayashi, R. Chornock, A. Henden, A. C. Updike, S. B. Cenko, N. R. Tanvir, I. A. Steele, A. Cucchiara, A. Gomboc, A. Levan, Z. Cano, C. J. Mottram, N. R. Clay, D. Bersier, D. Kopač, J. Japelj, A. V. Filippenko, W. Li, D. Svinkin, S. Golenetskii, D. H. Hartmann, P. A. Milne, G. Williams, P. T. O’Brien, D. B. Fox, and E. Berger. GRB 091024A and the Nature of Ultra-long Gamma-Ray Bursts. *ApJ*, 778:54, November 2013. doi: 10.1088/0004-637X/778/1/54.
- I. Vurm and A. M. Beloborodov. Radiative Transfer Models for Gamma-Ray Bursts. *ArXiv e-prints*, June 2015.

- F. Y. Wang, Z. G. Dai, and E. W. Liang. Gamma-ray burst cosmology. *New A Rev.*, 67: 1–17, August 2015. doi: 10.1016/j.newar.2015.03.001.
- E. Waxman. γ -Ray Burst Afterglow: Confirming the Cosmological Fireball Model. *ApJ*, 489:L33–L36, November 1997. doi: 10.1086/310960.
- R. A. M. J. Wijers and T. J. Galama. Physical Parameters of GRB 970508 and GRB 971214 from Their Afterglow Synchrotron Emission. *ApJ*, 523:177–186, September 1999. doi: 10.1086/307705.
- R. A. M. J. Wijers, M. J. Rees, and P. Meszaros. Shocked by GRB 970228: the afterglow of a cosmological fireball. *MNRAS*, 288:L51–L56, July 1997.
- R. Willingale, P. T. O’Brien, J. P. Osborne, O. Godet, K. L. Page, M. R. Goad, D. N. Burrows, B. Zhang, E. Rol, N. Gehrels, and G. Chincarini. Testing the Standard Fireball Model of Gamma-Ray Bursts Using Late X-Ray Afterglows Measured by Swift. *ApJ*, 662:1093–1110, June 2007. doi: 10.1086/517989.
- R. Willingale, F. Genet, J. Granot, and P. T. O’Brien. The spectral-temporal properties of the prompt pulses and rapid decay phase of gamma-ray bursts. *MNRAS*, 403: 1296–1316, April 2010. doi: 10.1111/j.1365-2966.2009.16187.x.
- S. E. Woosley and J. S. Bloom. The Supernova Gamma-Ray Burst Connection. *ARA&A*, 44:507–556, September 2006. doi: 10.1146/annurev.astro.43.072103.150558.
- L. Xiao and B. E. Schaefer. Estimating Redshifts for Long Gamma-Ray Bursts. *ApJ*, 707: 387–403, December 2009. doi: 10.1088/0004-637X/707/1/387.
- T.-F. Yi, G.-Z. Xie, and F.-W. Zhang. A Close Correlation between the Spectral Lags and Redshifts of Gamma-Ray Bursts. *Chinese J. Astron. Astrophys.*, 8:81–86, February 2008. doi: 10.1088/1009-9271/8/1/08.
- D. Yonetoku, T. Murakami, T. Nakamura, R. Yamazaki, A. K. Inoue, and K. Ioka. Gamma-Ray Burst Formation Rate Inferred from the Spectral Peak Energy-Peak Luminosity Relation. *ApJ*, 609:935–951, July 2004. doi: 10.1086/421285.
- D. Yonetoku, T. Murakami, R. Tsutsui, T. Nakamura, Y. Morihara, and K. Takahashi. Possible Origins of Dispersion of the Peak Energy-Brightness Correlations of Gamma-Ray Bursts. *PASJ*, 62:1495–, December 2010. doi: 10.1093/pasj/62.6.1495.
- D. Yonetoku, T. Nakamura, T. Sawano, K. Takahashi, and A. Toyonago. Short Gamma-Ray Burst Formation Rate from BATSE Data Using E_p - L_p Correlation and the Minimum

- Gravitational-wave Event Rate of a Coalescing Compact Binary. *ApJ*, 789:65, July 2014. doi: 10.1088/0004-637X/789/1/65.
- S. A. Yost, D. A. Frail, F. A. Harrison, R. Sari, D. Reichart, J. S. Bloom, S. R. Kulkarni, G. H. Moriarty-Schieven, S. G. Djorgovski, P. A. Price, R. W. Goodrich, J. E. Larkin, F. Walter, D. S. Shepherd, D. W. Fox, G. B. Taylor, E. Berger, and T. J. Galama. The Broadband Afterglow of GRB 980329. *ApJ*, 577:155–163, September 2002. doi: 10.1086/342175.
- B. Zhang. Open questions in GRB physics. *Comptes Rendus Physique*, 12:206–225, April 2011. doi: 10.1016/j.crhy.2011.03.004.
- B. Zhang and P. Mészáros. An Analysis of Gamma-Ray Burst Spectral Break Models. *ApJ*, 581:1236–1247, December 2002. doi: 10.1086/344338.
- B. Zhang and A. Pe’er. Evidence of an Initially Magnetically Dominated Outflow in GRB 080916C. *ApJ*, 700:L65–L68, August 2009. doi: 10.1088/0004-637X/700/2/L65.
- B. Zhang and H. Yan. The Internal-collision-induced Magnetic Reconnection and Turbulence (ICMART) Model of Gamma-ray Bursts. *ApJ*, 726:90, January 2011. doi: 10.1088/0004-637X/726/2/90.
- B. Zhang, B.-B. Zhang, F. J. Virgili, E.-W. Liang, D. A. Kann, X.-F. Wu, D. Proga, H.-J. Lv, K. Toma, P. Mészáros, D. N. Burrows, P. W. A. Roming, and N. Gehrels. Discerning the Physical Origins of Cosmological Gamma-ray Bursts Based on Multiple Observational Criteria: The Cases of $z = 6.7$ GRB 080913, $z = 8.2$ GRB 090423, and Some Short/Hard GRBs. *ApJ*, 703:1696–1724, October 2009. doi: 10.1088/0004-637X/703/2/1696.
- B.-B. Zhang, E.-W. Liang, and B. Zhang. A Comprehensive Analysis of Swift XRT Data. I. Apparent Spectral Evolution of Gamma-Ray Burst X-Ray Tails. *ApJ*, 666:1002–1011, September 2007. doi: 10.1086/519548.
- B.-B. Zhang, B. Zhang, K. Murase, V. Connaughton, and M. S. Briggs. How Long does a Burst Burst? *ApJ*, 787:66, May 2014. doi: 10.1088/0004-637X/787/1/66.
- Z. Zhang, G. Z. Xie, J. G. Deng, and W. Jin. Revisiting the characteristics of the spectral lags in short gamma-ray bursts. *MNRAS*, 373:729–732, December 2006. doi: 10.1111/j.1365-2966.2006.11058.x.
- H. Zitouni, N. Guessoum, W. J. Azzam, and R. Mochkovitch. Statistical study of observed and intrinsic durations among BATSE and Swift/BAT GRBs. *Ap&SS*, 357:7, May 2015. doi: 10.1007/s10509-015-2311-x.

Y.-C. Zou and T. Piran. Lorentz factor constraint from the very early external shock of the gamma-ray burst ejecta. *MNRAS*, 402:1854–1862, March 2010. doi: 10.1111/j.1365-2966.2009.15863.x.